UNIVERSITY OF CALIFORNIA SAN DIEGO

SAN DIEGO STATE UNIVERSITY

Structure-function effects of mutations in domains of Inducible Tyrosine Kinase

A dissertation submitted in partial satisfaction of the requirements for the degree

Doctor of Philosophy

in

Biology

by

Roman Myroslavovych Levytskyy

Committee in charge:

University of California, San Diego
Professor Ananda Goldrath
Professor Cornelis Murre

San Diego State University
Professor Constantine Tsoukas, Chair
Professor Ralph Feuer
Professor Roland Wolkowicz

2012

The Dissertation of Roman Myroslavovych Levytskyy is approved, and it is acceptable in quality and form for publication on microfilm and electronically:

_____

_____

_____

_____

_____

Chair

University of California, San Diego

San Diego State University

2012

TABLE OF CONTENTS

LIST OF ABBREVIATIONS

AH	Armenian hamster
Amp	ampicillin
AP	Antarctic phosphatase
APS	ammonium persulfate
ATP	Adenosine-5'-triphosphate
ATP	adenosine triphosphate
BSA	bovine serum albumin
CD28	cluster for differentiation 28
CD3ε	Cluster for differentiation 3 epsilon chain
CD4	cluster for differentiation 4
CFP	cyan fluorescent protein
Co-IP	co-immunoprecipitation
CsA	Cyclosporin A
Cy5	cianine dye 5
CypA	Cyclophillin A
DIC	Differential interference contrast microscopy
DIUF	deionized ultra-filtered
DMEM	Dulbecco's Modification of Eagles Medium
DMSO	Dimethyl sulfoxide
DTT	Dithiothreitol

Dy405	DyLight 405 dye
EDTA	Ethylenediaminetetraacetic acid
ELISA	enzyme-linked immunosorbent assay
ERK	extracellular signal-regulated kinase
FACS	fluorescence activated cell sorting
FCS	fetal calf serum
FP	fluorescent protein
FRET	fluorescence resonance energy transfer
FWD	forward
GFP	green fluorescent protein
GαAH	goat anti-Armenian hamster
GαH	goat anti-hamster
GαM	goat anti mouse
GαR	goat anti-rabbit
HEPES	4-(2-hydroxyethyl)-1-piperazineethanesulfonic acid
Hi-Fi	High Fidelity
HRP	horseradish peroxidase
ICCS	intracellular cytokine staining
IFNγ	interferon gamma
IL	interleukin
IM	ionomycin
IP	immunoprecipitation

ITAM	immunoreceptor tyrosine-based activation motif
ITK	Inducible Tyrosine Kinase
KAc	potassium acetate
Kan	kanamycin
LAT	linker for activation of T cells
LB	Luria Bertani medium
MαGFP	mouse anti-GFP
MαItk	mouse anti-Itk
MαLAT	mouse anti-LAT
MαpY	Mouse anti-phosphotyrosine
MαpY511	Mouse anti-phosphotyrosine 511
NP-40	nonyl phenoxypolyethoxylethanol
PAAG	polyacrylamide gel
PBS	phosphate buffered saline
PCR	polymerase chain reaction
PF	paraformaldehyde
PGS	protein G-sepharose
PhosphoFlow	phosphorylation sensitive flow cytometry
PLCγ	Phospholipase C gamma 1
pM	picomoles
PMA	phorbol-12-myristate-13-acetate
PMSF	phenylmethanesulfonylfluoride

PPIase	Peptidyl-Prolyl Isomerase
PVDF	Polyvinylidene fluoride
pY	phosphotyrosine
RE	restriction enzyme
REV	reverse
RPM	rotations per minute
RPMI	Roswell Park Memorial Institute medium
R-poly-αItk	rabbit polyclonal anti-Itk antibody
RαM	rabbit anti-mouse
RαSLP-76	rabbit anti-SLP-76
SAM	S-Adenosyl methionine
SDS	Sodium dodecyl sulfate
SH1	Src homology domain 1
SLP-76	SH2 domain containing leukocyte protein of 76kDa
SOC	Super Optimal broth with Catabolite repression
TAE	Tris, acetic acid and EDTA buffer
Taq	Thermus aquaticus
TBST	Tris-Buffered Saline and Tween 20
TC	tissue culture grade
TEMED	Tetramethylethylenediamine
Tiff	Tagged Image File Format
TMB	3,3',5,5' tetramethylbenzidine

TOPO TA	DNA Topoisomerase I Thymine Adenine Cloning Vector
Tris	tris(hydroxymethyl)aminomethane
U	activity units
WTB	western transfer buffer
YFP	yellow fluorescent protein
YT	yeast-tryptone medium
ZAP-70	zeta-chain-associated protein kinase 70
β-ME	beta-mercaptoethanol

LIST OF FIGURES

LIST OF TABLES

ACKNOWLEDGEMENTS

I would like to thank Dr. Constantine Tsoukas for his mentorship, support, and direction, my committee members Dr. Roland Wolkowicz, Dr. Ralph Feuer, Dr. Ananda Goldrath, and Dr. Cornelis Murre for agreeing to serve on my committee despite their busy schedules and for providing valuable suggestions on the direction of my project.

I would like to thank Dr. Sandy Bernstein for patiently giving me a lot of advice in the beginning of my studies in the PhD program, and for his initiative with PhD/MBA program.

I would like to thank David Guimond for advice and help in solving and troubleshooting multiple technical problems, Nupur Hirve for work on PH domain mutants, especially on FYF mutant, Dr. Juris Grasis for advice on technical problems and data interpretation.

Also I would like to thank Ritz Zhang for developing Itk-CY biosensor, David Guimond for initial development of the FRET assay in our lab, and initial assessment of the Itk biosensor FRET, Dr. Tomasz Zal for sharing his expertise on FRET assay.

I would like to thank Jason Rudy for his help in multiple subclonings and site directed mutagenesis efforts, Roma Munday and Alexa Spilsbury for help in site directed mutagenesis.

I would like to thank Dr. Amy Andreotti for providing the template BtkSH3 construct, and Dr. Karsten Sauer for collaboration on FYF project.

I would like to thank Brett Hilton for help and training in flow cytometry, Dr. Robert Zeller for allowing use of his Zeiss AxioVision microscope, and Dr. Forest Rohwer for allowing use of his PCR Gradient MasterCycler machines.

I would like to thank Dr. Greg Harris, Patty Swinford, Sandra Talley, Medora Bratelin, and Cathy Pugh for being available, helpful, and efficient in solving all the administrative issues I have encountered.

I would also like to thank Krystal Herman and Sunny Levy, who were members of the lab when I just joined. Also big thanks to Wolcowicz lab, McGuire lab, Rohwer lab, Zeller lab, and Glembotsky lab for being friendly and helpful.

I would like to thank my co-authors for letting me use in the Results section of my dissertation part of the data from the following papers:

1. ***Levytskyy R.M., Hirve N., Rigaud S., Sauer K., Zal T., Tsoukas C.D.*** Effects of the mutation in FYF motif of the Pleckstrin Homology (PH) domain of Itk (in preparation)
2. ***Levytskyy R.M., Hirve N., Guimond D.G., Min L., Andreotti A.H., Tsoukas C.D.*** In Vivo Consequences of Disrupting the Transphosphorylation and Intermolecular Self-Association of the Inducible T Cell Kinase (ITK) (Submitted to Journal of Biological Chemistry)

VITA

Education:

2005-2012 – PhD in Biology San Diego State University and University of California, San Diego. Major: Molecular and Cellular Biology. Research in Immunology (Structure-function relation of protein domains in Inducible Tyrosine Kinase mutants in cell lines and in transfected primary KO mouse lymphocytes).

2003-2004 – M.S. in Biochemistry Ivan Franko National University of Lviv, Lviv, Ukraine. Department of Biology. Major: Biochemistry. GPA 4.0. Master's Diploma thesis: "Determination of cytotoxic activity of alkaloid-derived substances on the model of mitogen stimulated human lymphocytes".

- Graduated *summa cum laude.*

1999-2003 – B.S. in Biochemistry Ivan Franko National University of Lviv, Lviv, Ukraine. Department of Biology. Major: Biochemistry. GPA 3.9. Bachelor's Diploma thesis: "Role of Nitric Oxide in apoptosis of Jurkat T-cell line and normal human lymphocytes".

Publications, patents, and presentations:

1. ***Levytskyy R.M., Hirve N., Rigaud S., Sauer K., Zal T., Tsoukas C.D.*** Effects of the mutation in FYF motif of the Pleckstrin Homology (PH) domain of Itk (in preparation)
2. ***Levytskyy R.M., Hirve N., Guimond D.G., Min L., Andreotti A.H., Tsoukas C.D.*** In Vivo Consequences of Disrupting the Transphosphorylation and Intermolecular Self-Association of the Inducible T Cell Kinase (ITK) (Submitted to Journal of Biological Chemistry)
3. ***Levytskyy R.M., Hirve N., Tsoukas C.D.*** Functional effects of the structural mutants of Itk domains. Abstract and poster presentation, Graduate Research Symposium, SDSU, April 8th, 2011
4. ***Levytskyy R.M., Tsoukas C.D.*** Spatiotemporal behavior, intracellular signaling and interactions of Itk in T cells. Abstract and poster presentation, 36th La Jolla Immunology Conference, Salk Institute, October 12-14th, 2010
5. ***Levytskyy R.M., Hryvul T.M., Stoika R.S.*** Method of detection of nitrite ions in solutions (UA(Ukraine) patent No. 76576)
6. ***Levytskyy R.M., Filyak Y.Z., Stoika R.S.*** Correlation between generation of nitric oxide and cell viability in human peripheral blood cells and Jurkat T-cell line//Experimental Oncology, 2004, Vol.26, No.3, p.217-220

7. ***Levytskyy R.M., Lozinsky R.P., Panchyshyn O.J., Negrych T.I., Stoika R.S.*** Dualism of nitric oxide action in apoptosis//Animal Biology, 2003, Vol.5, No.1-2, p.39-51
8. ***Levytskyy R.M., Panchyshyn O.J., Hryvul O.T., Makukh J.M., Stoika R.S.*** Impact of dexametazone on nitrite production by T-leukemic cells of Jurkat T-cell line//Materials of all-Ukrainian students' conference in Lviv State Academy of Veterinary Medicine, Lviv: Lviv State Academy of Veterinary Medicine, 2003, Vol. 2., 87 p.
9. ***Hryvul O.T., Makukh J.M., Tsarik R.V., Levytskyy R.M., Korobov V.M.*** Blood indices of bloodstock bulls//Materials of international students' conference in Lviv State Academy of Veterinary Medicine, Lviv: Lviv State Academy of Veterinary Medicine, 2001, 114 p.

Activities and community service

- Abstract reviewer for 2011 AAPS Annual Meeting and Exposition
- Abstract reviewer for 2011 AAPS National Biotechnology Conference

- Volunteer at Biotechnology Industry Organization

- Volunteer Judge in biological sciences at San Diego Science and Engineering Fair

- Volunteer Assistant Event Captain at San Diego Regional Science Olympiad

- Member of *Toastmasters International*, *Professional Men's Toastmasters #624*
    - Received a Competent Communicator (CC) recognition

- Co-organizer of international conference at Ivan Franko National University of Lviv (2000) dedicated to the centenary of genetics

Awards:

Won several biology contests while high school and undergraduate student (24 major awards including: Silver Medal at Ecological Projects Olympiad in Istanbul, Turkey (1999), 2 first prizes at Soros Foundation All-Ukrainian Contest in the field of Biology (1998 and 1999), winner of All-Ukrainian Biology and Ecology Olympiad (1999), 5 times prize winner of All-Ukrainian Biology Olympiad).

Foreign languages:

- ✓ Ukrainian,
- ✓ Russian
- ✓ Polish

Research skills

Cell culture
- Suspension and adherent eukaryotic cell culture (mammalian, insect, yeast)

Bacterial cultures

Animal protocols (small animals)

Transfections
- Biorad, Amaxa, Lipofectamine in cell lines and primary cells

Nucleic acid preparation
- DNA preps using various methods (regular preps, ethanol precipitation, endotoxin free preps)
- RNA isolation

Cloning
- Restriction digests, ligations, subcloning from and into different vectors, direct PCR fragments subcloning, TA vector subclonings
- Vector design, sequence comparison, etc.
- Vector NTI

PCR
- PCR, RT-PCR, qRT-PCR, Gradient PCR
- Site-directed mutagenesis

DNA and RNA gels, comet assay

ELISA

Western Blotting, CoIPs

Immune cell stimulation
- Antibody, antigen, and chemical agent driven cell stimulation
- T-cell/B-cell conjugation assays

Biochemistry
- Enzymatic reactions, enzyme kinetics, enzyme-based assays

Flow cytometry
- Surface marker staining, intracellular staining
- Multiparameter staining and analysis
- FACS, Phosphoflow
- Intracellular Cytokine Detection (ICCS)
- Experience with BD FACS Aria and BD FACS Canto
- DIVA, FlowJo

Microscopy
- Slide preparation, antibody and chemical agent staining on the slide
- Epifluorescent microscopy, live imaging, FRET, Confocal microscopy
- Electron microscopy (basic skills)

Image processing
- Advanced image analysis and processing using ImageJ
- Writing scripts and plugins for ImageJ

Statistical analysis
- Excel, Prizm, SigmaPlot, Origin

ABSTRACT OF THE DISSERTATION

Structure-function effects of mutations in domains of Inducible Tyrosine Kinase

by

Roman Myroslavovych Levytskyy

Doctor of Philosophy in Biology

University of California, San Diego, 2012

San Diego State University, 2012

Professor Constantine Tsoukas, Chair

The dissertation is studying structural mutants of various domains of the Inducible Tyrosine Kinase (Itk), and their relation to functionality of this protein in immune cells. Using cell lines as well as primary cells from $Itk^{-/-}$ mice, and employing systematic functional study approach this work is exploring effects of several mutations (Y511F, BtkSH3, FYF) on immediate, and far downstream signaling of Itk under conditions of TCR induced stimulation. Structural (FRET), as well as biochemical and molecular biology techniques were used (western

blotting, flow cytometry, ELISA). It was shown that Itk does not exhibit noticeable differences neither in structure, nor in localization in resting cells, but changes conformation and localization patterns under stimulation in T-cell-APC system. This event is pronounced in statistically significant manner in wild type Itk, but is disrupted to different extent in mutants. PH domain mutant FYF is the only one from those explored that has disrupted localization pattern, and surprisingly, nonfunctional activation residue mutant Y511F preserves intact localization. However, all mutants show disruption in structural pattern when compared to wild type Itk. Another novel finding is related to Itk-SLP-76 interaction, which proved to be disrupted in BtkSH3 mutant that lacks noncanonical SH3 domain interactions, pointing on important role of noncanonical SH3 interactions in signaling of Itk in complex with SLP-76, and as a result in activation of Itk. All mutants show some extent of disruption in Y511 phosphorylation, which has a direct effect on downstream events as assessed by PLCγ phosphorylation, and reflects defects in structure and localization patterns, with mutants being significantly deficient comparing to wild type. This results in even more pronounced effect in Th2 cytokine production, and this dissertation provides the first evidence of the influence of these mutants on Th2 cytokines, which are the signature cytokines of Itk. The dissertation proposes explanations of the mentioned phenomena, underlines an importance of different parts of Itk molecule in its functionality, and makes

possible to apply the data acquired here to further understand the role of Itk in deeper detail with possible clinical implications in the future.

INTRODUCTION

TEC kinases

TEC family is the largest family of kinases after Src family, and consists of five members: Itk, Btk, Tec, Rlk, and Bmx (1). One of the features of Tec kinases that differentiates them from Src kinases is the absence of myristoylation site and presence of PH domain that allows them to become targeted to the membrane (2). All Tec kinases share similarities in activation mechanism (3). They all require phosphorylation by a Src family kinase and then autophosphorylation on tyrosine residue in SH3 domain to become activated (3).

Interestingly, domain functions of Tec kinases compared to Src family kinases are closer to that of Csk kinase than Src kinase (4). In Src kinase, SH2 and SH3 domain play an inhibitory function – isolated kinase domain is fully active, and the addition of SH2 and SH3 domains inhibits activity (4). Introduction of point mutations that disable SH2 or SH3 domain has a positive effect on kinase activity (3). The opposite is true for Csk kinase and Tec kinase family. In this case, SH2 and SH3 domains enhance the activity, and isolated SH1 domain has low kinase activity (3).

One of the TEC kinases closely related to Itk is Rlk. It was shown to perform a similar and overlapping function. However, under Th2 skewing conditions, its expression is reduced while Itk expression stays constant (5). At the same time, Rlk expression is less reduced in Th1 cells, which may point to the specific importance of Itk in differentiated Th2 cells (5). Rlk is believed to supplement Itk function, having

an additive effect in some cases, while in other cases having an opposite effect, thus making these two proteins not completely interchangeable (5). A notable feature of Rlk is an absence of the PH domain in contrast to other TEC kinases (2).

Itk structure

Itk contains SH1, SH2, SH3, TH, and PH domains typical for Tec kinases (6), as displayed in Figure 1. SH1 domain occupies residues 357-622, SH2 domain 241-340, and SH3 domain 179-228, which are connected by short peptide linkers (7). Subsections below characterize each Itk domain in detail.

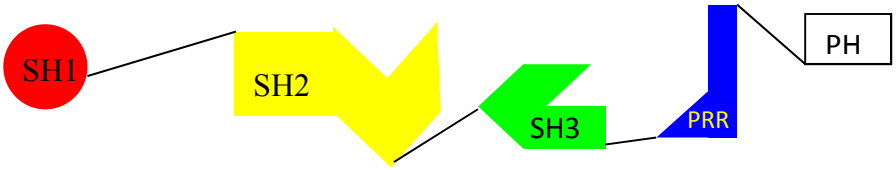

Figure 1. Schematic domain structure of Itk

SH1 domain

Isolated SH1 domain of Itk was synthesized, crystallized, and characterized by multiple groups (8). The domain has an activation loop encompassing amino acid residues 502-521, with Y511 serving as an activating switch after it gets phosphorylated (8,9). Other residues of importance in the catalytic center of the domain are Glutamine 406, Lysine 391, and Asparagine 500 (8,10). The structure of Itk SH1 domain is similar to SH1 domains of other kinases, including Src kinases, and consists of two terminal loops with the linker region in between (8,6). One of the

differences with Src kinases is the absence of c-terminal area with phosphotyrosine sites, which points at a different activation mechanism for the TEC kinases (6).

Kinase domains of Itk and Btk are very close in structure in phosphorylated and unphosphorylated form (8). However, the major difference is that in inactive conformation, the ATP binding pocket of Itk resembles that of an active conformation, while in Btk, inactive conformation has one of the loops closing off the binding pocket (8).

While in other kinases, the active center usually undergoes significant structural changes under activation, usually bringing domain loops closer together to properly orient ATP molecule for hydrolysis (8), in Itk after Y511 phosphorylation the structure of the SH1 domain barely changes (8,10). This leads to an interesting observation that while in other kinases phosphorylation of the tyrosine residues might be necessary to remove the loops blocking the catalytic center of the domain, in Itk the phosphorylation of Y511 does not seem to have much influence on loop position, thus making the active center of the enzyme constitutively capable of binding ATP, which contrasts with other proteins in the Tec family, such as Btk, and Src family, such as Lck (8,10). This also suggests that other domains of Itk might play a crucial role in regulating its activity (8,10).

SH1 domain was studied intensively the last several years in an effort to design new selective inhibitors of Itk activity that might be used as therapeutic agents for autoimmune diseases and organ transplantation (10,11,12,13,14). However, it turned out that other domains might be better targets for inhibitor development, as SH1

domain of Itk showed the same ATP binding with or without catalytic domains, but did not show the same activity (10).

SH1 domain is known to phosphorylate tyrosines on two targets – Y180 in the SH3 domain of the same Itk molecule (9) and Y783 residue in between SH2 and SH3 domains of PLCγ (15). This phosphorylation *in vivo* depends on SH2 domains of respective proteins that bind the nonphosphotyrosine site on SH1 domain of Itk, and guide phosphorylation sites to the catalytic pocket on the SH1 domain (16). SH1 domain by itself shows low activity *in vitro*, but addition of the linker that is normally located between SH1 and SH2 domains significantly enhances kinase activity (3). SH2 domain addition increases it even further. This was proven by attaching SH2 domain to isolated peptide substrate, which increased kinase activity several fold (16,17). Mutations in this linker area cause loss of function in Itk molecule (17). However, addition of other domains seems to have no additional effect in contrast with Csk kinase, in which addition of both SH2 and SH3 domains positively influences enzymatic activity (3).

Residue W355, in the linker between SH2 and SH1 domains, turns out to be critical for Itk kinase activity, and is believed to take part in interaction between regulatory domains of Itk and kinase domain, similar to the homologous region of Src and Csk kinases (3). Residue K390 is a critical residue inside kinase domain active site, and its mutation K390R renders kinase domain inactive (3,9). It was shown that Itk has regulatory tyrosine in SH1 domain, and that phosphorylation of this residue - Y511 is important for Itk kinase activity (3,9). Y511F mutants of Itk that cannot get

phosphorylated on 511 residue demonstrated significantly lower kinase activity in various assays, and significant decrease in transducing signal to downstream targets, resulting in lower phosphorylation of PLCγ and lower IL-2 production (9). However, Y511F still exhibited higher overall activity than K390R (9).

SH2 domain

There is a wealth of information about Src family SH2 domains, but structure and function of SH2 domains of other proteins was less intensively studied. SH2 domain of Src binds a phosphorylated tyrosine at the C-terminus of the protein as a way of regulating Src activity (6). In Itk and other Tec kinases, C-terminus has a different structure, even though SH2 and SH3 domains have similar structure to that of Src (18,6). Also, it was shown that to be activated, Itk has to interact with phosphotyrosines that are not homologous to C-terminal tyrosine of Src (6). This led to a hypothesis that SH2 domain of Itk has a regulatory role and plays a part in molecule activation (18).

It was long known that events like tyrosine phosphorylation (19) and *cis*/*trans* proline isomerization (6,20) can affect the structure of binding sites and regulate signaling that way, and that SH2 domain of Itk does contain proline sequences that fit the isomerization pattern. They can undergo isomerization, and this event might play a regulatory role (21,6), shown in Figure 2A. This led to the discovery of evidence that Itk activity can be regulated by CypA, a direct target of CsA (18). CypA is one of the PPIases that promotes the transition between *cis* and *trans* proline conformations in solution (6,22). Itk has one of the prolins – P287 that is susceptible to conformational change by CypA (18,6).

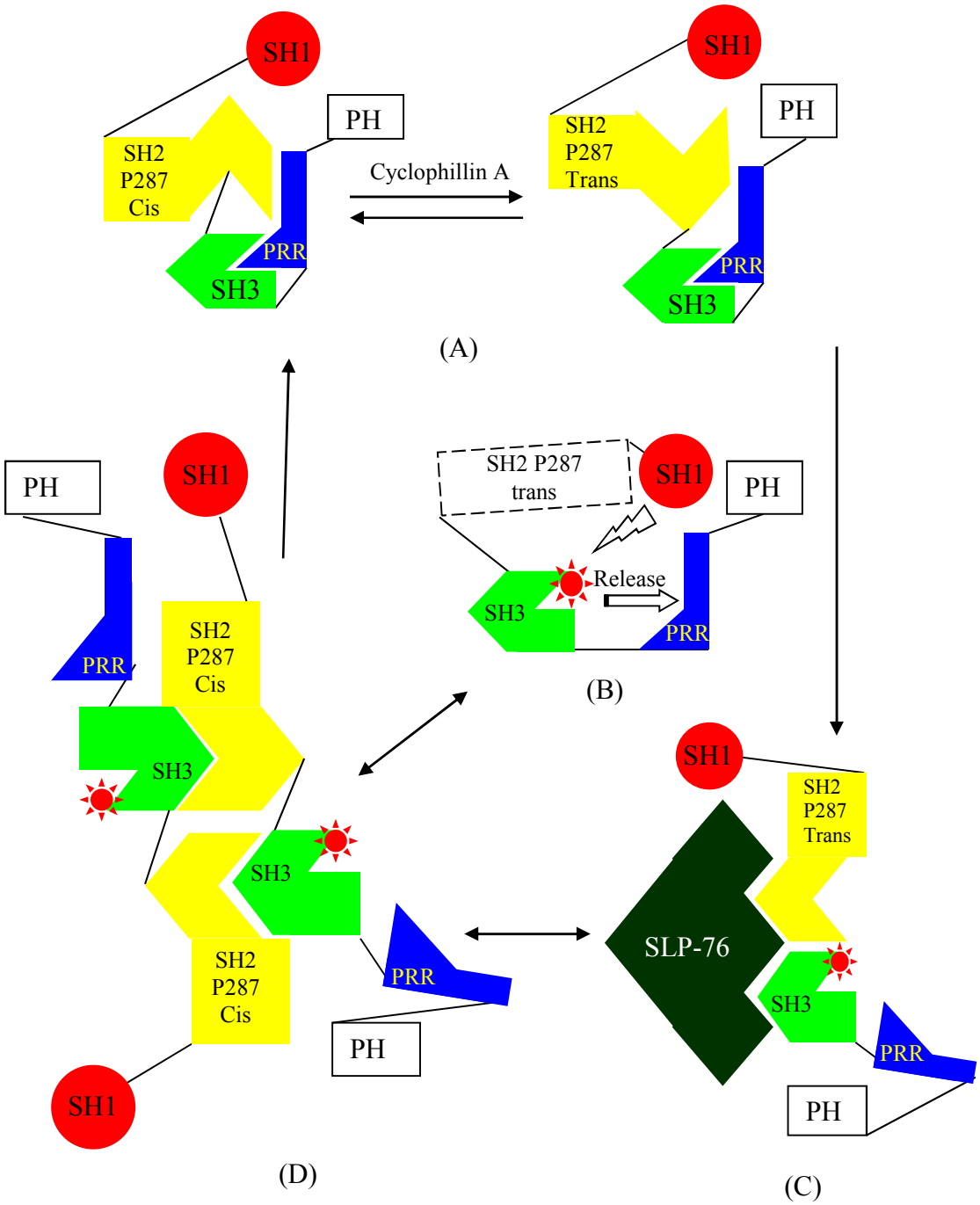

Figure 2. Simplified scheme of Itk conformational changes according to literature data.

A) SH3 domain in intramolecular fold, SH2 domain fluctuating between P287 *cis* and *trans*

B) After activation by Lck, Itk autophosphorylates on Y180, releasing PPR ligand from SH3 binding pocket, and now favoring noncanonical SH3 ligands

C) Itk bound to SLP-76 in SH2 P287 *trans*, and SH3 phosphorylated at Y180 residue

D) Dimer formation with SH2 P287 *cis* bound to SH3 domain of other Itk molecule

- Y180 phosphorylation is shown as red star.

In solution SH2, domain of Itk can have one of the two predominant conformations that differ in conformation of one proline residue - P287, which can be either *cis* or *trans* (18). Structural mutation of this proline into glycine locks the SH2 domain in a conformation mimicking permanent *trans* conformation of P287, and at the same time prevents interaction with CypA (18).

This *cis-trans* conformational change influences not only areas of the SH2 domain in immediate proximity to P287, but also more remote areas of the domain (18,20). Itk seems to be unique in contrast to other proteins that contain proline isomerization switches because of the changes in the molecule that happen not only in SH2 regions that are close to the proline residue, as in HIV-1 capsid (20), but also in regions of the SH2 domain that are farther away (23). Interestingly, it was shown that these two different conformations of SH2 domain of Itk have a different affinity for different substrates - while P287 *cis* conformation has higher affinity for the SH3 domain of other Itk molecules, P287 *trans* conformation has higher affinity for phosphopeptides (24). Thus, it was suggested that proline isomerization plays a role in switching interactions between ligands (18). It was also shown that CypA inhibits the phosphorylation signaling cascade downstream of Itk, but does not affect upstream events, and this effect can be reversed by CypA inhibitor CsA (18). It was suggested that the natural activation sequence of events consists of the phosphotyrosine of another molecule binding the pY pocket in SH2 domain of Itk, at the same time displacing CypA while keeping P287 still in *trans*. This leads to interaction of the flanking aminoacids adjacent to phosphotyrosine with a binding pocket in SH2

domain of Itk that is located close to pY pocket (pY+3), and is a result of conformational change from *cis*-*trans* isomerization of P287 (18). Further, it was shown that addition of the phosphopeptide significantly shifts the SH2 domain conformation equilibrium in solution toward P287 *trans* form (21).

The NMR experimental data revealed that phosphotyrosine binding pocket of the SH2 domain does not undergo major changes and is overlapping in both, *cis* and *trans* conformations (25,21). However, the pY+3 pocket does exhibit very different conformation in P287 *cis* versus P287 *trans* (18,21). This binding site (pY+3) is responsible for the recognition of flanking aminoacids of the phosphopeptide (21). Conformational changes in SH2 domain of Itk resulting from binding of the phosphopeptide are thought to positively influence the activity of SH1 domain, and ultimately the activity if Itk as a whole, while binding of SH3 domain to *cis* SH2 domain is thought to inhibit activation (21). *Trans* conformation of P287 SH2 makes it impossible to bind SH3 domain because of the steric hindrance this conformation creates in relation to SH3 domain binding pocket (23). This proline switch is unique to Itk, and does not have homologous proline in other Tec kinases except for Ptk, a Tec kinase of Zebrafish (23).

It is believed that in Btk, SH2 domain plays a role in switching on the PLCγ phosphorylation, which is a later event that happens after the Btk activation events mediated by the PH domain (26). In B cells, SH2 domain binds to PLCγ via SLP-65, thus providing an additional level of regulation by requiring two separate upstream events – Syk (analog of ZAP-70 in T-cells) phosphorylating PLCγ and SLP-65

(analog of SLP-76 in T cells) binding to Btk before PLCγ can be phosphorylated by Btk and become active (26).

It was shown that KO mice lacking CypA demonstrate increased Th2 cytokine production. Also, it was pointed out that Itk was the likely candidate in the signaling cascade that is affected. Later research showed that, indeed, Itk input into cytokine production is regulated by CypA under TCR stimulation conditions (5). Lack of CypA increased significantly the production of IL4, as well as other Th2 cytokines (IL5 and IL13), while the production of Th1 cytokine IFNγ stayed constant (5).

A similar effect was demonstrated by transfection of P287G Itk into the cells of the wild type mice. It increased the production of Th2 cytokines, showing that *trans* P287 conformation of the SH2 domain is the active one, and that CypA may play a key role in the regulation of Itk activity *in vivo* (5). Also, P287G and wild type Itk increased IL4 expression when transfected into $Itk^{-/-}$ mouse cells, but kinase dead Itk mutant K390R did not, which suggests that SH2 domain exerts its effect on IL4 production via regulation of the kinase domain (5). This effect also resembles the effects in NFAT transgenic animals, and confirms the Itk role in this pathway (5).

It was shown that SH2 domain of Itk is critical in interaction of Itk with LAT. Itk with either deletion of SH2 domain or with a point mutation affecting critical active binding pocket residue (R265K) resulted in a loss of inducible Itk phosphorylation and a loss of LAT binding. At the same time, deletion of other mutants, except kinase domain, did not disrupt either of the events (27). This shows the significance of SH2 domain in upregulation of activity if Itk.

Two conformations of SH2 domain – *cis* and *trans* are separated by a relatively high energy barrier, and, for this reason, switch from one to another in solution is slow without involvement of other proteins that act as Itk signaling partners. CypA lowers the energy barrier, and thus allows for quicker conformation change (6,20). This could allow locking Itk in predominant conformation, for example, into SLP-76 bound *trans* P287 SH2 conformation in case when phosphorylated SLP-76 would be in excess at the immunological synapse site (26), shown in Figure 2C. SH2 domains of most proteins bind only canonical phosphotyrosine residues, while Itk also has an affinity to its own SH3 domain, where binding is not directly related to recognizing phosphotyrosine (6). Binding of SH2 domain to SH3 domain of other Itk molecule forms a dimer that is believed to be inactive (6). SH2 domain of Itk on substrate molecule acts as an adapter in docking the substrate to the SH1 domain catalytic pocket. In experiments to elucidate the minimum required substrate part of the whole Itk molecule, it was proven that SH2 domain is necessary for SH3 domain autophosphorylation. It was suggested that SH2 domain of the substrate molecule binds to the corresponding site on the SH1 domain, and orients the substrate site for phosphorylation (16). This binding to the SH1 domain does not require interaction with phosphorylated tyrosine residues, which are the conventional substrate for the SH2 domain (16). Introducing substitutions in arginine residues that are responsible for phosphotyrosine binding did not affect interactions with SH1 domain (16). It was also shown that isolated SH2 domains compete for this binding site, and may be used for inhibiting Itk activation (16).

One of the problems intensively studied by NMR was noncanonical binding between SH2 and SH3 domains of Itk (28). It was shown what mutation in active site of SH2 domain W208K prevents both, canonical phosphotyrosine-dependent binding, and noncanonical SH3 domain binding (28). Residues K280 and N286 in CD loop of SH2 domain turned out to be important for SH3 domain binding. They have positive charge, and can readily interact with phosphorylated Y180, or its analog – Y180E, that introduces negative charge, mimicking phosphorylation. Mutation of K280A and N286A completely abrogated SH3 domain binding by SH2 domain (28). It also seems that noncanonical ligand binding by Itk SH2 domain has similarities to noncanonical binding of ubiquitin by Sla1. Even though ubiquitin and Itk SH3 domain have very different overall structures, the binding sites in both cases share similarities in amino acid residues that make contact with the ligand (28).

It was suggested that Itk undergoes multimerization, not just dimerization at the membrane (29). A model was suggested that assumes multimer formation due to sequential SH2-SH3 domain binding in different Itk molecules, which also positions PH domains on one side, and makes a possibility for reinforcement of multimer structure by additional bonds between PH domains (28).

SH3 domain

SH3 domains usually bind highly conserved sequence polyproline containing sequences, in case of Itk - PXXP, which is considered to be the canonical binding substrate for Itk SH3 domain (30). SH3 domain of Itk was solved in different configurations, and its structure is well known (30). First attempts consisted of studying free SH3 domain, and SH3 domain bound to its canonical substrate – PPR region of TH domain of Itk (30). Later studies focused on SH3 bound to nonconventional substrate – SH2 domain (28). For binding with PXXP ligand, three residues are important – Y180, Y225, and W208. They were shown to change location in ligand-bound SH3 domain compared to free domain (30). This binding is performed in similar fashion by SH3 domains of other proteins like Grb2. They have homologous tyrosine residues to Y180 and Y225, which exhibit similar behavior under binding the ligand (30).

SH3 domain of Itk has a canonical ligand in PPR domain of Itk that has a PXXP structure (KPLPPTP) characteristic of classical SH3 domain ligands (31), interaction is shown in Figure 2A. This interaction within the molecule is believed to be inhibitory (32). It was proven to exist in vivo, and Itk in this conformation appeared to be inactive (33,34).

Noncanonical binding of a *cis* P287 SH2 domain of Itk by SH3 domain of Itk (displayed in Figure 2D) has some resemblance to binding the PPR region, as the SH2 region that binds to SH3 binding pocket has structural similarity with the PPR region,

even though this SH2 region does not contain either the proline motif or any prolins at all (23).

In some experiments in the literature, SH3 domain deletion was demonstrated to be insignificant for inducible Itk activation and binding to LAT (27). Experiments with deletion of domains or introducing point mutations affecting critical residues in binding pockets showed that SH3 domain deletion or introduction of W208 mutation (critical residue in SH3 binding pocket) did not affect LAT binding or inducible Itk activation (27). However, other experiments that used specific inhibitor peptide mimicking SLP76 polyproline region showed interference with Itk activity, blocking Itk phosphorylation, and suggesting that SH3 binding to polyprolin sequence does play a role in normal Itk signaling (35). It was shown that Y180F mutant is partially deficient in Itk function (6). Most probably activation of Itk requires Y180 phosphorylation in SH3 domain (shown in Figure 2B) and binding of phosphotyrosine by SH2 domain simultaneously, and shifting equilibrium from dimer formation by occupying binding sites (6). To get autophosphorylated on Y180 Itk requires a presence of SH2 domain to properly orient the tyrosine residue for phosphorylation. Single SH3 domain cannot act as a substrate for the intact Itk molecule (16). Residue Y180 lies within a hydrophobic pocket in SH3 domain that is conserved among Tec kinases (28). It is believed that phosphorylation of Itk is most efficient when Itk is in dimer conformation, thus making the dimer a possible necessary prerequisite step before activation (6). Y180F mutant partially disables kinase activity, but less so than Y511F mutant in SH1 domain. This points to Y180 being less critical than Y511 in

activation of Itk (9). Even though Y180F mutant does not influence kinase activity of the SH1 domain directly, it displays steric hindrance for the phosphorylation substrates by intramolecularly locking PPR in SH3 binding pocket, and blocks the active center of the kinase domain, thus significantly lowering the rate at which it is able to phosphorylate its substrates (4). Y180E mutation that mimics tyrosine phosphorylation by using acidic residue instead, behaved the opposite way. This mutation caused loss of PPR region binding, and significantly increased binding of SH2 domain of another Itk molecule, thus locking Itk molecules in dimer formation (4).

SH3 domain deletion mutants of Itk demonstrate higher activation than wild type, and point to a negative regulatory function that SH3 domain performs (36). Interestingly, when assessed in model insect cell system, W208K mutant of Itk that disrupts SH3 domain interactions by inactivating key residue in SH3 binding pocket has normal Y511 and Y180 phosphorylation, as well as downstream PLCγ and ERK phosphorylation (9). However, in Itk-/- mouse model W208K mutant showed significantly lower IL-2 production and ERK phosphorylation, in the range similar to Y511F mutant (9).

It turns out that Itk has a complex mode of activation, consisting of two steps before becoming fully activated, first - phosphorylation of Y511 residue by Lck, and then phosphorylation of Y180 by the same Itk molecule (9,4). To become activated, Itk also has to be bound to phosphorylated LAT first (9). Another necessary condition for Itk activation seems to be binding to SLP-76 (35).

In Btk, the function of Y224 (homolog of Y180) appears to be identical to that of Y180 in Itk, with identical mechanisms involved (9). SH3 domain of Btk has similar structure, and can bind canonical PXXP sequence. However, SH3 domain of Btk significantly differs from that of Itk in the backbone structure, and more resembles that of Src and Fyn. Also, it has two alternative conformations in contrast to three in Itk. (37). SH3 domain of Btk was also shown to be involved in forming intramolecular folds and intermolecular dimers. However dimer formation is believed to be caused by canonical sequence binding, unlike that of Itk that relies on noncanonical SH2-SH3 binding for dimer formation (38). Even though Btk SH3 domain exhibits similar mechanism of activation by conformation change - phosphorylation of tyrosine residue Y223 (homologous to Y180 in Itk) leads to release of PXXP substrate (37,39), its interactions with nonconventional ligands should substantially differ, as well as interactions where SH3 domain acts as a ligand.

SH3 domain of Tec was also resolved and showed similar structure and functionality to Btk and Itk SH3 domains with only minor differences - PPR region being more similar to Btk than to Itk (40).

In Src family kinases, SH3 domain plays an important negative regulatory role by binding to PPR region in the linker between SH2 and SH1 domains, and also by providing phosphotyrosine for the SH2 domain to bind preventing Itk activation. In Btk and Itk, the mechanism of activation is cardinally different, and these domains play practically opposite function exerting positive regulatory control. Even though Tec shows similar mechanics to Btk and Itk, its SH3 exerts negative regulation on Tec

kinase activity (40). Similar intramolecular binding was suggested for Btk, and was confirmed in experiments with PPR peptide, PPR mutations, and mutations in Y223, also pointing to Y223 (homolog of Y180 in Itk) playing a regulatory role by destabilizing canonical ligand binding after tyrosine phosphorylation (31,41). Experiments comparing SH3 domains of Itk and Rlk in binding PPR substrates demonstrated that Rlk has a similar dynamic to Itk in terms of intramolecular and intermolecular binding via SH3 domain (42,43).

One of the canonical ligands of Itk SH3 domain is CD28, a co-stimulatory receptor playing a role in T-cell responses. It has a PXXP site on its cytoplasmic region, and Itk was shown to specifically bind to it upon CD28 crosslinking. Binding to CD28 might be a minor pathway leading to Itk pre-activation via bringing it to the signaling cluster near the membrane and facilitating contact with Lck and PIP3 (44).

Binding sites for Itk SH3 domain on SLP-76 are canonical PXXP sequences, and are located close to Y145 residue that serves as binding site for Itk SH2 domain (15), shown in Figure 2C. It is believed that mode of binding – intramolecular versus binding with SLP-76 might be concentration dependent, and a matter of competition for the same binding site in SH3 domain (28,35). When Itk is recruited to the signaling complex, the concentration of SLP-76 is high, and it outcompetes intracellular substrate binding (28,15). SH3 and SH2 domains of Itk are believed to act in concert in SLP-76 binding (15).

TH domain

It was predicted from the NMR and other structural data that most Tec kinases, including Itk, Btk, and Tec are able to form dimers, as well as intramolecular folds. Intramolecular folds with SH3 domains binding conventional substrates are predominantly made possible by binding PRS-1 type PPR regions, and intermolecular associations are more stable by binding PRS-2 type PPR regions. Itk has only one PRS-1 PPR region, which makes dimers by SH3 binding conventional ligands unlikely, while Btk and Tec have both, PRS-1 and PRS-2 regions, and can form dimers with conventional SH3-PXXP binding (40). However, it was shown in experiments with mutations in PRR region of Btk that both, PRS-1 and PRS-2 sites are important for forming dimers, and PRS-1 has an even higher chance of doing so. It was also shown that canonical SH3-TH domain interactions are not the only ones that contribute to dimer formation in Btk, because even with all prolins at binding sites mutated, some Btk still formed dimers. The data also suggested that tyrosine phosphorylation of Y224 (homolog of Y180 in Itk) constitutes a mechanism of activation of this kinase by promoting a release of the PXXP substrate from SH3 binding pocket (45). It is also assumed that the PPR region of Itk might bind SH3 domains of other proteins when not interacting with SH3 domain of Itk (32).

The sequences of Itk PPR regions differ from optimal binding sequences for the SH3 domains, and one of the reasons is the flexibility that switching between intramolecular and intermolecular binding offers compared to one mode of binding (46). Even though in the experiments performed in vitro Itk does have higher activity

because of release of the intramolecular fold when PPR region is deleted or mutated, it shows decreased activity in experiments performed in vivo, which might point to a role PPR region plays in binding some of the Itk signaling partners, presumably facilitating Lck interaction (36).

PH domain

PH domains of various proteins share a common folding structure, and thus bind very similar substrates (47). In Btk, it was shown that PH domain is required for activation (49). Its function is docking the protein to the membrane, switching on autophosphorylation, and allowing phosphorylation by Lyn and Syk (analogs of Lck in B-cells), placing its function upstream of that of SH2 domain (26,48). It is suggested that PH domain of Btk may, along with PH domain of PLCγ, play a role of attaching the whole signalosome to the membrane (26,49). A similar sequence of events and functionality was also proposed to take place in T-cells with Itk and its signalosome partners by analogy with Btk in B cells (26). Experimental data confirmed these assumptions, as indeed, PH domain of Itk demonstrated involvement with Itk recruitment to the membrane (50,51).

Previous studies already showed that there is a possibility of PH domains being responsible for Itk dimerization, as disabling SH2 and SH3 interactions did not completely abrogate dimerization (28). Deletion or certain mutations of Itk PH domain do not have a negative influence on kinase activity of Itk *in vitro* (4), but disrupt Itk function in vivo (52,51,15). Interestingly, deletion of the PH domain causes Itk to have spontaneous enzymatic activity *in vitro* which might suggest that PH domain is shielding the active center of the kinase domain when Itk is not activated (49). It was demonstrated that Itk lacking PH domain is not capable of localizing to the cell membrane, and neither does it get phosphorylated. If the Itk lacking PH domain is supplemented with another means of getting targeted to the membrane, it still does not

recover inducible activation, which suggests PH domain role in activation above that of simple membrane targeting facilitator (51).

PH domain can bind either proteins or inositol compounds that have phosphorylated D-3 position (52,49). Among different protein substrates that PH domains of Tec kinases were shown to bind are PKC, Actin, and βγ-subunits of G proteins (52,53).

As far as PI3K generates inositol compound that has phosphorylated D-3 position, it takes an active part in regulating Itk PH domain targeting to the membrane, and ultimately, Itk activity (52,49). Inhibition of PI3K function by Wortmannin disrupts Tec kinase function by preventing recruitment of PH domains to the membrane via blocking PIP3 production (52). Apart from PIP3, another compound that has affinity to PH domains is IP4, which was shown to be necessary for Itk recruitment to the membrane (49). Neither PIP3, nor IP4 are necessary for Itk function in vitro, which suggests that their function is sole recruitment of Itk to the signaling complex at the membrane (49). IP4 augments PIP3 binding, and it is believed that it promotes PH domain conformation with high affinity to both, PIP3 and IP4, and in physiologic conditions in vivo gets replaced by PIP3 at the membrane due to high concentration of PIP3 there. IP4 binding might also have a synergistic effect on conformation of other PH domains, which might be in the multimer with PH domain that bound IP4 (49).

In Btk, a PH domain mutation R29C disrupts signaling function of Btk (52), and was found both in human (Bruton's agammaglobulinemia) and mouse (Xid)

disease (52,54). Another mutation of Btk PH domain E41K increases phosphoinositol binding and makes Btk hyperactive in vitro (52,47). However, similar mutation in related kinases Bmx and Tec decreases their activity (52). Mutations of PH domain R29C and F26S are notable for being discovered in disease phenotype in Btk in mice and in humans (54,55). They all have defects of different severity in phosphoinositol binding in Btk, and also show a similar picture in Tec and Itk (54). F26S mutation is believed to disrupt the binding pocket for PIP3, but not the structure of the whole domain (55).

PH domains of Tec kinases have a characteristic motif (FYF motif) consisting of F25 (F26 in Itk), Y112 (Y90 in Itk), and F114 (F92 in Itk), and which is believed to be in the phosphoinositol binding pocket and is relevant to PIP3 binding (55).

Proteins involved in Itk signaling

There are multiple proteins involved in the signaling cascade launched by TCR/CD28 stimulation signals. General summary of the main proteins involved, interactions between them, and regulatory phosphorylation sites in the phosphorylation cascade are displayed in Figure 3. The following subsections contain a brief overview of these individual proteins in relation to Itk signaling.

PLCγ

PLCγ is an important signaling protein in calcium signaling path. It needs to be phosphorylated by both, Itk and a Syk kinase (ZAP-70) on two different sites to become active (26). In case of Btk, phosphorylation of PLCγ requires intact PH and SH2 Btk domains (26). Also, it was shown that PLCγ interacts with Syk and can get phosphorylated by Syk on multiple tyrosine residues (56). LAT serves as a recruitment site for PLCγ, which binds to phosphorylated Y132 residue of LAT (57). PLCγ contains five tyrosine phosphorylation sites, but only Y775 and Y783 are important for the activation (57).

Phosphorylation of Y783 residue of PLCγ is performed by Itk SH1 domain in a similar way to SH2 Itk autophosphorylation. Interestingly, the flanking aminoacids of these two phosphorylation sites are very different, and do not have common or homological sequences. It was shown that this is possibly due to SH2 domains of substrate Itk and PLCγ molecules exhibiting docking function, allowing the correct exposure of the phosphorylation site to active site of the Itk kinase domain (16).

Figure 3. Schematic representation of phosphorylation signaling cascade downstream from TCR/CD28 stimulation that controls Th2 cytokine production.

Phosphotyrosines are marked with red stars. Tyrosine phosphorylation interactions are marked with red lines, other interactions are marked with black lines. Phosphorylation events by the same protein are marked with the same line style. Proteins that are known to directly bind to each other are shown as overlapping.

*The figure is highly schematic. Sizes and shapes are not in proportion with real sizes and shapes of the proteins and cell components. Location of the phosphorylation sites is also highly schematic and does not reflect their precise location on real protein structures.

‡For the simplicity purposes the figure represents major, but not all interactions between the proteins in signaling cascade (for example, CD28 binding to Itk is not shown).

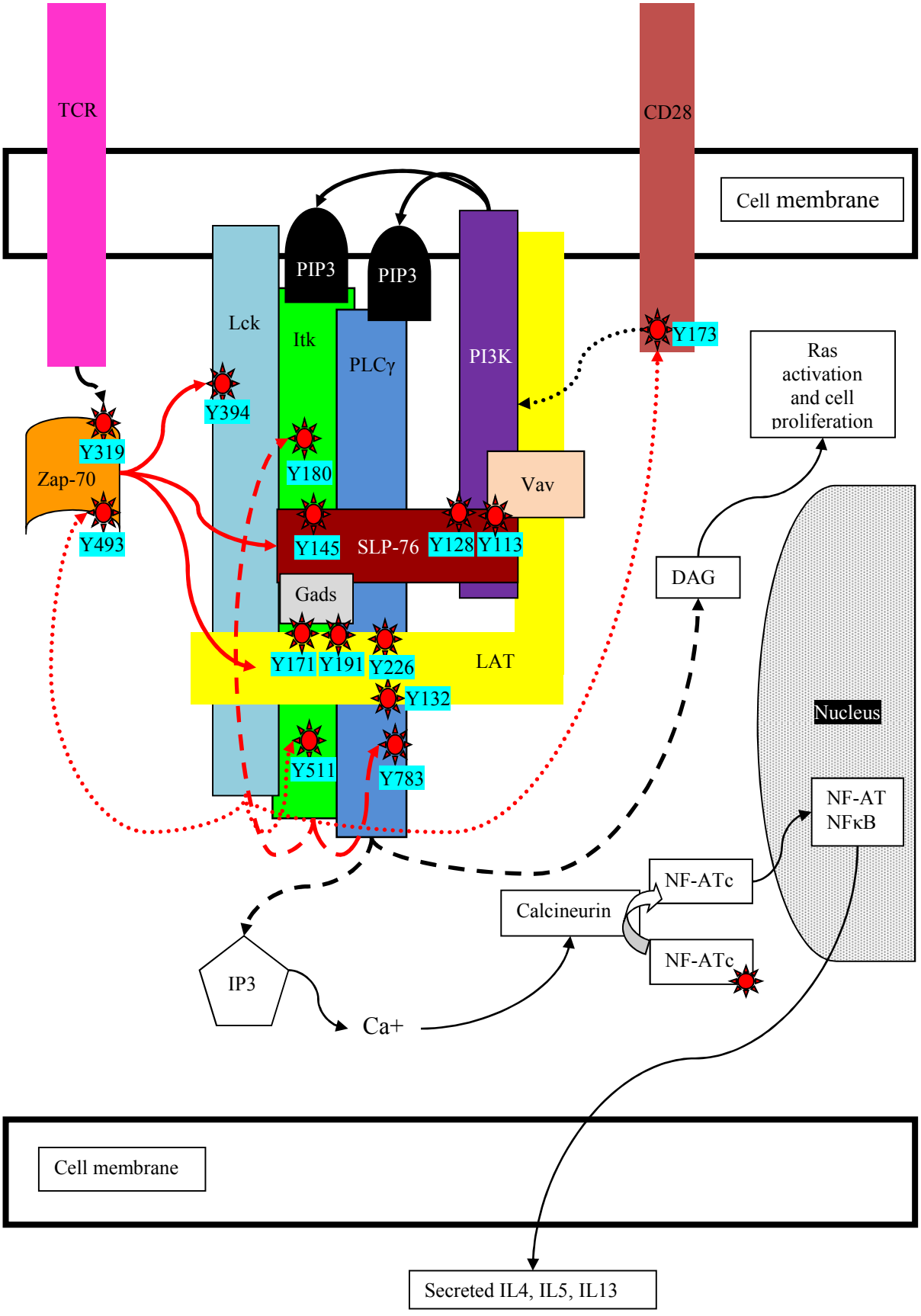
TCR
CD28
Cell membrane
PIP3
PIP3
Lck
Itk
PLCγ
PI3K
Y173
Ras activation and cell proliferation
Y394
Y319
Zap-70
Y493
Y180
Vav
Y145
SLP-76
Y128
Y113
Gads
DAG
Y171
Y191
Y226
LAT
Y132
Nucleus
Y511
Y783
NF-AT NFκB
NF-ATc
Calcineurin
NF-ATc
IP3
Ca+
Cell membrane
Secreted IL4, IL5, IL13

Activated PLCγ enzymatically breaks PIP2 producing IP3 and DAG (58). This initiates Ca^{2+} release by IP3 interacting with CRAC channels and activation of PKC and Ras that get activated upon interaction with DAG (57). Ca^{2+} release ultimately leads to activation of nuclear transcription factors, such as NFAT and NFκB (59). The cellular version of NFAT gets dephosphorylated upon binding of Ca^{2+}-calcineurin complex, and becomes a nuclear version upon translocation to the nucleus, where it binds specific promoter regions, including those involved in interleukin production (60).

Lck

Lck belongs to a family of Src kinases and becomes activated at the early stages of TCR signaling (61). Lck SH2 domain has an affinity toward binding ZAP-70, and can phosphorylate it (26). Lck as well phosphorylates Y511 of Itk and activates it (4,62). Another target for enzymatic activity of Lck is Y173 in CD28, which in phosphorylated form is necessary for PI3K binding (44).

Zap-70

Zap-70 belongs to a family of Syk kinases, and is recruited by the ITAMs in TCR complex, where it is phosphorylated by Lck on Y493 (61,63). Even though Syk kinases do not directly phosphorylate Tec kinases, they promote their recruitment by phosphorylating adaptor proteins that Tec kinases bind, thus bringing them to the area that is saturated with Src kinases that directly phosphorylate Tec kinases, and is also saturated with Tec kinase substrates, like PLCγ (15). Zap-70 phosphorylates multiple intracellular targets upon activation, among them LAT, SLP-76 (4), and PLCγ (61). Recruitment of ZAP-70 is one of the early events following the TCR stimulation, and reaches its maximum less than a minute after stimulation (15).

SLP-76

SLP-76 is an adaptor protein in T-cells homologous to SLP-65/BLNK in B-cells (26). It consists of SH2 domain, SH3 domain, and N-terminal domain that houses phosphotyrosine sites (64). It also plays a role in the activation of PI3K by binding its regulatory p85 subunit. This requires SLP-76 phosphorylation and localization to the membrane. After this binding, the catalytic subunit of PI3K p110 is activated and produces PIP2 and PIP3 that play a critical role for membrane recruitment of proteins with PH domains (64,53).

It was proven that SLP-76 binds to Itk SH2 domain and contains a peptide that is binding to the pY and pY+3 sites in *trans* P287 Itk SH2 domain (26,65). The binding is direct, and shows the same mechanism as binding of SLP-65/BLNK to Btk SH2 domain. In fact, isolated SH2 domains of these proteins were used interchangeably to pull respective SLP phosphoproteins out of cell lysates via GST pull-downs (26). This interaction between Itk/Btk SH2 and SLP-76/65 is very selective. Other SH2 domains (like that of Lck) do not have specific affinity to SLP-76, and bind to their substrates with less selectivity (26).

In experiments with SLP-76 mimicking polyproline rich peptide, it was also shown that SLP-76 interacts with SH3 domain of Itk (35). The peptide blocked this interaction, preventing the binding of SLP-76 to Itk, and also preventing Itk phosphorylation on Y511 residue, and as a result, disrupting Itk signaling (35). Together with LAT and PLCγ, SLP-76 forms a signaling complex in T-cells (26,15,66) that was shown to influence specifically PLCγ phosphorylation, which is

greatly reduced in SLP-76 deficient cells (67). The sites that bind to Itk SH2 domain on SLP-76 are phosphorylated by ZAP-70, facilitating the interaction between Itk and SLP-76 (15). Phosphorylation on tyrosine residues Y113, Y128, and Y145 is required for SLP-76 activity (15,64). This phosphorylation occurs at the immunological synapse during T-cell-APC interaction (64). Y145 is the residue that when phosphorylated, interacts with SH2 domain of Itk, and it seems to be the most important phosphorylation site involved in SLP-75 signaling (15,68). Tyrosine residues Y113 and Y128 are required for p85 binding and also modulate the signal from TCR stimulation (64,68). Y113 residue is important for p85 activation, but not by direct binding, but by a proxy of another adaptor protein Vav that binds both, SLP-76 and p85 (64).

LAT

LAT is an adaptor protein that gets phosphorylated on multiple tyrosine residues by ZAP-70 under TCR stimulation. It serves as an assembly backbone for many signaling proteins involved in TCR signaling that helps them localize and stay around the contact site (69,70).

To become activated, LAT needs to get palmytoilated (69,71,72). After this modification, it goes to the membrane and localizes at lipid raft areas (71). LAT forms the basis of the signalosome by binding adaptor proteins like SLP-76 and Vav either directly (70), or through other adaptor proteins (64). Tyrosine phosphorylation on Y171 and Y191 is required for LAT functionality (64). However, there are other residues that also take part in kinase recruitment to LAT (73).

LAT was shown to be required for the localization of SLP-76 (64,15) and PLCγ (66). LAT also colocalizes with TCR/CD3 upon activation (27). It was demonstrated that LAT is critical for inducible Itk activation. It is believed that there are several direct and indirect (facilitated by adaptor proteins like Grb-2 and Gads) binding interactions between LAT and Itk (15,74). Experiments with LAT-deficient cell lines show that Itk cannot be activated there. However, activation is rescued by transfection of transgenic LAT (27). Moreover, it was shown that LAT binding to Itk depends on Itk SH2 domain (27).

TCR/CD3 and CD28

TCR is a receptor complex, consisting of several signaling proteins that have ITAM sequences on their cytoplasmic portions (61). Src kinases phosphorylate ITAMs under receptor stimulation (15). After this event, ITAMs recruit a myriad of nonreceptor tyrosine kinases of Src, Syk, and Tec families, which in turn transfer and amplify the signal further (61). Syk kinases bound to phosphorylated ITAMs get phosphorylated and activated by Src kinases (15). CD28 mainly acts as a costimulatory receptor for the TCR complex (61,44).

TCR and CD28 are both required for complete T cell activation (44), and have synergistic effect on crosslinking (61,75). These two receptor molecules are acting as elements of a single signaling complex, and it is known that CD28 can bind TCR ζ-chain (44,61). CD28 was shown to be capable of binding Itk, and can play an accessory function in Itk activation (44,76). Also CD28 is involved in PI3K activation by providing a phosphotyrosine binding site for SH2 domain of PI3K (as shown in Figure 3), and in this way is performing an additional activation step that facilitates generation of PIP3 and thus recruiting Itk PH domain to the membrane (44).

Functional role of Itk

ITK-deficient mice ($Itk^{-/-}$) show decreased phosphorylation of PLCγ, and Th2 cytokine production (5,9,77). They also show a decrease in IL2 production (9,77), developmental deficiencies in Th2 development, and peripheral immune response (5). $Itk^{-/-}$ cells show defects downstream from PLCγ phosphorylation that can be overcome by using a PMA/ionomycin combination, which directly influences Ca^{2+} signaling and avoids the amplification pathway that goes through kinase cascade that involves SLP-76-LAT signalosome including Itk and PLCγ (78).

Because of the direct effect of Itk on PLCγ, it plays a role in Ca^{2+} signaling, and $Itk^{-/-}$ cells remind cells where calcineurin is disabled by addition of inhibitors (79). However, the negative effect of $Itk^{-/-}$ on Ca^{2+} signaling, though drastic, is not complete, which suggests that Itk only plays an amplification role (79).

Tec family kinase Rlk was shown to play a role in PLCγ1 phosphorylation, and production of IL-2 and IFNγ in T cells, thus overlapping in function with Itk. However, they differ in IL-4 production, which is believed to be more influenced by Itk (52). Rlk is believed to be downregulated in Th2 cells, but upregulated in Th1 cells, opposite from Itk, while both of them are at similar levels in undifferentiated Th0 cells (52). There is also evidence that other Tec kinases can have functions that duplicate Itk and Rlk, to some extent (52). Even though it was not shown directly that Rlk phosphorylates PLCγ, and $Rlk^{-/-}$ cells have normal PLCγ phosphorylation, it was shown that in double knockouts, $Itk^{-/-}Rlk^{-/-}$ PLCγ phosphorylation is impaired more than in $Itk^{-/-}$ single knockouts (78). Also another hint at the role of TEC kinases in

Ca^{2+} signaling is that cells deficient in Itk or Tec have impaired NFAT activation (80,81), which depends on prolonged Ca^{2+} signaling (82). Another product of PLCγ activity is DAG that activates Ras-GRP in T-cells and leads to Ras/MAPK pathway activation (83).

Itk in T-cell development

It was shown that Itk plays a role in positive selection in CD4 cells, as cells from $Itk^{-/-}$ mice were less efficient at this process (84). $Itk^{-/-}$ thymi tend to have slightly decreased numbers of $CD4^+$ SP cells, and increased numbers of $CD8^+$ SP cells (84). It seems like the absence of Itk affects early stages of CD4+ cell development causing lower numbers of single positive cells to form. However, those that did form, seemed to be normal (84). It was demonstrated that absence of Itk diminishes the efficiency of negative selection (85). Itk is important in CD4 helper cell development and is believed to play a significant role in Th2 type cell differentiation (81,86,87). It was shown that Itk deficient cells have disrupted IL4 production (84). One of the aspects of Th2 response that is disrupted in $Itk^{-/-}$ mice is the response to parasitic infection (78,88). Another aspect is disrupted response to Ova-induced asthma (89).

It was shown that Itk and Rlk are important for development of conventional $CD8^+$ cells, and knockouts almost completely lack them (90). Itk also plays a significant role in development of conventional αβ CD4 and CD8 cells (91,92). $Itk^{-/-}$ cells lack conventional CD8 cells, but have large numbers of innate-like CD8 cells that have memory markers and express IFNγ (93,94). It is believed that Itk plays a role in inhibiting selection that allows development of conventional cells (93). $Itk^{-/-}$ thymi also develop large numbers of CD4γδ cells, which can produce Th2 cytokines and stimulate excessive production of IgE by B cells (92,95).

$Itk^{-/-}$ mice show defects in CXCL12 chemokine induced T-cell recruitment to the lungs (96). Similarly, Jurkat cells expressing inactive Itk mutants showed reduced CXCL12 induced activation of CDC42 and RAC (97).

It was shown that Itk expression can be activated by binding GATA3 to the DNA region close to the Itk enhancer (87), and that GATA3 expression can't be sustained for a long time in $Itk^{-/-}$ cells (86). Also, Itk plays a role in downregulation of T-bet, as $Itk^{-/-}$ cells have higher T-bet levels under stimulation (87). It was also shown that in low-level stimulation, $Itk^{-/-}$ lymphocytes behave differently than wild type - they undergo Th1 differentiation instead of Th2 (87).

It was shown that Itk-/- cells can differentiate into either Th1 or Th2, and also keep the correct proportion between Th1 and Th2. However, they are severely deficient in functionality of the Th2 cells that formed, which results in decreased production of IL4 – a signature Th2 cytokine (86).

Clinical implications of Itk

In $Itk^{-/-}$ mice, symptoms of asthma are greatly reduced after sensitization compared to a wild type mouse (89). They show reduced inflammation, T cell proliferation, and reduced T-cell infiltration, as well as reduced Th2 cytokine production (89). This, in turn, leads to reduced airway hyperresponsiveness, preventing the symptoms of asthma (100). It was also demonstrated that in order to exhibit asthma symptoms, Itk has to be kinase active, as mice possessing kinase inactive Itk do not exhibit asthma symptoms after sensitization (101). However, it is worth noting that different strains of mice – BALB/c versus C57BL/6 have different susceptibility to sensitization, and thus a different propensity to develop asthmatic response (102).

Mouse models of asthma show that this disease is dependent mostly on IL4 and IL13 – Th2-type cytokines (98), even though Th1 cytokines are also important (99). Asthmatic response in this model is caused by sensitization with OVA while in natural environment, it is caused by exposure to bacterial LPS (99). It turns out that there are two types of asthma, depending on the amount of LPS in the exposure – low amounts cause type 2 response, while low dose causes type 1 (99).

Even though Itk is well known for its role in artificially induced asthma in the mouse model (103), it was also shown that certain forms of asthma in human patients are a result of mutation in Itk promoter, as this mutation occurs significantly more often in asthmatics than in healthy people (104). Several groups are developing Itk

inhibitors (mainly kinase domain inhibitors) for possible use in asthma treatments (105,106).

Among the diseases that might be related to abnormalities of Itk function are dermatological diseases, such as atopic dermatitis and psoriasis. They are believed to have excess T cell activation directly related to Itk hyperfunction (107).

An interesting observation about the clinical implications of related protein Btk is that its mutations have a specific phenotype XLA, which is a human disease characterized by low levels of circulating B cells and low immunoglobulin in blood serum (47). In Btk, there are mutations in all of the domains that can cause XLA (37,108). These mutations disrupt Btk function, and result in developmental defects in B cell lineage (47). Mice have a similar disease called XID (55). Most clinically relevant XLA mutations are in PH domain (47). Some of them disrupt folding of the PH domain, like T33P or V64F, others affect binding site for PIP3, like F26S (47). R29C and R29H, however, are believed to disrupt protein binding by PH domain (47,55). There are no known analogs of XLA or XID in relation to Itk, which might point at differences in their functional pathways in T and B cells.

Another mutation linked directly to human disease was discovered in SH2 domain of Itk. Patients had severe complications and defective immune regulation, which manifested itself under EBV infection and proved to be lethal. This mutation R335W is a mutation of a conservative residue that disrupts SH2 folding (109).

Not only point mutations, but also translocations and fusions of Itk molecule were studied as underlying cause of human disease. Itk and Syk fusion protein is known to cause T-cell lymphoma (110).

Yet another interesting connection of Itk with disease is depletion of $CD4^+$ cells in AIDS. It was shown that Itk might be a major factor in HIV particle replication in $CD4^+$ cells, and blocking Itk with inhibitors reduces HIV replication rate (111). Itk also seems to play a role in viral entry due to actin polarization role and in transcription from HIV LTR due to Itk involvement in NFAT activation (112). It was shown that inactivating Itk lowers p24 levels, and decreases the speed of viral production in the cell culture (112).

Because of the increased number of innate $CD8^+$ cells, $Itk^{-/-}$ is more efficient at clearing some parasitic infections (94). Another interesting aspect is because $Itk^{-/-}$ cells are defective in Th2 development and responses, they don't easily develop Th2-dependent asthma (94).

It was noted that Itk plays a role in eliminating viral infection based on studies of $Itk^{-/-}$ mice that demonstrated reduced antiviral response and reduced viral clearance for some virus infections (113). This effect seems to be cytokine-dependent, as addition of cytokines rescued the functional deficiency (113).

MATERIALS AND METHODS

Antibodies

Phosphoflow antibodies against pItk pY511 clone 24a/BTK, pPLCγ1 pY783 clone 27/PLC and pZAP-70 pY319 clone 17A/P-ZAP70 were labeled with Alexa 647 and obtained from BD Biosciences, San Diego, CA. Anti-Itk IP antibody (rabbit polyclonal), anti-Itk blotting antibody clone 2F12, anti-phosphotyrosine antibody clone 4G10, anti-LAT antibody clone 2E9, and anti-SLP-76 antibody clone AS55 were ordered from Upstate (now division of Millipore). Anti-GFP antibody clone 7.1 was ordered from Roche, Indianapolis, IN. Anti-mouse CD3e and anti-mouse CD28 antibodies were ordered from BD Pharmingen, San Diego, CA. Dy405 conjugated anti-golden Syrian & Armenian Hamster antibody was purchased from Rockland, Gilbertsville, PA. Goat anti-Armenian Hamster antibody was purchased from Jackson ImmunoResearch, West Grove, PA.

Chemicals and reagents

Chemicals were ACS Grade from Fisher Scientific, Hampton, NH unless otherwise specified. Molecular biology reagents were Molecular Biology Grade from Sigma, St. Louis, MO unless otherwise specified. Also, the following reagents were used: BSA (Fraction V, Calbiochem, San Diego, CA), Acrylamide (HPLC grade, Sigma, St. Louis, MI).

Cell lines

Jurkat clone JTag cells (a kind gift of Dr. Altman, La Jolla Institute of Allergy and Immunology, La Jolla, CA) and Raji cells (a kind gift of Dr. Kathy McGuire, San Diego State University, San Diego, CA) were cultured in RPMI 1640 (supplemented with 10% serum, 0.2 M Glutamine, 100U/ml penicillin, 100µg/ml streptomycin, 20mM HEPES) in 37^{o}C humidified incubator with 5% CO_2 atmosphere.

Mouse thymocyte nucleofection

Thymocytes were isolated from thymi of wild type (C57BL6, from Jackson Laboratories, Bar Harbor, ME) or Itk$^{-/-}$ mice (bred on C57BL6 background, a kind gift of Dr. Littman, New York University School of Medicine, New York, NY) 6-12 weeks of age by separating cells through nylon mesh. Cells were nucleofected using Amaxa Nucleofector II machine with 10µl of 1.5 µg/ml DNA solution in Tris-EDTA buffer following manufacturer's instructions, and after transfection cultured in proprietary Lonza Nucleofector medium, supplemented with 10% FCS in 37^{o}C humidified incubator with 5% CO_2 atmosphere.

Skewing and cytokine production

The method uses amended combination of the skewing methods described in the literature (81,86,87,114). Thymocytes were collected 4 hrs after Nucleofection, counted, resuspended 2x10^{6} cells per ml in Lonza Medium supplemented with 1 µg/ml αCD28, 20 µg/ml αIL12, 10% serum, 0.2 M Glutamine, 100U/ml penicillin, 100µg/ml

streptomycin,, and transferred 200,000 cells per well into 96-well U-bottom plates coated with αCD3ε. Plates were placed in 37^{o}C humidified incubator with 5% CO_2 atmosphere overnight. Next day cells were supplemented with 5 ng/ml IL2 and 10ng/ml IL4. After 2 days cells were pelleted, resuspended in fresh RPMI 1640, supplemented with1 μg/ml αCD28, 10% serum, 0.2 M Glutamine, 100U/ml penicillin, 100μg/ml streptomycin, 20 mM HEPES,, and transferred into 96-well U-bottom plates coated with αCD3ε. After 24 hrs supernatants were collected and assayed for cytokine content using commercially obtained kits from eBioscience. IL13 detection range was 31-2,000 pg/ml, IL4 and IL5 detection range was 8-500 pg/ml (as defined by the range of concentrations used by us when building manufacturer-suggested calibration curve).

Conjugate formation

Raji cells were stained with Cy5-ester (Amersham Cy5 Mono-Reactive dye pack by GE Healthcare), washed several times with PBS, and preloaded with 10μg/ml SEE (Toxin Technology, Sarasota, FL) in RPMI 1640 medium for 2 hours in 5% CO_2 atmosphere at 37^{o}C. After SEE loading, 1M Raji cells were mixed with 1M transfected JTag cells in 400 μl RPMI 1640 medium in Eppendorf tubes on ice (4^{o}C). Then the mixture was pelletted at 200G for 5 min, half of the supernatant was discarded, and cells were resuspended in leftover supernatant. Tubes were transferred to 37^{o}C waterbath for 3 min, and then immediately fixed with equal volume of 4%

paraformaldehyde in PBS for 10 min. Contents of the tubes was pelletted, and washed with PBS, then resuspended in 40 µl PBS, and mounted on two microscopy slides.

DNA constructs

Constructs were designed using Vector NTI 10 Software (Invitrogen, Carlsbad, CA). Template CY construct was designed by Ritz Zhang (San Diego State University, San Diego, CA) from CMV pEYFP-N1 and CMV pECFP-C1 vectors (both from Clontech, Mountain View, CA). pME vectors were designed on the basis of pME18S-FL3 Itk-GFP vector, previously described in (51). For growing vectors, subcloning efficiency E.coli DH5α strain (Invitrogen, Carlsbad, CA) was used. For growing non-CpG methylated DNA, E. coli strain GM2163 (Fermentas, Vilnius, Lithuania) was used. DNA for primary cell transfections was purified with endotoxin-free purification kits (MaxiPrep, Qiagen or MaxiPrep, Macherey-Nagel, Bethlehem, PA), following manufacturers' instructions. DNA for subcloning and cell line transfections was purified using Wizard preps (Wizard PCR Preps DNA purification system, Wizard MiniPrep DNA purification system, and Wizard MegaPrep DNA purification system, all from Promega, Madison, WI) following manufacturer's instructions. For restriction digests and backbone dephosphorylation restriction enzymes and Antarctic phosphatase were used respectively (all from New England Biolabs, Ipswich, MA) following manufacturer's recommendations. For ligation, T4 DNA Ligase (New England Biolabs, Ipswich, MA) was used following manufacturer's recommendations.

Site-Directed Mutagenesis

Template DNA molecule was methylated using CpG Methyltransferase (M.SssI, New England Biolabs, Ipswich, MA) following manufacturer's recommendation. Then PCR was performed using forward and reverse primers (synthesized by Invitrogen, Carlsbad, CA) and Platinum Blue PCR SuperMix (Invitrogen, Carlsbad, CA) or HiFi Taq Polymerase (Invitrogen, Carlsbad, CA), following manufacturer's recommendations on Eppendorf Mastercycler Gradient PCR machine (Eppendorf, Hamburg, Germany) following manufacturer's instructions. List of primers is located in Appendix 2. List of primers used for subclonings and site-directed mutagenesis. Mutants were constructed in collaboration with Nupur Hirve, Jason Rudy, Roma Munday, and Alexa Spilsbury (all from San Diego State University, San Diego, CA). Wild type Itk-GFP, K390R, and R29C mutants were subcloned from original vectors designed by Dr. Keith Ching and Dr. Juris Grasis (San Diego State University, San Diego, CA). W208K mutant was subcloned by David Guimond (San Diego State University, San Diego, CA) from a vector created by Dr. Juris Grasis (San Diego State University, San Diego, CA).

Microscopy and FRET analysis

Microscopy was performed using Zeiss AxioVision Imaging System (Carl Zeiss, New York, NY) with 0.5 Neutral Density filter and . Morphological conjugates were selected by DIC using stable conjugate criteria by Montoya et al. (115) and imaged with CFPex-CFPem, YFPex-YFPem, CFPex-YFPem, and Cy5ex-Cy5em filters as described in (116,117). For image analysis a plugin was written in Java

(source code shown in Appendix 4. Source code of ImageJ plugin) for ImageJ image analysis software package (NIH, Bethesda, MD). Before analysis images were aligned by vector-spline regularization using TurboReg plugin for ImageJ.

Localization index was calculated as a ratio between YFP intensity at proximal to the APC site of the T cell versus YFP intensity at the opposite end of the T cell as described in (51).

Immunoprecipitation and Western Blotting

Twenty million cells were lysed on ice in 500 µl of lysis buffer (1% NP-40, 20 mM Tris, 0.4 mM EDTA, 150 mM NaCl, 5µg/ml leupeptin, 5 µg/ml pepstatin A, 1µM sodium orthovanadate, 1 µM PMSF) for 1 hr, then lysate was pelleted at 14,000 rpm in a microcentrifuge at 4^{o}C for 20 min. Ten microliters of the lysate was aliquoted into a separate tube to be used as a control, the rest of the supernatant was transferred into new Eppendorf tube, supplemented with IP antibody (amount varied per manufacturers recommendation), and left tumbling overnight at 4^{o}C. For immunoprecipitations, the following antibodies were used: Anti-Itk (rabbit polyclonal, Upstate, Temecula, CA). Next day tubes with immune complexes were supplemented with 20 µl of Protein G Sepharose (GE Healthcare, Little Chalfont, Buckinghamshire, UK), and tumbled for 2 hrs at 4^{o}C. After this the pellet was washed several times with lysis buffer, and proteins were denatured by boiling in Laemmli buffer for 5 min. Proteins were resolved by SDS-PAGE gels (6%, 7.5% or 9% depending on the size of the target protein), and transferred into PVDF membrane (Pall Life Sciences, Port

Washington, NY). For western blotting, the membrane was blocked with 5% BSA in TBST for 1 hr, washed several times with TBST, then exposed to primary antibody for 1 hr, washed several times with TBST, exposed to secondary antibody for 30 min, and washed several times with TBST. For band detection, SuperSignal West Pico Chemiluminescent Substrate (Pierce, Rockford, IL) or WEST-Easy western blotting detection system (Nacalai USA, San Diego, CA) were used following manufacturers' recommendations. The signal was captured by scientific grade photo film (Kodak, Rochester, NY) in a series of exposures. For blotting, the following antibodies were used: Anti-Phosphotyrosine (clone 4G10, Millipore, Temecula, CA), Anti-LAT (Upstate, Temecula, CA), Anti-Itk (clone 2F12, Upstate, Temecula, CA).

Fold increase was established by calculating experimental signal to loading ratio for each lane, and then dividing stimulated lane ratio over respective nonstimulated lane ratio.

Stimulation for phosphoflow

Technique is a modified version of protocols described in the literature (118).

Thymocytes 24 hr after transfection were collected, spun down, and resuspended in 500µl ice cold RPMI 1640 medium containing Armenian Hamster anti-mouse αCD3ε (BD Pharmingen) for phosphoflow or Armenian Hamster anti-mouse αCD3ε and Syrian Hamster anti-mouse αCD28 (both from BD Pharmingen) for ICCS. After 1hr cells were washed with RPMI 1640 medium, then resuspended in 500µl of fresh ice-cold RPMI 1640 medium containing premixed cocktail of Goat

anti-Armenian Hamster antibody (Jackson ImmunoResearch, West Grove, PA), and Goat Anti-Armenian & Syrian Hamster Dy405 antibody (Rockland, Gilbertsville, PA) in 1:7 proportion. After 30 min on ice, samples were transferred to 37^{o}C waterbath for 1 min, and then immediately fixed in 2% paraformaldehyde for 10 min.

Stimulation for western blotting

Jurkat cells were resuspended in RPMI-1640 medium at 5x106 cells per ml, supplemented with 5μg/ml OKT3 antibody, mixed, and held on ice for 1 hr. Then cells were pelleted, washed three times with ice-cold RPMI-1640 medium, supplemented with 5μg/ml rabbit-anti-mouse antibody, and held on ice for 30 minutes. After this, cells were transferred to 37oC for 1 minute. Then cells were pelleted, and resuspended in ice cold NP-40 lysis buffer supplemented with 1μM leupeptin, 0.1μM aprotonin, 1μM pepstatin A, 1mM PMSF, and 0.5μM sodium orthovanadate.

Phosphoflow

Phosphoflow protocol was a modification of previously published methods (119,120). After stimulation cells were fixed in 2% paraformaldehyde for 10 min, then they were pelleted down in U-bottom flow cytometry tubes, and supernatant was discarded. Next the pellet was resuspended by vortexing, and then resuspended in 1 ml of ice cold 95% methanol. Sample was stored in 4^{o}C overnight. Next day cells were washed several times in 3 ml of FACS buffer (0.5% BSA in PBS), blocked for 1 hr with 110μg/ml Mouse IgG, and stained with respective anti-phosphotyrosine antibody

(mouse anti-Btk-p551, mouse anti-ERK1/2-p202/204, mouse anti ZAP-70-p319, mouse anti-PLCγ1-p783) for 1hr at room temperature. All phosphoflow antibodies were BD Phosflow antibodies from BD Biosciences, tagged with Alexa 647 or PE-Cy7. Then cells were washed in FACS buffer several times, and resuspended in 200 µl FACS buffer for measurement on FACS Aria (BD Biosciences). Mouse IgG1 fluorescence controls from BD Bioscience were used as isotype controls.

Flow cytometry analysis

Data acquired from flow cytometry was analyzed using BD FACS Diva 4.0 (BD Biosciences, San Diego, CA) and FlowJo 7 (FlowJo Software, Ashland, OR) software.

Cytokine production by ELISA

Total cytokine production was determined in original and serially diluted supernatants using ELISA kits (IL-4 and IFNγ by BD Biosciences, San Diego, CA; IL-5 and IL13 by eBioscience, San Diego, CA) and following manufacturer's instructions. The product was measured in 96-well ELISA plates (BD Biosciences, San Diego, CA) on eMax Precision Microplate Reader (Molecular Devices, Sunnyvale, CA) using SoftMax Pro v5.0 software.

Statistical analysis

Statistical analysis was performed using Excel 2007 (Microsoft, Seattle, WA), GraphPad Prism 4.0 (GraphPad Software, San Diego, CA), and SigmaPlot 10.0 (Systat Software, Chicago, IL).

RESULTS

Itk constructs

Several Itk fusion constructs were designed in order to visualize Itk, and gather insights about its structure. Mutants of different domains of Itk were designed on the basis of the information available from the literature that were known or were predicted to completely or partially disrupt one or more Itk functions (available mutants are summarized in Table 1).

Table 1. List of Itk mutants available in different vectors (pME-CY for studies in JTag cells, and CMV-GFP for studies in primary $Itk^{-/-}$ cells)

	Mutant	pME CY	CMV GFP	Affected Domain
1	F26S	+	+	PH
2	R29C	+	+	PH
3	Y90F	+	+	PH
4	F92S	+	+	PH
5	PPR1	+	-	PPR
6	PPR2	+	+	PPR
7	Y180E	+	+	SH3
8	Y180F	+	+	SH3
9	W208K	+	+	SH3
10	R265K	+	+	SH2
11	P287G	+	+	SH2
12	K390R	+	+	SH2
13	Y511F	+	+	SH1
14	Btk-SH3	+	+	SH3
15	Btk-PPR	+	-	SH3 + PPR
16	Y180E-P287G	+	+	SH3 + SH2

Two different vectors were used as the backbone for the construct: pME vector under SRα promoter, and pECFP/pEYFP vectors under CMV promoter. SRα based vectors allow high expression of the protein of interest in cell lines containing large T

antigen as a transgene (121), and CMV vectors allow efficient expression of protein of interest in primary cells (122).

Out of all mutants that were constructed, three turned out to be particularly interesting. These were the BtkSH3 mutant, Y511F mutant, and FYF mutant. BtkSH3 mutant is an Itk molecule with SH3 domain from related kinase Btk. It was predicted that this mutant would prevent Itk SH3 interactions with SH2 domain of other Itk molecules, as well as interaction with other Itk signaling partners. There was some information available on this mutant derived from in vitro structural studies (34,24). Y511F mutant has phenylalanine substitution in place of the tyrosine that serves as an activation trigger for Itk after Lck phosphorylates Y511 site, which is located in the activation loop of the kinase domain of Itk (62). This mutant was known to disable some of the Itk functionality (9), even though it did not disrupt the kinase domain activity by itself (8). FYF mutant was constructed in our lab based on the presumed role of the FYF motif in PH domain of Itk (47). This motif was thought to be important in recognizing PH domain substrates, targeting Itk to the membrane, and possible influence on overall Itk functionality.

Biochemical properties

All constructs were assessed for expression (Figure 4) to make sure that cloning was performed successfully and did not involve frame shift or other design flaws. All constructs showed predicted correct size on western blots, and were detected by anti-Itk antibody.

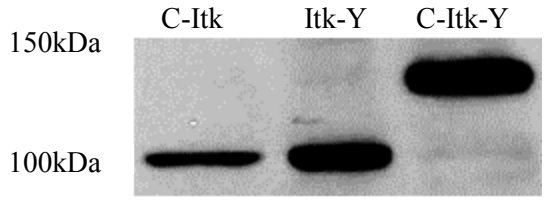

Figure 4. Wild type construct expression.
Sample expression of wild type Itk constructs tagged with fluorescent proteins: single-tagged (on C- or N-termini, C-Itk and Itk-Y, respectively) and double-tagged (on C- and N-termini, C-Itk-Y). JTag cells were transfected with respective DNA constructs, lysed 48 hours after transfection, immunoprecipitated with αGFP, immune complexes were resolved by SDS-PAGE gel, transferred to PVDF membrane, and blotted with αItk antibody. Bands were visualized by chemiluminescence, as described in Materials and Methods.

Then all wild type constructs were assessed for transphosphorylation to make sure that functionality of the Itk molecule stayed intact after tagging with fluorescent proteins (data not shown). After confirming that wild type constructs had normal expression and phosphorylation patterns, we assessed the mutants for phosphorylation properties under TCR stimulation (Figure 5). Endogenous wild type Itk in each sample served as loading and stimulation control. Total stimulation assessed by total lysate phosphorylation appeared uniform in all samples under stimulation (Figure 5a). Endogenous Itk showed uniform phosphorylation under stimulation in all samples (Figure 5c). Transfected wild type Itk revealed strong phosphorylation signal under

stimulation by αCD3ε crosslinking, as predicted (Figure 5b). Y511F mutant does not have a phosphorylation site at Y511 residue, and shows only very marginal total phosphorylation due to Y180 and other tyrosine residues, and is greatly reduced compared to wild type molecule (Figure 5b). FYF mutant showed reduction in phosphorylation on a scale similar to Y511F, and Btk-SH3 mutant showed some reduction in total phosphorylation comparing to wild type construct (Figure 5b).

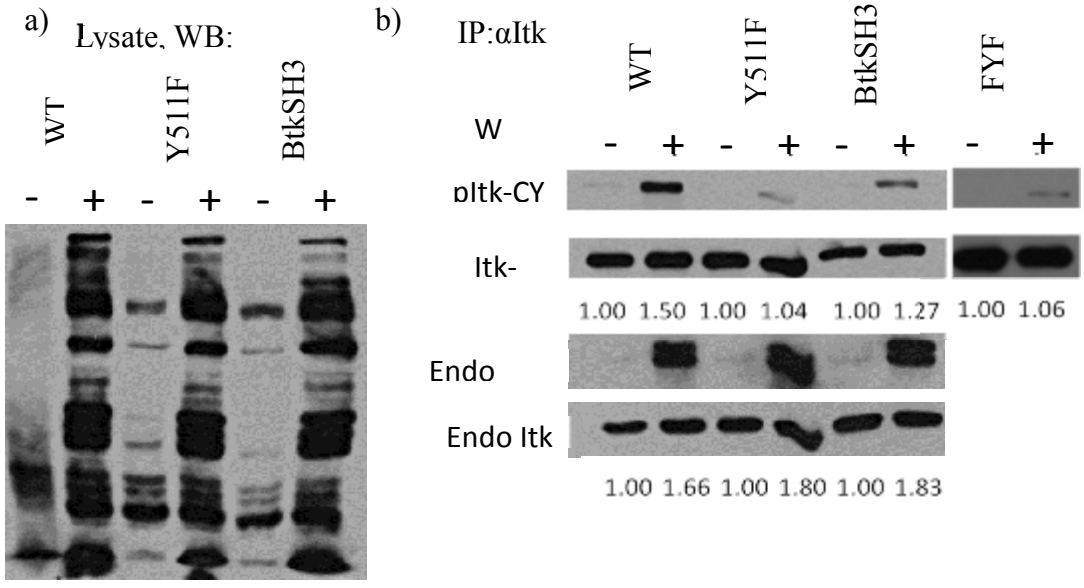

Figure 5. Effects of different Itk mutants on Itk phosphorylation.

Jurkat cells that had been transfected with the indicated ITK constructs were stimulated (+) or not (-) with anti-CD3ε antibodies and then lysed. A) Control for stimulation. Total lysate phosphorylation was assessed by immunoblotting with antiphosphotyrosine antibody, and stimulated lanes showed increase in phosphorylation; B) ITK in the lysates was immuno-precipitated (IP) with anti-ITK antibodies, immune complexes resolved by SDS-PAGE, proteins transferred onto PVDF membranes and immuno-blotted (IB) sequentially with anti-phosphotyrosine antibodies and anti-ITK antibodies as indicated. Bands were visualized by chemiluminescence as described in Materials and Methods section. Numbers under the panels represent the fold-increase in band signal intensity (phosphorylation) compared to the respective non-stimulated control calculated as described in the Materials and Methods section. Results are those from one of three replicate experiments with similar results. Y511F and FYF phosphorylation is significantly reduced while phosphorylation level in all endogenous samples is comparable.

This data was further confirmed by the phosphoflow technique, using a specific antibody that only recognizes pY511 residue (Figure 6). The results obtained from the experiment confirmed data from the western blotting experiment. Y511F showed significant reduction in Y511 phosphorylation signal compared to wild type construct, and BtkSH3 construct showed somewhat reduced specific phosphorylation compared to wild type. This confirmed previous literature data on Y511F mutant (9), but also showed BtkSH3 mutant properties in a T cell system, which had previously been assessed only in the insect cell system (34).

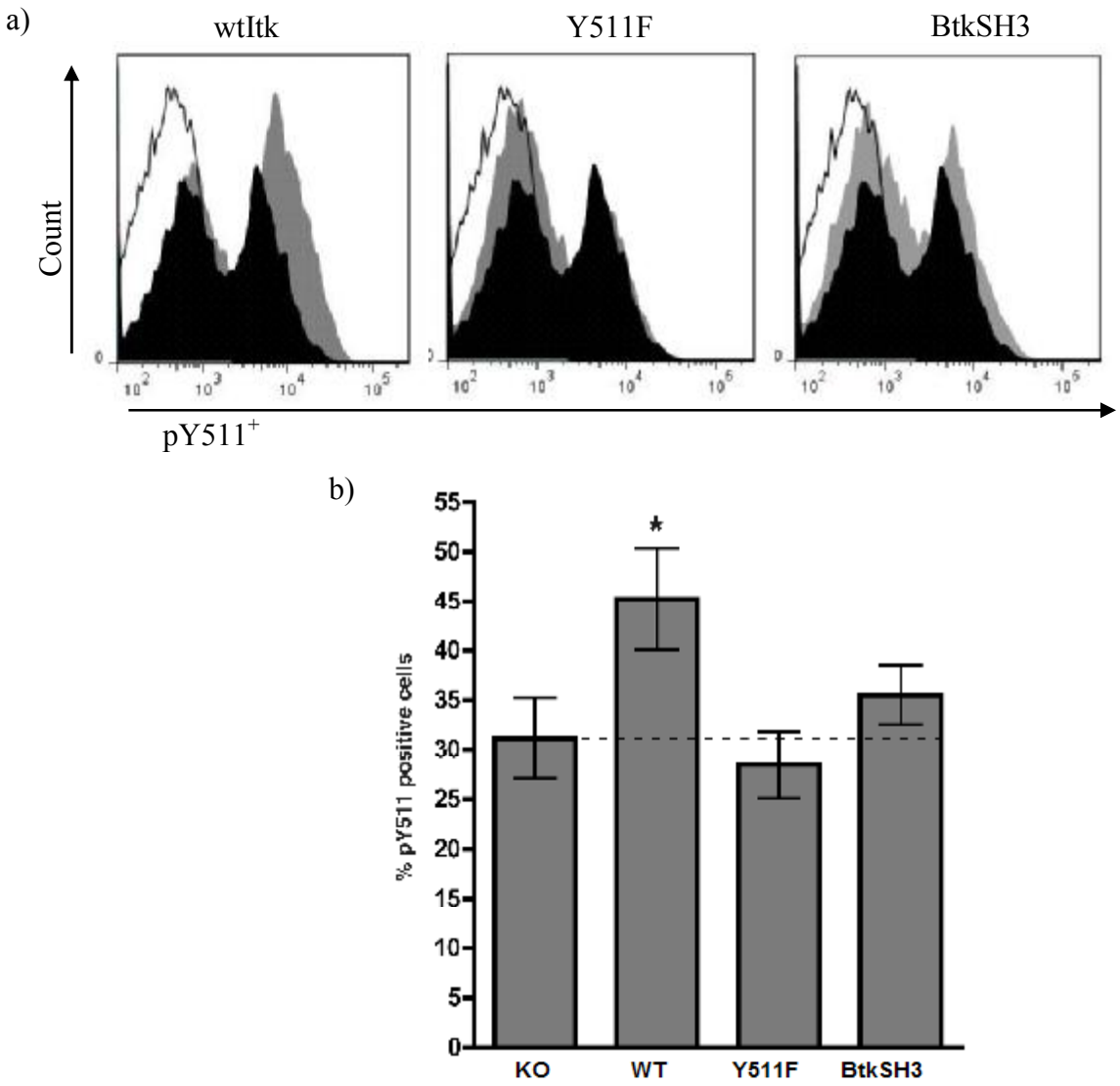

Figure 6. Itk pY511 phosphorylation by flow cytometry in transfected mouse thymocytes.

One representative experiment and a cumulative experiment bar graph are shown. A) Murine thymocytes from ITK-deficient mice, nucleofected with the indicated ITK constructs, were stimulated with anti- CD3ε antibodies for 1 minute and then analyzed for ITK phosphorylation using Alexa 647-tagged antibodies that react with ITK pY511, as described in Materials and Methods section. Results are displayed as cell number (linear scale) vs. fluorescence intensity (logarithmic scale). In each panel the open histogram represents non-transfected/non-stimulated cells and the black histogram mock nucleofected cells. Gray histograms represent ITK-WT (left panel), -Y511F (middle panel), and –BtkSH3 (right panel) nucleofected cells. The results are those of one representative experiment; B) average (±SEM) percentage of pY511 positive cells of three replicate experiments (including the experiment depicted in panel A) performed as described in panel A. The * denotes that the average of pY511 positive cells in WT-ITK nucleofected group is significantly different from the rest of the groups at $p<0.05$ (student's t test). The dotted line demarcates the specific anti-pY511 reactivity.

FRET assay validation

One of the methods that allow studying conformation of the protein in a living cell is FRET (Fluorescence Resonance Energy Transfer). This method allows measuring the relative conformation state of the molecule by fusion-tagging the protein of interest with fluorescent proteins with overlapping emission and excitation spectra (like CFP and YFP).

To use FRET biosensors, it has to be established first whether fluorophores are at a close enough distance to allow energy transfer (116). To obtain this information, we used a photobleaching technique that involves burning out the acceptor fluorophore by removing the neutral density filter for a few minutes, and then measuring changes in donor emission. When the acceptor is photobleached, energy transfer cannot occur, and all the excitation energy is transformed into donor emission energy (116). The difference between donor emission before and after photobleaching using the same amount of energy can be used to calculate the amount of energy transfer from one fluorophore to another (116). In an example (Figure 7), energy transfer was about 8%. Average energy transfer in the experiments was around 9±3%. This is in the usual range of biosensors involving FRET methodology (116,117,123), with a similar error range (116). Theoretically, possible maximum transfer is around 40% (116).

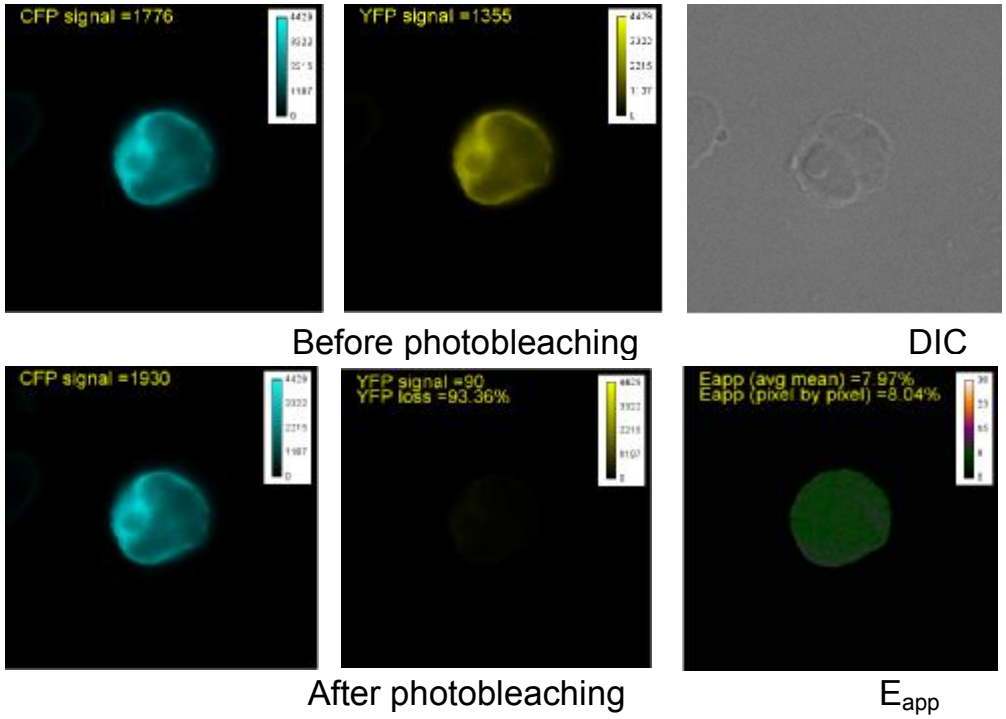

Figure 7. Sample YFP photobleaching.

JTag cells were transfected with C-Itk-Y, fixed with paraformaldehyde, transferred to the slides and subjected to 3 minute YFP photobleaching. FRET efficiency was calculated based on raw pre- and post photobleaching images using area average and pixel-by-pixel approaches. Color table method was used to visualize intensities. Calibration bars on the images show color correspondence to intensities on fluorescence images or E_{app} values (in %) on E_{app} image.

After the confirmation of energy transfer using photobleaching technique, it is possible to use a more efficient technique, eFRET (116). This technique is based on using a three-filter set to capture differences in energy transfer without using the time-consuming photobleaching technique. When establishing the validity of the biosensor, we applied the eFRET technique. In an example (Figure 8), the energy transfer efficiency was about 10%, with average energy transfer from several experiments being around 9±3%.

These two techniques showed that the fluorophores in our biosensor were correctly oriented, and at an appropriate distance for the energy transfer to occur.

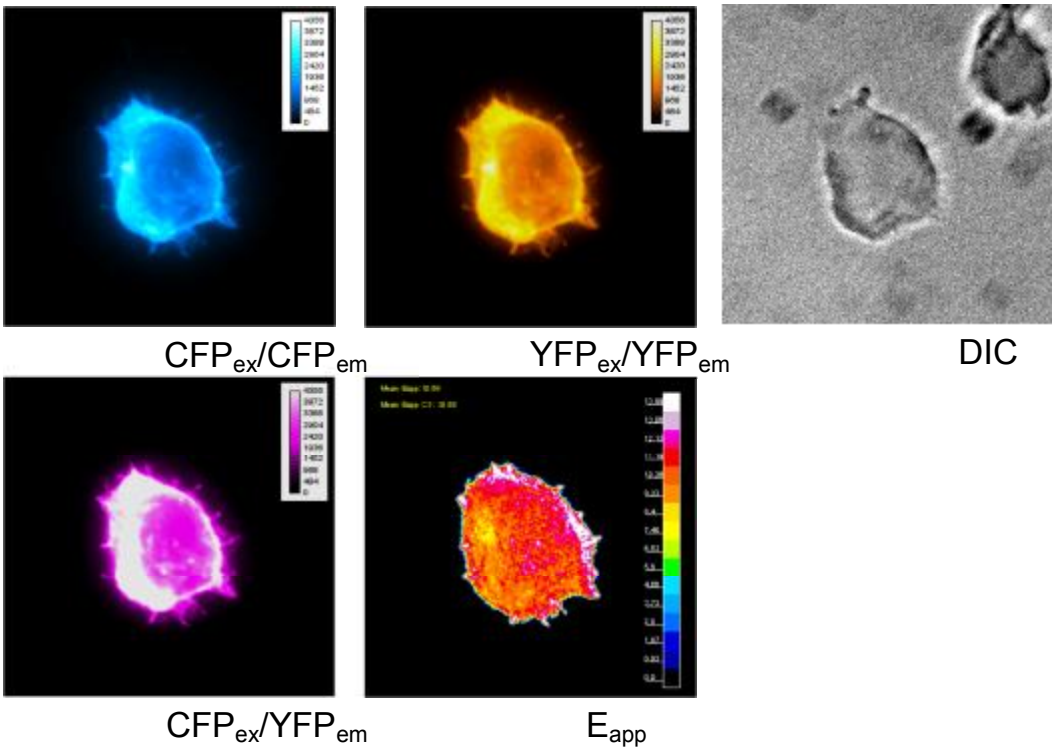

Figure 8. Sample EFRET experiment.

JTag cells were transfected with C-Itk-Y, fixed with paraformaldehyde, and transferred to the slides. EFRET efficiency was calculated based on raw images acquired according to sensitized emission method using area average and pixel-by-pixel approaches. Color table approach was used for visualizing fluorescent images and isolinear mapping was used to visualize Calibration bars on the fluorescent images show color correspondence to intensities. Calibration bar on E_{app} image shows color correspondence to values within isolinear surfaces of E_{app} intensity (in %). Limits of each surface differ from the limits of the previous one by 1/16 of the maximal E_{app}.

We determined whether intracellular distribution of FRET signal in resting cells is uniform, and whether there are significant fluctuations between measurements of the cytoplasmic region of the same cell. We did not find a significant difference between different cytoplasmic areas within a resting cell (Figure 9a).

The next step in validating the biosensors was to investigate whether our system suffers the effects of crowding – i.e. whether the transfection efficiency, localization or any other means of achieving unequal concentration of the fluorophores, would influence the measured energy transfer that could lead to potential errors in evaluating structural changes. Using both photobleaching and EFRET techniques it was shown that FRET in resting cells transfected with C-Itk-Y does not correlate with YFP intensity (data from photobleaching is shown in Figure 9b; data from eFRET is shown in Figure 10). This assay was necessary to prove that changes in FRET signal do not preferentially result from random molecule collisions, but from the true conformational change.

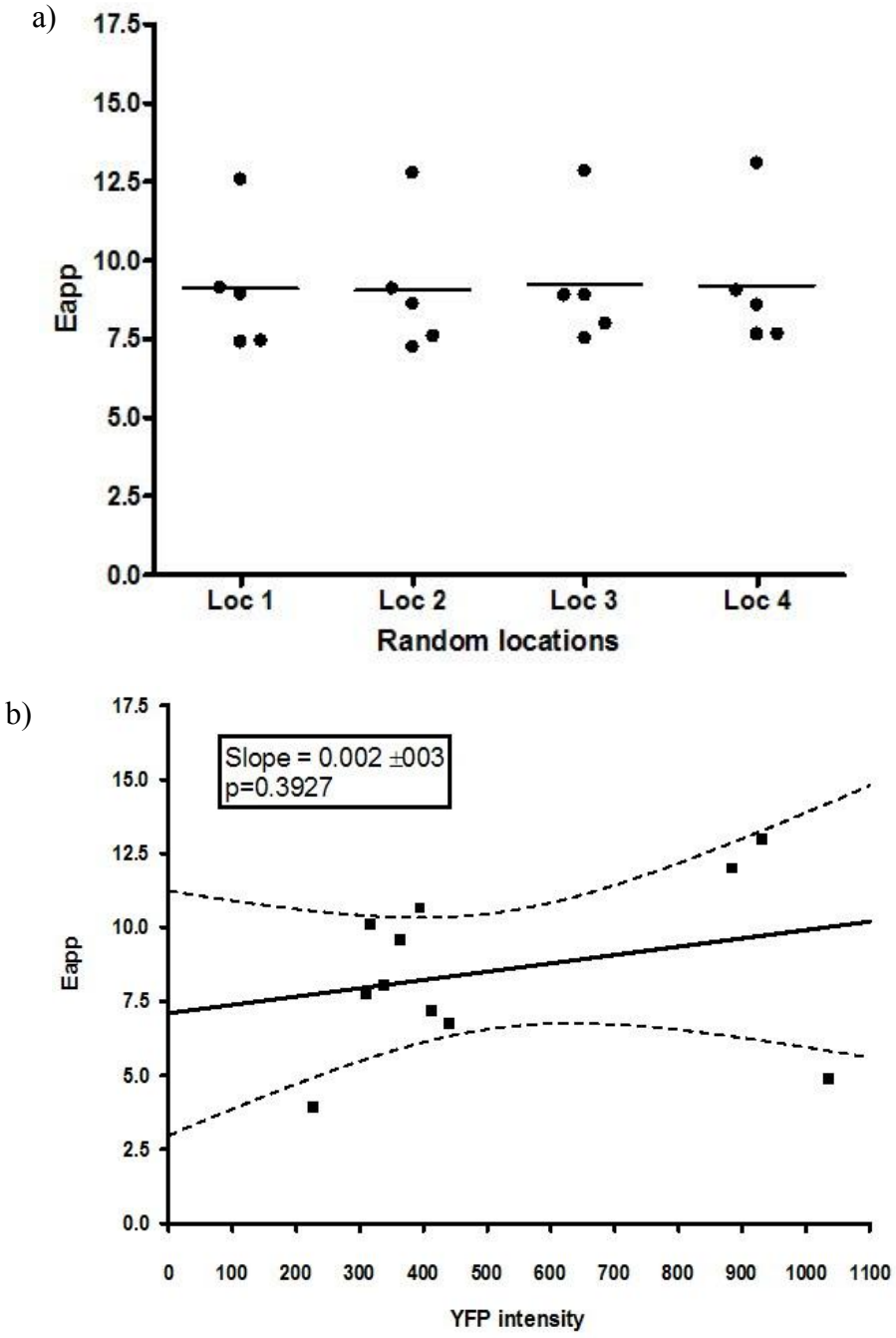

Figure 9. FRET sensitivity in JTag cells transfected with Itk-CY.

The sensitivity of FRET assay was tested in Itk-CY transfected JTag cells at nonstimulated state. A) Sensitivity. EFRET was measured in four random locations in resting cells (fixed at 4^{o}C) transfected with C-Itk-Y; B) dependence of Eapp on YFP intensity. Resting cells (fixed at 4^{o}C) transfected with C-Itk-Y were subjected to YFP photobleaching (3 min, ~70-90% YFP loss) on the slide. FRET efficiency was calculated in three random locations based on pre- and postphotobleached images. Solid line represents linear regression fit line, 95% confidence interval for linear regression fit is outlined by dashed lines.

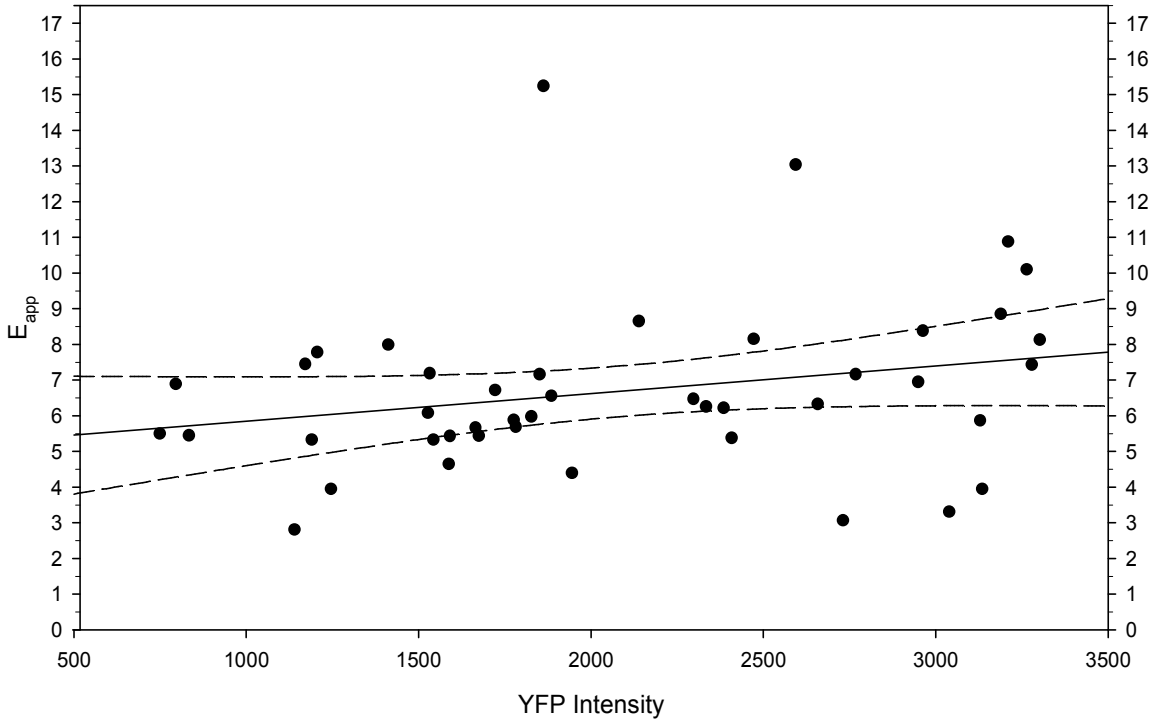

Figure 10. Crowding effect on eFRET

eFRET data was calculated for 45 resting JTag cells transfected with Itk-CY and showing different expression levels (ranging from 600 to 3300 arbitrary units of YFP fluorescence intensity). Most data points fell into 99% confidence interval for linear distribution fit, and no significant correlation between expression level and eFRET was found.

FRET in resting cells

To assess whether mutations may have a measurable effect on Itk conformation without stimulation, FRET studies were performed in resting JTag cells transfected with Itk mutants. First, wild type biosensors were assessed for fluorescence distribution pattern, and for FRET distribution inside the cytoplasm (representative images shown in Figure 11). Fluorescence distribution was used as a proxy of wild type Itk localization at resting state. It proved to be located in the cytoplasm showing higher distribution toward the thicker part of the cell, possibly because of the additive effect of epifluorescence through thicker portions of the cytoplasm (Figure 11a). eFRET showed a uniform distribution inside the cytoplasm that was independent of Itk concentration (Figure 11b).

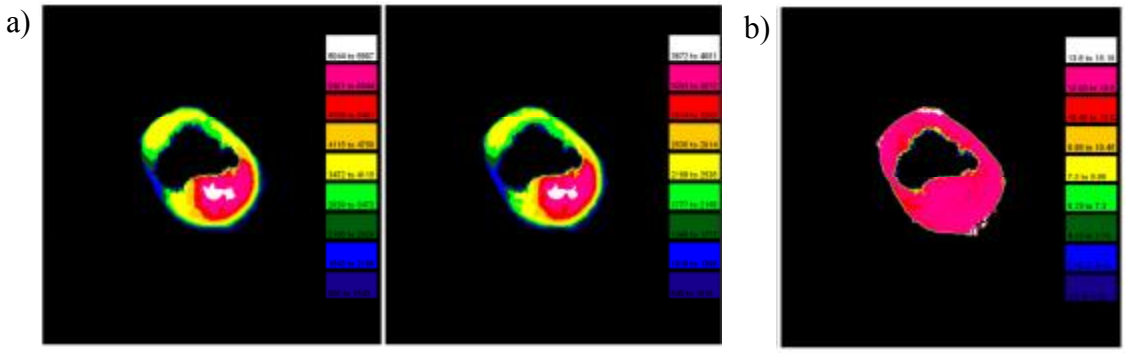

Figure 11. Wild type Itk-CY localization and eFRET in resting JTag cells transfected with wild type Itk-CY construct

Sample resting JTag cell is shown 48 hours after transfection with Itk-CY, and fixed with 2% paraformaldehyde before mounting on the slide. A) CFP (left) and YFP (right) fluorescence mapped inside the cell according to increasing intensity (blue to white, 10% increments); B) eFRET mapped inside the cell according to increasing intensity (blue to white, 10% increments)

We tested the possibility of disrupting eFRET signal by overexpressing nonfluorescently tagged (using H902 tag – HIV-derived tag epitope, one of the common nonfluorescent fusion tags) wild type Itk molecules alongside wild type Itk-CY constructs on assumption that an excess of untagged Itk might be able to form complexes with Itk-CY and block energy transfer from CFP to YFP by separating them apart due to resulting conformational change. The experiments did not show a significant difference in eFRET on addition of the excess of nonfluorescent H902-tagged Itk in concentration up to 4x in excess of the fluorescently tagged Itk, determined as 4x amount of transfected DNA (Figure 12).

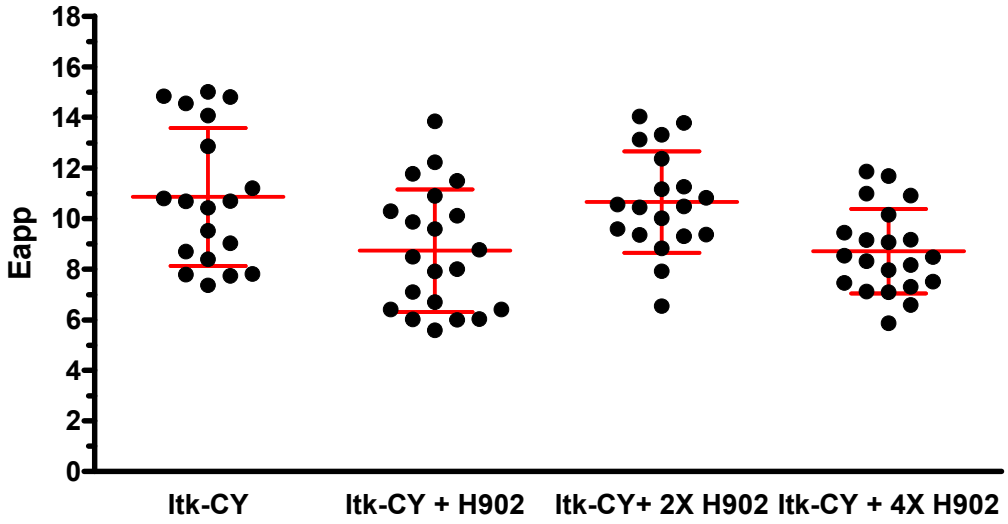

Figure 12. Competition of fluorescently tagged and nonfluorescently tagged Itk

eFRET was assessed in JTag cells transfected with Itk-CY and with combination of Itk-CY and excess of nonfluorescently tagged H902-Itk (excess assessed by the amount of DNA used for transfection comparing to Itk-CY DNA). Transfected cells were collected 48 hours after transfection, fixed in 2% paraformaldehyde, mounted on the slide, and assessed for FRET (Eapp) as described in Materials and Methods section. Eapp calculated for each cell is shown as a black dot, mean and standard deviation for each group are shown as red error bars.

The opposite approach was also used to clarify whether endogenous Itk already present in JTag cells has a competition effect on transfected fluorescently tagged Itk. For this purpose, 293T cell line was used that does not express endogenous Itk, and Eapp values were compared to those received from JTag cell line (Figure 13). There was no significant difference in Eapp between JTag cells expressing Itk-CY and 293T cells expressing Itk-CY.

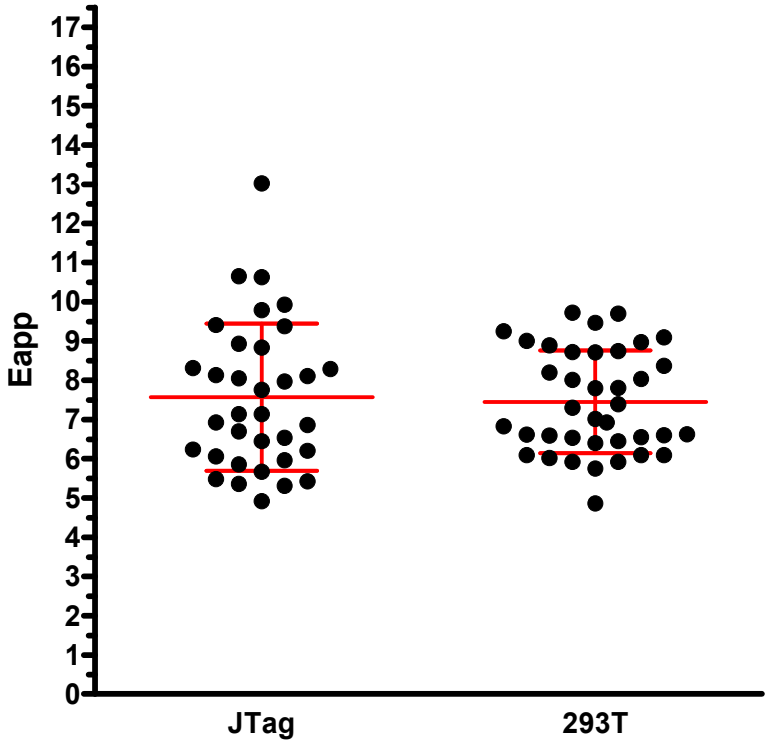

Figure 13. Effect of endogenous Itk on eFRET

Itk-CY was transfected into JTag cells that express endogenous Itk, and into 293T cells that do not express endogenous Itk. Transfected cells were collected 48 hours after transfection, fixed in 2% paraformaldehyde, mounted on the slide, and assessed for FRET (Eapp) as described in Materials and Methods section. Eapp calculated for each cell is shown as a black dot, mean and standard deviation for each group are shown as red error bars.

To determine whether transfected Itk in resting cells forms head-to-head, head-to-tail, or tail-to-tail complexes that would bring single CFP and YFP tags on different Itk molecules into a close proximity, single-tagged (YFP or CFP) Itk molecules were cotransfected into JTag cells. There was no significant difference in Eapp in head-to-head, head-to-tail, or tail-to-tail combination. Eapp levels were approximately two fold lower than that of the Itk-CY biosensor, and close to the background (Figure 14).

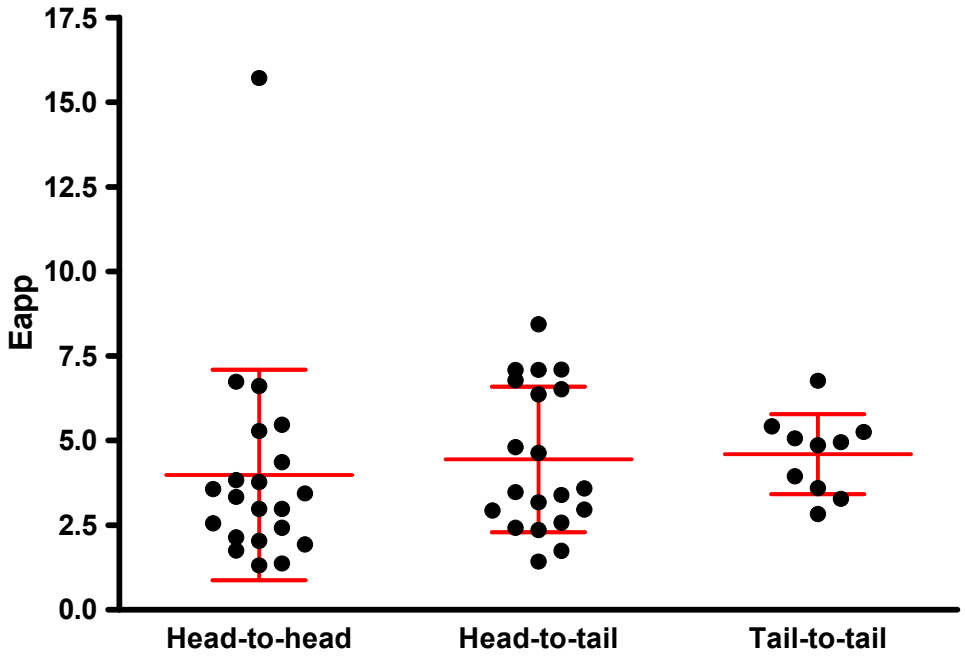

Figure 14. Single fluorescently tagged Itk constructs cotransfection

JTag cells were cotransfected with a pair of CFP- and YFP-tagged constructs in equal proportion. Head-to-head (N-terminal to N-terminal), Head-to-tail (N-terminal to C-terminal), and Tail-to-tail (C-terminal to C-terminal) combinations were assessed. Transfected cells were collected 48 hours after transfection, fixed in 2% paraformaldehyde, mounted on the slide, and assessed for FRET (Eapp) as described in Materials and Methods section. Eapp calculated for each cell is shown as a black dot, mean and standard deviation for each group are shown as red error bars.

Mutants were tested to assess whether any of them changes conformation at resting state, resulting in change of Eapp. No significant difference was observed between Eapp of different CY tagged mutants at resting state.

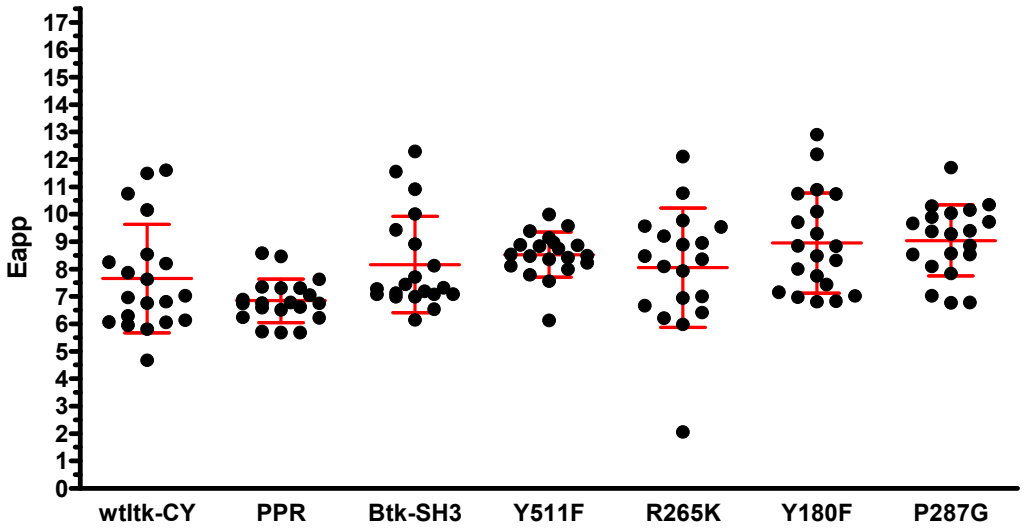

Figure 15. eFRET in JTag cells transfected with CY-double tagged Itk mutants

Transfected cells were collected 48 hours after transfection, fixed in 2% paraformaldehyde, mounted on the slide, and assessed for FRET (Eapp) as described in Materials and Methods section. Eapp calculated for each cell is shown as a black dot, mean and standard deviation for each group are shown as red error bars.

JTag-Raji conjugate system

One of the useful models for immunological processes that is close in functionality to immunological signaling in live organisms is a T-cell-APC model (124). JTag-Raji conjugation system mediated by SEE similar to the system used by Montoya et al. (115) was employed in this project as a model of immunological conjugate. SEE is a superantigen that binds to MHCII complex on APC, promoting T-cell activation and conjugate formation (125).

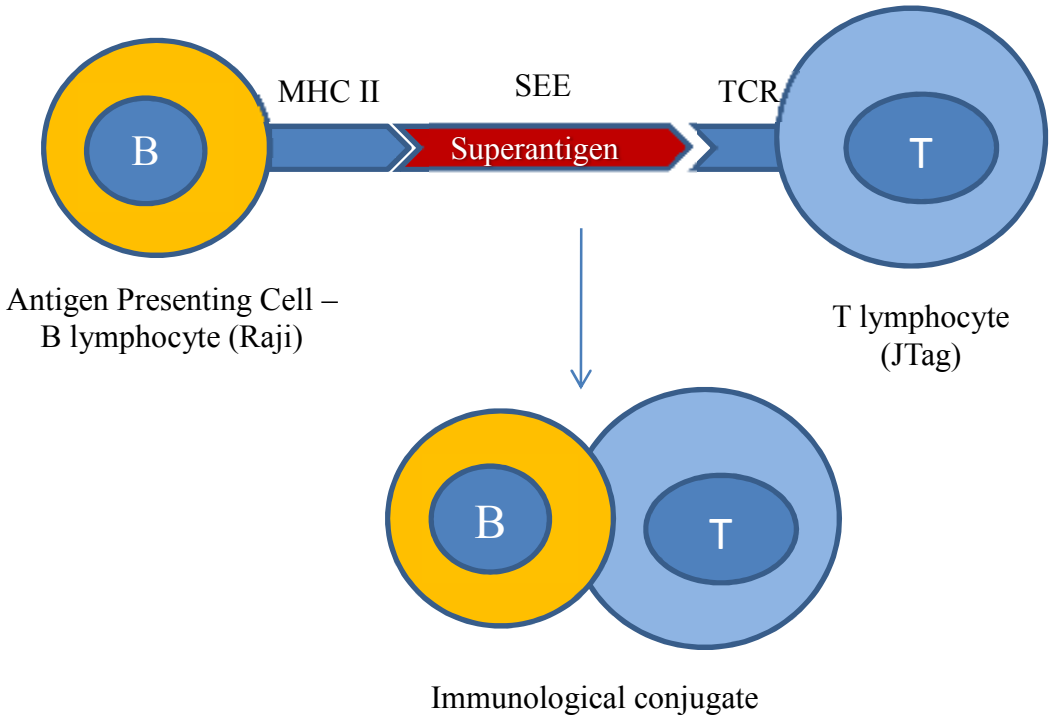

Figure 16. Schematic representation of JTag-Raji system
*MHC, TCR, and SEE representations are not shown in real shape or in real proportion to the cell

Localization in JTag-Raji conjugates

It was known from the literature that Itk localizes to the membrane upon TCR induced stimulation (51). However, kinetics of Itk localization in T-cell-APC conjugates were unclear. To clarify the details and timeframe of Itk localization, time kinetics of the localization was assessed by calculating localization index in conjugates from samples stimulated for different lengths of time by putting them in 37^{o}C water bath (Figure 17). It was shown that maximum localization is reached three minutes after placing the samples into the water bath.

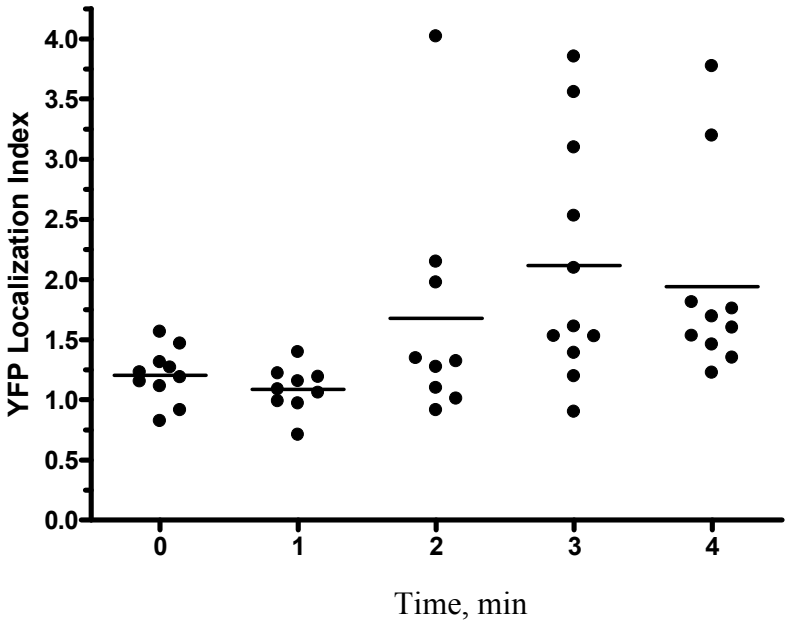

Figure 17. Localization kinetics

JTag cells were transfected with wild type Itk-CY, chilled on ice, and mixed with Raji cells preloaded with SEE. Cells then were incubated in 37^{o}C waterbath for indicated length of time (0, 1, 2, 3, and 4 minutes), and immediately fixed by adding equal volume of ice cold 4% paraformaldehyde. Then cells were mounted on the slide, and assessed for Itk localization as described in Materials and Methods section.

After establishing optimal conditions for measurement of localization, mutants were tested for deficiencies in localization (Figure 18). FYF mutant showed partial disruption of the localization function, and demonstrated significantly lower localization index compared to wild type construct. Y511F and BtkSH3 mutants surprisingly, showed no significant effect on localization.

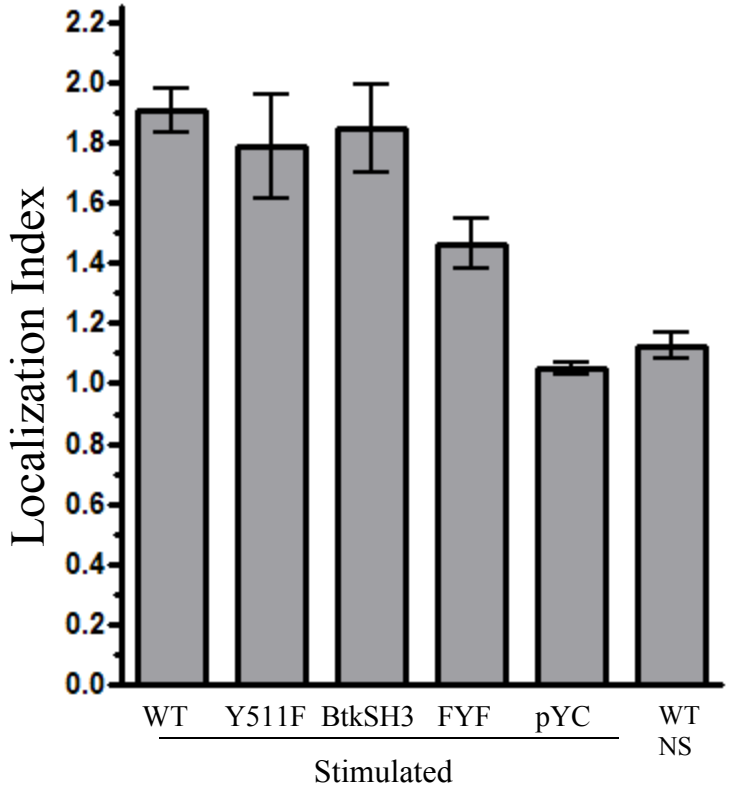

Figure 18. Localization of mutants in JTag-Raji conjugates

Jurkat cells transfected with fluorescent protein chimeric constructs of WT-ITK, ITK-Y511F, ITK-BTKSH3, FYF or with a construct containing fluorescent protein without ITK (pYC), as a transfection control, were incubated with Raji cells that had been pre-treated with SEE for 3 minutes at 37°C, or kept on ice (NS sample). Cells were then fixed in paraformaldehyde and analyzed using epifluorescence microscopy. Results of three replicate experiments, performed and analyzed as described in Materials and Methods section, are displayed as the average Localization Index (±SEM) for each ITK construct calculated as described in the Materials and Methods section. WT/NS denotes non-stimulated cells transfected with WT-ITK, as negative control. The number of conjugates analyzed in each group are WT, N=114; Y511F, N=37; BTKSH3, N=32; FYF, N= 55; pYC, N=10, WT/NS, N=10.

FRET in JTag-Raji conjugates

To assess conformational changes in Itk under stimulation, JTag-Raji conjugates were used. Raji cells were labeled with Cy5, and preloaded with SEE, while JTag cells were transfected with Itk-CY constructs. Then Eapp was calculated on the basis of images. To distinguish conjugates in stimulated cells from two randomly colocalized cells, we used stable conjugate criteria from Montoya et al. (115), which involved imaging only those conjugates that were morphologically qualified. Stable conjugates were considered those having T-cell that developed visible protrusions around APC (referred as "arms" further in the text), example is shown in Figure 19d-f. Conjugates with protrusions on only one side of the APC were discarded.

It was noted, that while wild type Itk localizes at the contact site uniformly (example shown in Figure 19e), as predicted, FRET distribution under stimulation shows an unanticipated pattern, forming high FRET area near the contact site with higher FRET at the "arms," and lower FRET at the center of the contact site (example shown in Figure 19f). Control samples of nonstimulated cells showed predicted uniform distribution pattern for FRET and localization (example shown in Figure 19a-c).

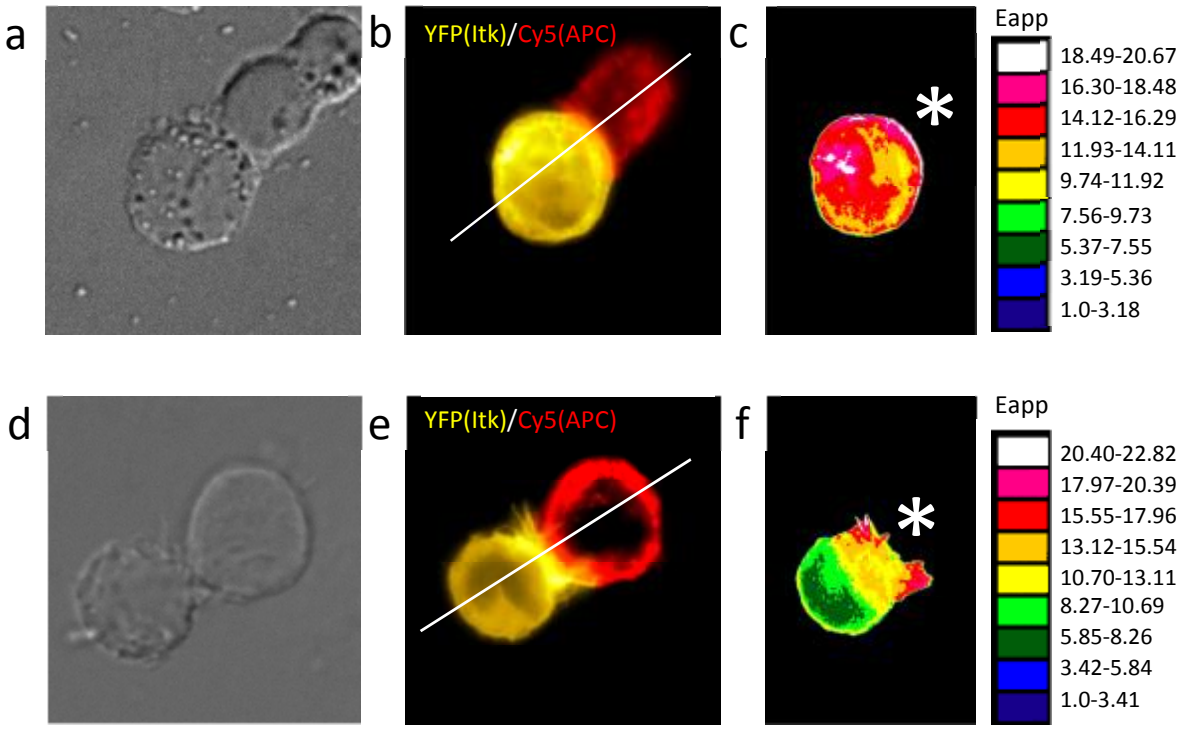

Figure 19. FRET in stimulated conjugate and nonstimulated cells

Jurkat cells transfected with CY-tagged chimeric construct of WT-ITK, were incubated with Raji cells that had been pre-treated with SEE and incubated for 3 minutes at 37°C or kept on ice. Cells were then fixed in paraformaldehyde, mounted on the slide, and analyzed using epifluorescence microscopy as described in Materials and Methods section. Shown are representative experiments displaying localization of ITK as YFP fluorescence intensity (panels b and e) in the presence (panels a-c) or absence (panels d-f) of stimulus (incubation in the water bath after SEE preloading). Differential interference contrast images are displayed in the panels a and d for the ease of the orientation. Eapp mapped inside the cell according to increasing FRET intensity (blue to white, 10% increments) is shown in panels c and f. APC position is marked with white asterisk, absolute Eapp values of each color on the Eapp map are shown on the right hand side from the respective map.

Kinetics of FRET pattern formation was assessed in JTag-Raji conjugates at different timepoints. The optimal time for pattern formation seemed to coincide with optimal localization time (compare Figure 17 and Figure 20), and was three minutes of 37^{o}C stimulation in a water bath.

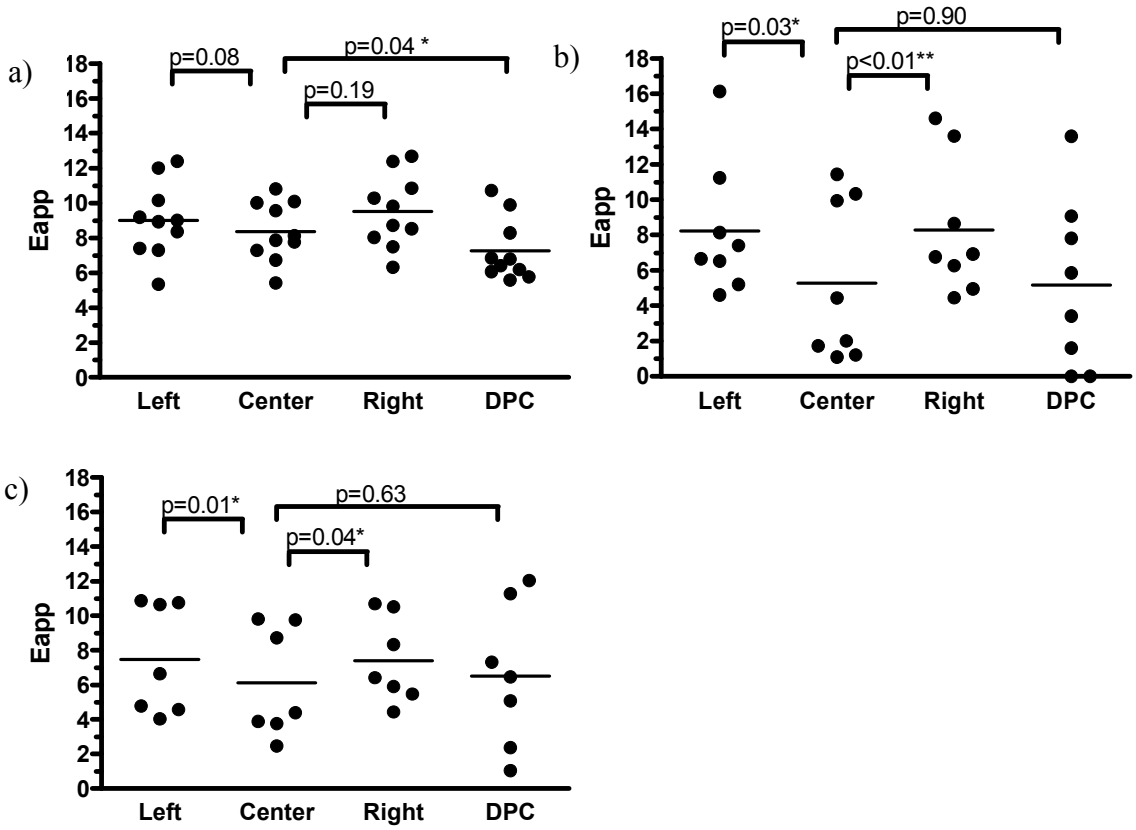

Figure 20. FRET pattern formation kinetics

Jurkat cells transfected with CY-tagged chimeric construct of WT-ITK, were incubated with Raji cells that had been pre-treated with SEE and incubated for 2 (a), 3 (b), or 10 (c) minutes at 37°C. Cells were then fixed in paraformaldehyde, mounted on the slide, and analyzed using epifluorescence microscopy as described in Materials and Methods section. FRET distribution patterns were analyzed by measuring Eapp in left, center, and right parts of the contact, and in the opposite site to the contact site – the distal pole complex (DPC) as a control location. Measurements in each individual cell are shown as black dots, mean is shown as a black line. Resulting numerical data was analyzed using Student t-test. P values are shown on top of a square bracket for each pair of locations. Most significant difference is seen at 3 min incubation.

To assess whether mutants affect FRET pattern formation in JTag-Raji conjugates, JTag cells were transfected with CY-tagged mutant Itk, mixed with Cy5 labeled Raji cells preloaded with SEE, and stimulated in 37^{o}C water bath for three min. After fixation and mounting on the slide, conjugates were imaged, and Eapp was calculated in the "arms" and the center of the contact site (see Table 2). Then ratio of the average of the sides, and center was derived to quantitatively determine the percent difference in Eapp at the center versus sides (see Table 2). There was a significant difference in Eapp between wild type construct and mutants. The FYF mutant showed a pattern identical to the negative control transfected with pYC construct. Y511F and BtkSH3 mutants showed partial disruption of the pattern.

Table 2. FRET patterns in Itk mutants

Construct	**Center**	**Sides**	**N**	**P**
WT	9.6±0.4	11.8±0.4	129	<0.0001
Y511F	13.4±0.5	14.2±0.4	29	0.2476
BtkSH3	10.4±0.5	11.2±0.5	32	0.2275
FYF	9.7±0.4	9.6±0.4	55	0.5973
pYC	21.1±0.6	21.0±0.6	21	0.6366

Interaction with SLP-76

To assess whether any of the mutations had an effect on binding the main signaling partner of Itk under stimulation, co-immunoprecipitation was performed (Figure 21). pY signal in total lysate served as a stimulation control. It was shown that Y511F mutant associates normally with SLP-76, while BtkSH3 has a moderate effect in decreasing the association.

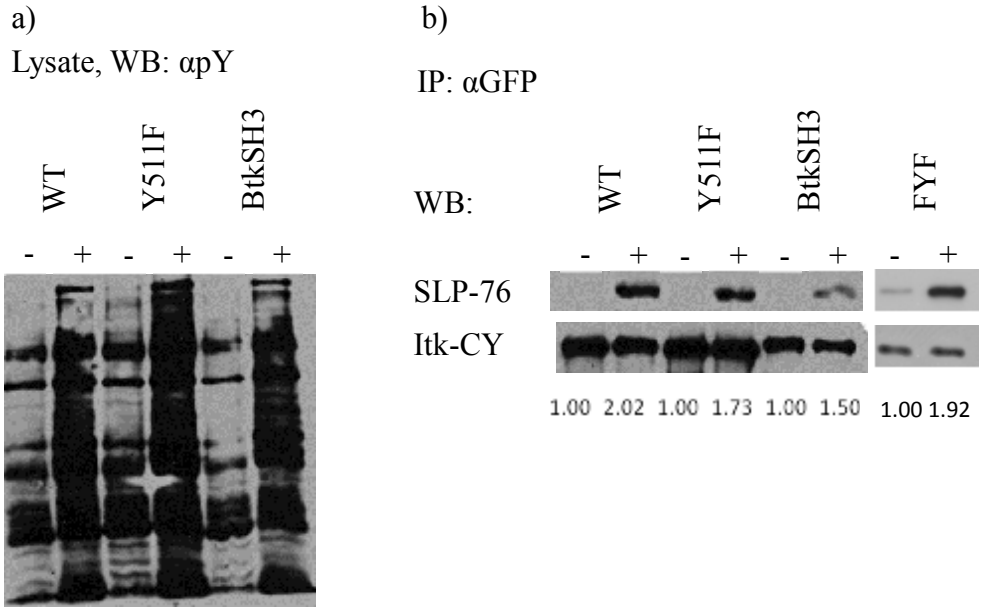

Figure 21. Association of Itk mutants with SLP-76

Jurkat cells that had been transfected with the indicated ITK-CY constructs were stimulated (+) or not (-) with anti-CD3ε antibodies and then lysed. A) Control for stimulation. Total lysate phosphorylation was assessed by immunoblotting with antiphosphotyrosine antibody, and stimulated lanes showed increase in phosphorylation; B) ITK in the lysates was immuno-precipitated (IP) with anti-GFP antibodies, immune complexes resolved by SDS-PAGE, proteins transferred onto PVDF membranes, and immuno-blotted (IB) sequentially with anti SLP-76 (top panel) and anti-ITK (bottom panel) antibodies. Bands were visualized by chemiluminescence as described in Materials and Methods section. Numbers under each blot represent the association index between each ITK-variant and SLP-76 calculated as described in the Materials and Methods section. Results are those from one of three replicate experiments.

Itk$^{-/-}$ mouse model system for assessing Itk signaling in Itk negative background

To assess signaling functions of Itk in a system that maximally resembles natural conditions Itk-/- mice thymocytes were used, having additional benefits of avoiding the influence of endogenous Itk on signaling function of transfected Itk, and possible interference with determining disruptive effects of particular mutants. The process used in the experiments is outlined in Figure 22.

Thymocytes were a particularly suitable model, as they allow reproducibly high and uniform nucleofection efficiency (Figure 23).

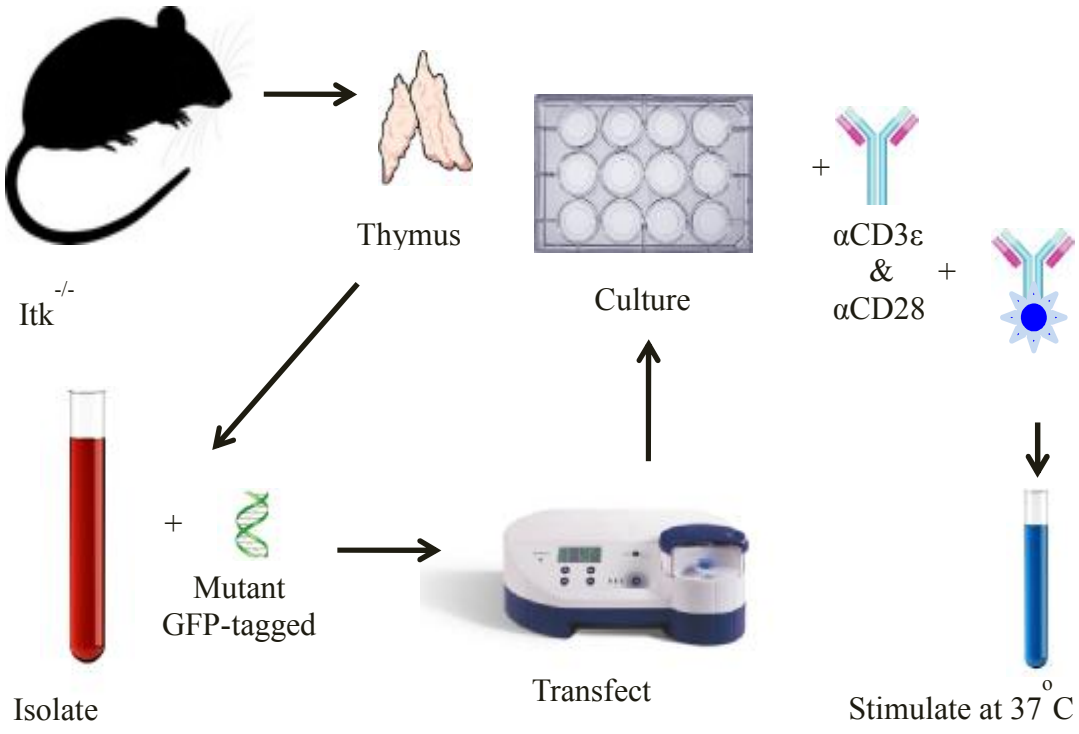

Figure 22. Schematic representation of Itk$^{-/-}$ mouse thymocyte model

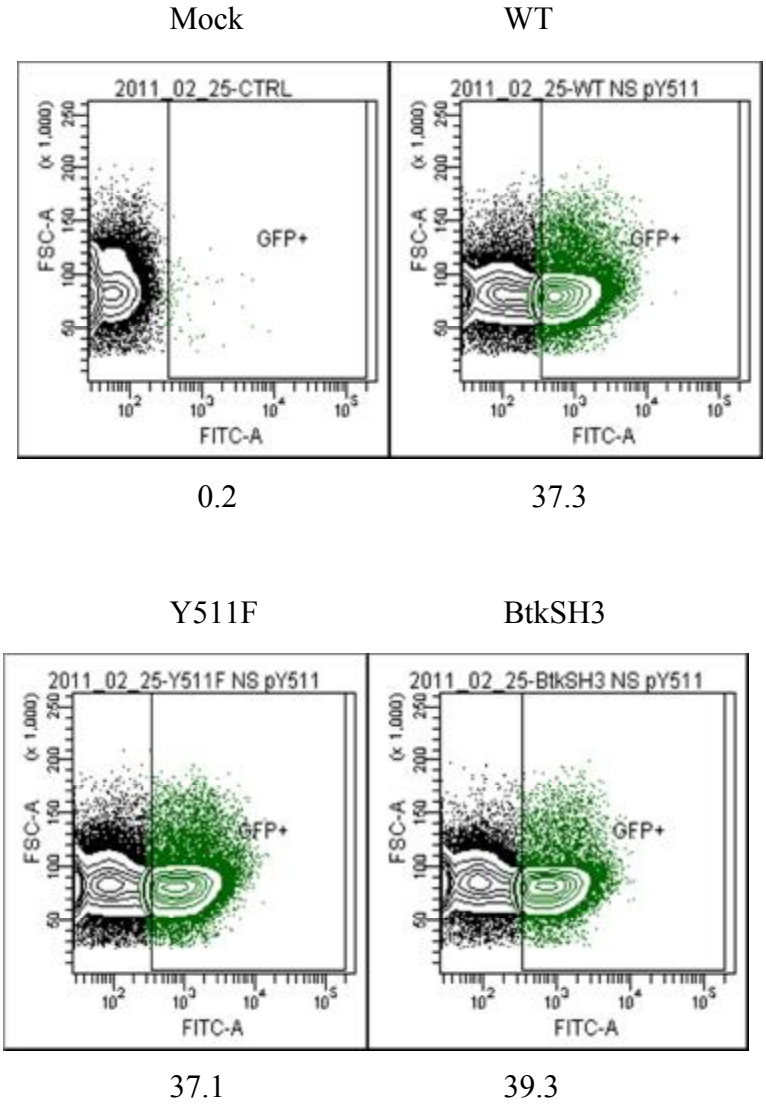

Figure 23. Nucleofection efficiency in thymocyte model.

Itk$^{-/-}$ mouse thymocytes were transfected with GFP-tagged wild type or mutant Itk as described in Materials and Methods section. Cells were analyzed for GFP expression signal and plotted versus forward scatter. GFP positive cells are marked green, percent GFP positive cells in the sample is indicated below each plot. Experiment showed high transfection efficiency for all tested constructs.

Downstream and upstream signaling

To assess whether immediate signaling downstream of Itk was affected in any of the mutants, PLCγ phosphorylation was assessed via phosphoflow experiments in $Itk^{-/-}$ mouse thymocytes nucleofected with a mutant of interest, stimulated, and labeled for cells binding stimulating antibodies. ZAP-70 was used as a negative control, because its phosphorylation precedes Itk phosphorylation, and is an upstream event that should not be affected by inactivation or hyperactivation of Itk. Representative pPLCγ experiment is shown in Figure 24, cumulative pPLCγ and pZAP70 experiments are shown in Figure 25.

PLCγ phosphorylation was significantly downregulated in Y511F and BtkSH3 mutants comparing to wild type, while there was no significant difference in ZAP70 phosphorylation.

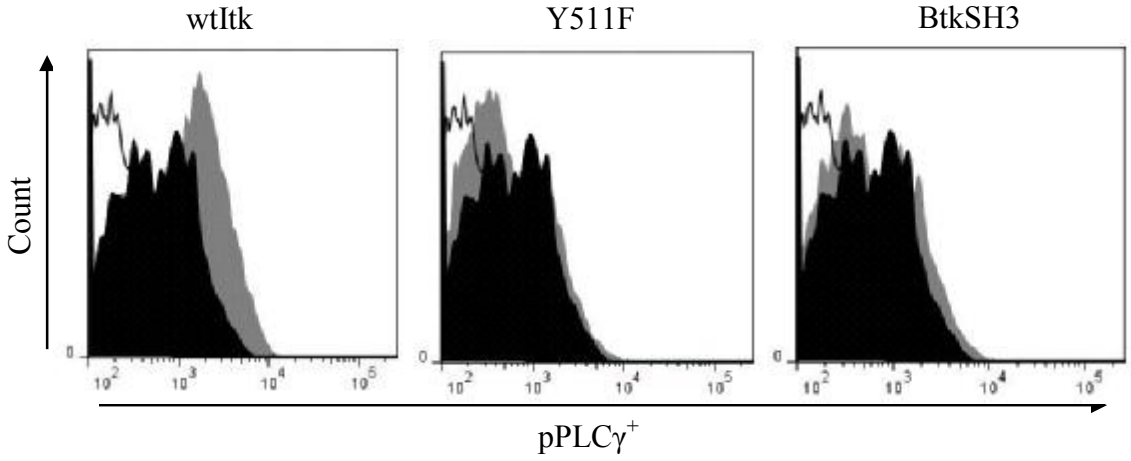

Figure 24. Reduced pPLCγ phosphorylation in mutants

Murine thymocytes from ITK-deficient mice, nucleofected with the indicated ITK constructs, were stimulated with anti mouse-CD3ε antibodies and then analyzed for PLCγ1 phosphorylation using Alexa 647-tagged antibodies that react with PLCγ1 pY783, as described in Materials and Methods section. Results are displayed as cell number (linear scale) vs. fluorescence intensity (logarithmic scale). In each panel the open histogram represents non-nucleofected/non-stimulated cells and the black histogram mock nucleofected cells. Gray histograms represent ITK-WT (left panel), -Y511F (middle panel), and –BTKSH3 (right panel) nucleofected cells. The results are those of one representative experiment out of four.

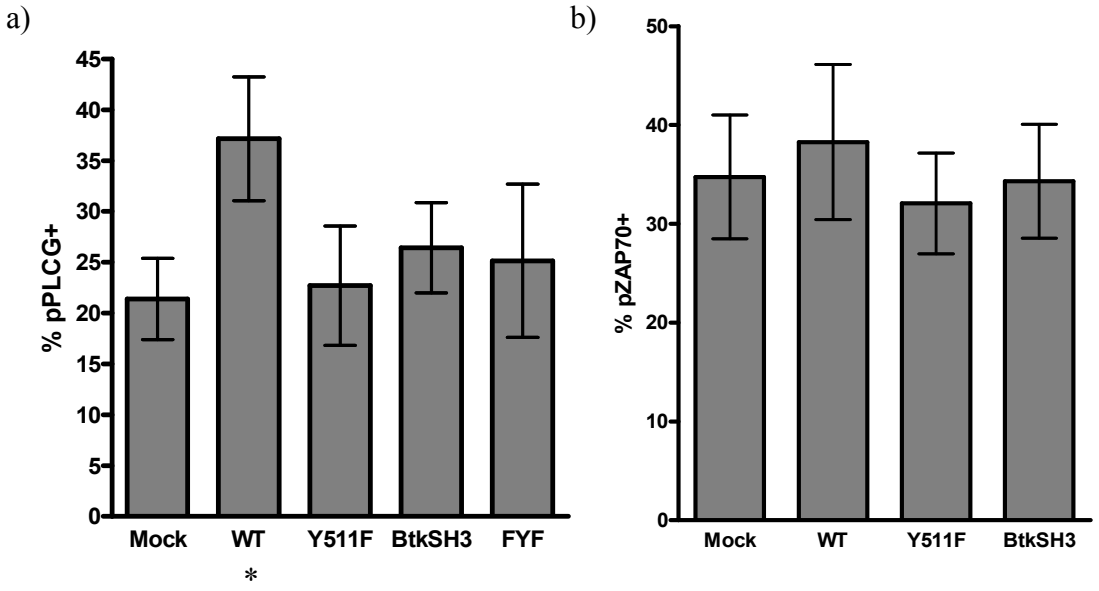

Figure 25. Cumulative phosphorylation in PLCγ and ZAP-70.

Average (±SEM) percentage of pY783 positive cells of three replicate experiments: A) Murine thymocytes from ITK-deficient mice, nucleofected with the indicated ITK constructs, were stimulated with anti mouse-CD3ε antibodies and then analyzed for PLCγ1 phosphorylation using Alexa 647-tagged antibodies that react with PLCγ1 pY783, as described in Materials and Methods section. The * denotes that the average of pY783 positive cells in WT-ITK nucleofected group is significantly different from the rest of the groups at $p<0.05$ (student's t test). The dotted line demarcates the specific anti-pY783 reactivity; B) average (±SEM) percentage of pY319 positive cells of four replicate experiments performed as described above, but analyzed for ZAP-70 phosphorylation using Alexa 647-tagged antibodies that react with ZAP-70 pY319. Each bar represents an average of at least four independent experiments.

Cytokine production

To assess the biological effects of Itk mutants, cytokines had to be assessed as a factor that plays the main role in pathogenesis of asthma and in normal immune system functioning. The cytokines that are relevant for these purposes were never assessed in these mutants, so assessment of type 2 cytokines was particularly interesting, as Itk was shown to have major influence on Th2 development pathway (86,126). Because most thymocytes are undifferentiated (127), and C57BL6 mice cells are more prone to Th1 type responses (128), it is necessary to skew cells toward a particular lineage (Th2 in our case) to be able to receive meaningful data on type 2 cytokine production.

Skewing was performed by blocking IL12 production after initial stimulation by αIL12, and stimulating Th2 development by adding a mixture of IL4 and IL2 to the culture medium. To establish the validity of this technique, we compared cells skewed toward Th2 developmental pathway with cells skewed towards Th1 skewed cells, and nonskewed cells. As predicted by available literature data (128), Th2 skewed cells demonstrated higher production of IL4 cytokine in wild type nucleofected cells under secondary stimulation (data not shown).

To elucidate the optimal range of secondary stimulus concentration that would be suitable to better distinguish Itk effects in type 2 cytokine production we performed stimulus titration in skewed cells (see Figure 26). Concentration around 0.2 μg/ml turned out to be optimal for assay resolution.

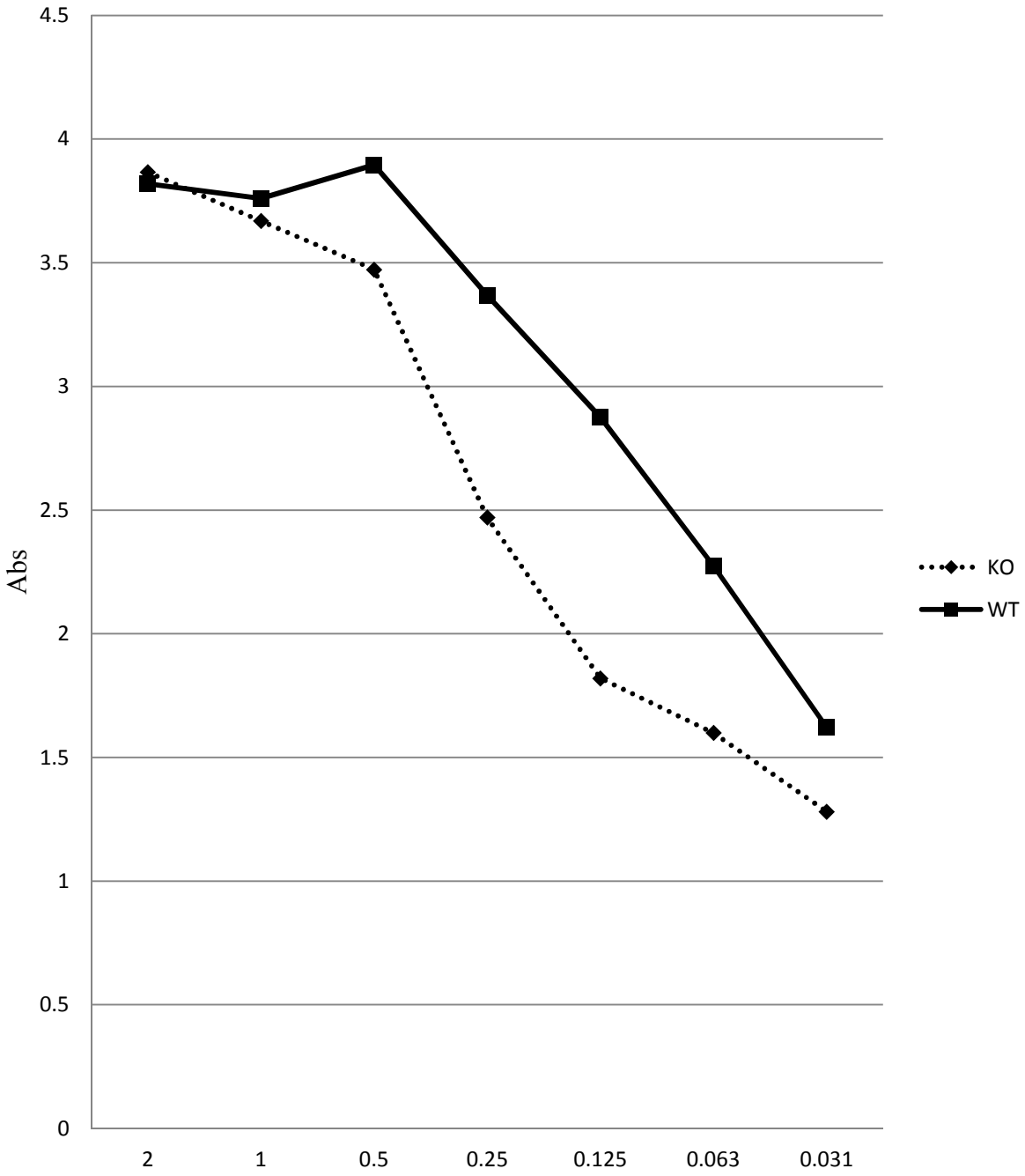

Figure 26. IL4 production in skewed thymocytes under different concentrations of secondary stimulus

Murine thymocytes were nucleofected with WT-ITK constructs or mock nucleofected, and then cultured under Th2 skewing conditions as described in the Materials and Methods section. Culture supernatants were assayed in duplicate for IL-4 using commercial ELISA assay kits and following manufacturer's recommendations.

After establishing optimal conditions, IL4 production was measured in medium of Itk$^{-/-}$ thymocytes nucleofected with mutants of interest, and skewed toward Th2 developmental pathway. Cumulative data of two independent experiments is shown in Figure 27. Y511F, the mutant incapable of getting phosphorylated by Lck; K390R, a kinase dead mutant; FYF, a mutant with disrupted structural motif in the PH domain; and Btk-SH3, a mutant with disrupted noncanonical ligand binding, all showed significant reduction in production of IL4 compared to wild type construct, with Y511F demonstrating drastic reduction to the level demonstrated by mock transfected Itk$^{-/-}$ thymocytes.

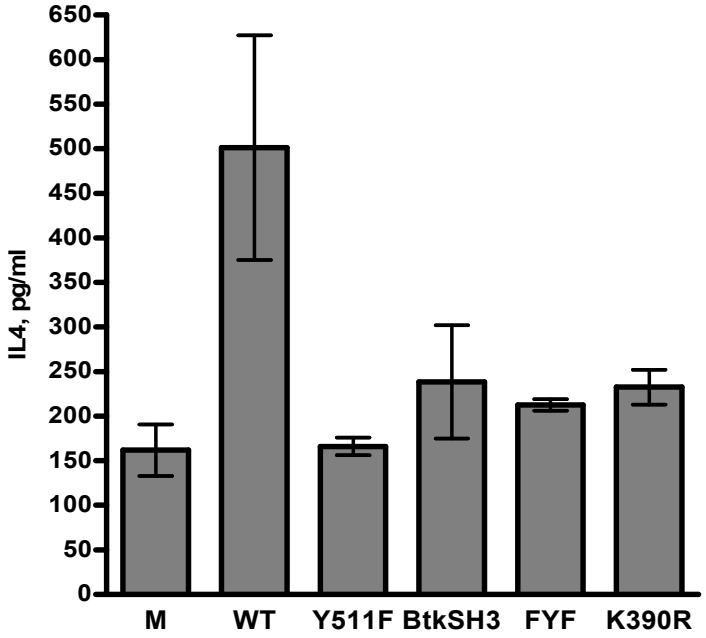

Figure 27. Deficient IL4 production by Itk mutants

Murine thymocytes were nucleofected with the indicated ITK constructs and then cultured under Th2 skewing conditions as described in the Materials and Methods section. Culture supernatants were assayed in duplicate for IL-4 using commercial ELISA assay kit and following manufacturer's recommendations. Results are displayed as the averages (±SEM) of three replicate experiments.

Measurement of IL13 and IL5 production in Th2 skewed cells showed a similar effect (see Figure 28). Y511F and Btk-SH3 transfected thymocytes showed significant reduction in production of both, IL13 and IL5 cytokines.

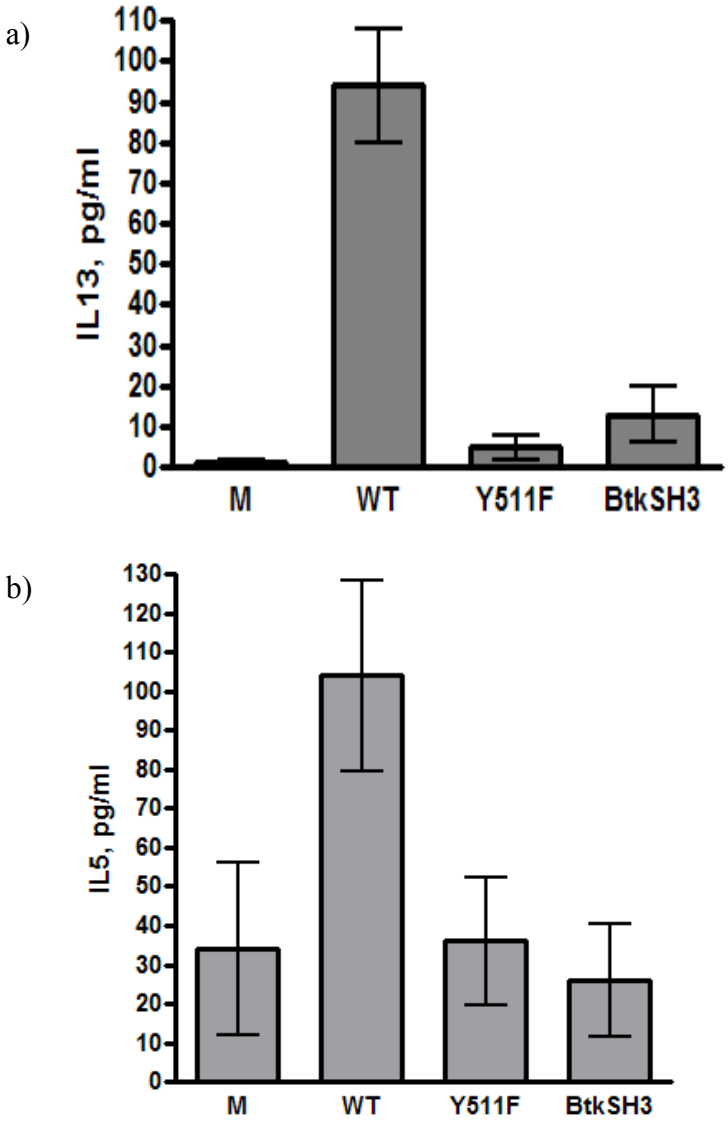

Figure 28. Deficient IL13 and IL5 production in mutants.

Murine thymocytes were nucleofected with the indicated ITK constructs and then cultured under Th2 skewing conditions as described in the Materials and Methods section. Culture supernatants were assayed in duplicate for IL-13 (A) and IL-5 (B) using commercial ELISA assay kits and following manufacturer's recommendations. Results are displayed as the averages (±SEM) of two replicate experiments for each cytokine.

Acknowledgement of use of published materials

Part of the data in this section was included in following publications:

1. ***Levytskyy R.M., Hirve N., Rigaud S., Sauer K., Zal T., Tsoukas C.D.*** Effects of the mutation in FYF motif of the Pleckstrin Homology (PH) domain of Itk (in preparation)

2. ***Levytskyy R.M., Hirve N., Guimond D.G., Min L., Andreotti A.H., Tsoukas C.D.*** In Vivo Consequences of Disrupting the Transphosphorylation and Intermolecular Self-Association of the Inducible T Cell Kinase (ITK) (Submitted to Journal of Biological Chemistry)

Permission for use of the published data in dissertation was received from all co-authors.

DISCUSSION

Spatial distribution of Itk at rest

We systematically characterized conformation and localization of various Itk mutants in relevant cells at rest – Jurkat T-cell line, and were the first to probe for different possible physiologically relevant scenarios of disrupting the Itk conformation at resting state.

We tested several mutants of SH3, SH2, SH1, and PPR domains in resting JTag cells, and were not able to find significant difference in FRET intensity or distribution compared to wild type (Figure 15). This result did not depend on presence of endogenous Itk (Figure 12, Figure 13). Our results conclusively show that at resting state, none of the available mutants disrupted resting Itk conformation(s), pointing on two possible scenarios: a) confirming the data presented by Qi et. al. in a similar system (33), and reaffirming the intramolecularly closed resting model by Andreotti et al (32), or b) showing that Itk does not assume a major conformation in the resting cell, and exists in multiple disordered semi-stable conformations (Andreotti A.H., oral communication). We also showed that neither overexpression (up to 4x excess as determined by amount of transfected DNA) of Itk (Figure 12) nor elimination of endogenous Itk (by using Itk deficient 293T cell line, Figure 13) has an effect at on an Itk conformation at rest. Overexpression of nonfluorescently tagged Itk along with fluorescently double-tagged Itk would cause changes in FRET if there were dimers formed because of the nonfluorescent Itk competing with fluorescent molecules in

dimer formation causing less FRET capable dimers found. This was not the case in our study, which may point to either absence of dimers, or to their presence in a dynamic range undetectable by the FRET biosensors. Absence of endogenous Itk, on the other hand, would increase FRET in case dimers were forming by making more FRET-capable dimers. This has not been the case either. These results are in contrast to a hypothesis in the literature that there exists a pool of oligomeric Itk in the cell where oligomerization is an intermediary step before activation (129).

There were also no detectable head-to-head, head-to-tail, or tail-to-tail Itk aggregation as measured by FRET from co-transfected single-FP labeled Itk molecules (Figure 14). In case of dimer formation in any of the possible molecule positions, we would expect to see restoring FRET from basal level to the level demonstrated by double FP tagged Itk construct. However, in contrast to previously reported observations by Qi et al (29), we were not able to detect dimer formation in any of the theoretically possible molecule positions, which may point to either one stable closed conformation or multiple disordered semi-stable conformations at rest.

These results can be interpreted as evidence that Itk either maintains stable conformation at rest or has multiple disordered conformations, and thus is relatively unaffected by point mutations in functional areas of various domains, and without evidence of aggregation or other interactions that disrupt N- and C-terminal relative locations. In contrast to data by Qi et al (29), we neither see higher Itk distribution at the membrane, nor detectable dimer formation at the membrane of the cells without stimulation. This might be caused by either artifacts of the system used by Qi et al.

(29) to measure aggregation (half-YFP complementation system), or the less relevant system used to express Itk constructs (lentivirus based overexpression in nonlymphoid cell line), or the changes might be of very small magnitude, which is effectively undetectable by FRET biosensors.

Spatiotemporal distribution of Itk under stimulation

We were the first to assess conformational change in Itk during TCR-induced stimulation, and in relation to its localization, and were the first to show that Itk forms a spatiotemporal pattern upon TCR-induced activation at the T cell-APC contact site.

First, we decided to assess the localization kinetics of the Itk (Figure 17). It was known from the literature that Itk localizes to the membrane under stimulation (51). However, considering that maximum localization timeline was unknown, and taking into account that we used a slightly different system, we performed a localization kinetics study of the wild type Itk. It turned out to have a maximum localization peaking at 3' after stimulation.

This time point was further used for localization and FRET studies in the mutants on the assumption that most likely the conformational change, if it occurs, is directly or indirectly linked to localization of Itk to the membrane.

Of the three mutants tested, only FYF mutant showed a significant disruption of localization, even though it was not completely absent as in case of negative controls (Figure 18). This finding reinforces the previously published knowledge about the importance of PH domain in Itk localization (51,52). However, it also shows that integrity of the FYF motif in the structure of the PH domain is important for proper function of the molecule and is related to membrane-binding capacity. This motif was shown to be a conservative part of PH domain in TEC kinases, and in Btk is believed to play a role in determining the binding specificity of the PH domain (55,130). It was also suggested that mutations in FYF motif in Btk might be

responsible for XLA-like symptoms (55). Other mutants surprisingly showed normal localization (Figure 18). Normal localization of the Btk-SH3 mutant eliminates a possibility of a direct link between SH3 domain noncanonical protein interactions and membrane localization, as could be inferred from the important role of SH3 domain interactions in Itk functionality (4,44,9). The fact that Y511F mutant demonstrates normal localization can be interpreted as evidence that membrane localization does not require Lck phosphorylation on Y511 residue, and is mediated by a different, possibly unrelated mechanism. This also points to the assumption that Itk localization is an earlier event than phosphorylation of Itk on Y511 residue.

When we used FRET technique to track possible conformational change under stimulation, surprisingly in wild type Itk we could see a clear reproducible FRET pattern in the area adjacent to the contact site between the T cell and the APC (Figure 19, Figure 20). Areas on the sides of the contact site including cytoplasmic protrusions semi-engulfing the APC (“arms”) showed significantly higher FRET signal than the middle section of the contact site (“center”). This observation hints at a differential Itk conformation pattern in the different areas of the contact site, resembling that of SMAC (131). Kinetics of the pattern roughly corresponded with the localization kinetics, so we could assume pattern formation and localization might be linked (Figure 20).

Surprisingly, all mutants showed significant disruption of the normal wild type Itk conformation pattern, and in FYF mutant it was completely disrupted (Table 2). This observation in combination with observations from resting cells shows that the

mutations we tested all contributed to an inability to change a conformation under stimulation to that of the wild type construct, and postulated that this effect might also have relevance to functionality of the molecule, as it is widely known that protein conformation has a direct influence on its function.

The above-mentioned observations underlined several important issues present in multiple published Itk studies to date. First of all, use of nonrelevant cell systems, including unstimulated cells (29), cell-free systems (24), overexpression in nonlymphoid cell systems (29), and similar methods would be inadequate, as they do not form a conjugate, and thus, cannot demonstrate separate areas of the contact site. The second issue is that studying Itk in cells without assessing multiple facets of its function may lead to missing important clues that could be detected with a more systemic approach and more targeted methods like the ones employed in our work.

Y511 phosphorylation and SLP-76 interaction

SLP-76 interaction showed unexpected results with Y511F mutant maintaining the interaction (Figure 21). The fact that Y511F mutant was able to bind SLP-76 shows that Y511 phosphorylation and SLP-76 binding are separate, and not directly related events, and that interaction of SLP-76 with Itk does not require previous phosphorylation of Y511 residue of Itk. On the other hand, Btk-SH3 mutant demonstrated a disrupted binding of SLP-76, which was quite unexpected. NMR data in the literature showed that Btk-SH3 mutant binds normally with a peptide mimicking binding sequence for Itk SH3 domain on SLP-76 (35). Our data suggest that other Itk domain interactions, presumably SH2 domain, may play a role in Itk-SLP-76 interaction either directly by binding of SLP-76 by SH2 domain of Itk, or indirectly by forming the appropriate conformation of Itk via SH2-SH3 interactions. The fact that the interaction was not completely disrupted can be attributed to the data from the literature that suggests that Itk and SLP-76 are a part of the SLP-76-LAT signalosome (66,65), and thus we can assume they could co-immunoprecipitate as part of the complex for example by being bound to a common partner LAT and several other supplementary proteins on condition the binding of the proteins in the complex is strong enough to withstand the manipulations during the immunoprecipitation.

We tested Y511 phosphorylation as one of the important milestones in Itk activation (62). As expected, Y511F showed low signal on par of that of the mock transfected sample in $Itk^{-/-}$ mouse system (Figure 6), and far below all other stimulated samples on western in JTag system (Figure 5). Btk-SH3 and FYF mutants showed

partial, albeit significant, disruption of Itk phosphorylation pattern, hinting at a possible link between conformation changes studied by FRET and Itk molecule functionality. Background phosphorylation in $Itk^{-/-}$ system can be explained with the specificity of the antibody, which is raised against homologous Btk phosphorylation signal, and thus we expected it to cross-react with other TEC kinases, notably with Tec and Rlk, which are relatively abundant in $Itk^{-/-}$ lymphocytes (132).

Phosphorylation assays were confirmed by two independent methods in two different systems, and showed similar results (Figure 5, Figure 6). However, phosphorylation data obtained for BtkSH3 mutant is in contradiction with data obtained by Min et al. (34). This can be explained by the use of different cellular systems to assess the situation. We tested our data in two systems – one relevant lymphoid cell line system, and an $Itk^{-/-}$ mouse system, and we think that both of them have a significant advantage compared to the nonlymphoid system used by Min et al. (34).

Signaling cascades

It was shown in the literature that $Itk^{-/-}$ mouse splenocytes tend to have lower PLCγ1 phosphorylation than wild type splenocytes as assessed by western blotting (77,87). However, there were no attempts to use a more quantitative approach. This is particularly important when trying to establish the influence on level of PLCγ1 phosphorylation by different mutants, which might have a partial effect that is hard to distinguish and/or quantify on a western blot.

The approach we used allowed us to do direct objective quantification of PLCγ phosphorylation as a downstream target of Itk activity (Figure 24). Our system also allowed studying effects of the mutants without interference from endogenous Itk and avoiding other artifacts of cell lines such as PTEN deficiency in Jurkat cells (133).

Effects of Y511F mutant were similar to those reported by Wilcox et al. (9), and showed significant decrease. However we found that in our system BtkSH3 mutant also showed decrease in activity, contrary to the data by Min et al. (34) that showed increase in PLCγ phosphorylation in a different cell system. This discrepancy can be explained by the fact that we used a more relevant ex vivo system – transfected $Itk^{-/-}$ thymocytes that mimic natural conditions for Itk functionality better. We were the first to research the effect of FYF mutant on PLCγ phosphorylation, and showed that it was disrupted as well. In combination with the localization data, this observation points to the importance of intact Itk membrane localization for the functionality of Itk, reinforcing the available data from the literature on Itk PH domain (51).

We used ZAP-70 phosphorylation as an upstream event to Itk activity to make sure that there is not a feedback loop upstream of Itk influencing the results (Figure 25), following similar logic used by Liu et al. (77) when studying $Itk^{-/-}$ effects. As expected, ZAP-70 did not show significant difference in phosphorylation under stimulation in cells transfected with different mutants.

High background in pPLCγ phosphorylation experiments can be attributed to the presence of TEC and Rlk in thymocytes. These kinases were shown by several authors to compensate to a certain extent the effects of the absence of Itk (132,78,134,2).

These results lead us to a conclusion that both, SH3 and PH domain integrity are necessary for Itk to efficiently phosphorylate its target PLCγ. Even though SH3 domain of Btk has some similarities in structure to SH3 domain of Itk, evidently they are not sufficient to maintain nonconventional protein interactions important for phosphorylating PLCγ. The fact that BtkSH3 mutant in our experiments also showed disrupted binding of SLP-76 might imply that nonconventional protein interactions of SH3 domain could have important function directly related to PLCγ phosphorylation. Our study of the FYF mutant reinforces the importance of the PH domain in Itk activity, and in particular of the FYF structural motif that has not been studied before. By combining information on PLCγ phosphorylation with data from localization experiments, we can suggest that disruption of the FYF motif prevents efficient long-term placement of Itk at the SLP-76-LAT signalosome. One of the hypothetical mechanisms might be the inability of FYF mutant to anchor at the membrane,

considering the role of PH domain in binding IP4 (49). Our findings show that Y511F, BtkSH3, and FYF mutants all negatively influence PLCγ phosphorylation, but apparently through completely different and not directly related mechanisms.

Cytokines

It was known that Itk plays role in production of Th2 cytokines as its signature cytokines (81,87), as well as IL2 (9,77) from experiments comparing $Itk^{-/-}$ splenocytes versus wild type splenocytes. It was shown that $Itk^{-/-}$ splenocytes have reduced IL4 production after primary and secondary TCR induced stimulation (87), and $Itk^{-/-}$ splenocytes, as well as Y511F mutant have reduced IL2 production (9). Also, it was shown that this effect depends on intensity of the stimulus (9,87). However, how production of IL4 and other relevant Th2 cytokines is affected by Y511F mutation, or other mutations remained unknown.

Miller et al. (87) who used the same C57BL6 $Itk^{-/-}$ mouse strain as ours, found that unskewed cells tend to differentiate into Th1 pathway under low stimulation, and thus produce IFNγ instead of IL4 (87). This necessitates skewing the cells towards Th2 pathway in order to elicit meaningful data on Th2 cytokine production. Another contributing factor to the lack of difference between wild type, mutants, and mock samples in unskewed cells is the presence of Rlk, which can partially substitute for lacking Itk (132,135).

Skewing cell into Th2 development path allowed separating the effects of Itk from other TEC kinases present in T cells, as it is known that expression of the Itk increases significantly under Th2 type stimulation (5,87). However, there is some background in the cytokine experiments in skewed knockout cells that might be attributed predominantly to Tec kinase, that was shown by others to increase expression after prolonged stimulation and differentiation, especially in Th2 cells

(136). Also, Tec seems to be optimally activated at the same conditions as Itk in our experiments by using TCR and CD28 stimulation (137). Rlk expression was shown to be low in Th2 skewed cells (132,135). Background in ELISA essays could also be caused by the same factors that influenced the background in our PLCγ1 phosphorylation experiments. However, the magnitude of this effect is lower, as far as cytokine production starts several steps downstream of Itk, and the signal could have a chance to go through several amplification steps.

As was expected on the basis of our PLCγ phosphorylation data, Th2 cytokine production was impaired in all tested mutants (Figure 27, Figure 28). This data complements the data by Wilcox et al. (9), which looked at IL2 production in Itk mutants, particularly in Y511F mutant, showing downregulation. Our data also confirms a stimulus strength dependent difference between $Itk^{-/-}$ and wild type thymocytes cytokine production (9), Figure 26. It was pointed out that Itk function most probably lies in amplification of weak stimulatory signals. However, there was only indirect evidence in the form of the effects on IL2 production (9), which is not the typical Th2 cytokine, and not the most critical for disease conditions such as asthma. We were the first to show that this effect holds true for Th2 cytokines, such as IL4, which have clinical relevance in several immune diseases (138,139).

From the cytokines tested, IL4 showed the highest differences dependent on intact Itk molecule presence (Figure 27), while IL13 and IL5 showed more moderate effects (Figure 28). This is in line with published experiments done by our group in $Itk^{-/-}$ mouse systems, which show that IL4 is a signature cytokine for Itk (35), as well

as by other groups (126,140). Our results also show that all the mutations of Itk studied in this work ultimately result in disruption of the Th2 function in T cells by inactivating the signal amplification role of the Itk. However each mutant acts through a different mechanism.

Conclusion

We showed that Itk is distributed randomly and uniformly in the cytoplasm at rest, and either has a uniform stable conformation, or has multiple semi-stable disordered sonformations. We were not able to see evidence of dimer formation at rest using different methods to probe for this possibility. Thus, within the sensitivity limitations of the FRET biosensor method, our work helps to support one of the models of Itk conformation proposed by August group (33), but not the other proposed by the same group (29). It also supports the conformational model developed by Andreotti et al. (32).

We were the first to show that, under stimulation, Itk undergoes conformational change, forming a specific spatiotemporal pattern with different conformations in the "arms" and the middle of the contact site. Mutations in different domains of Itk affect pattern formation, as well as functionality of the molecule.

Interestingly, only one of the mutants showed a significant defect in localization under stimulation – FYF mutant. The reason might be reduced functionality of PH domain, and inability to efficiently anchor molecule at the membrane, as this domain is known to interact with the membrane (49). None of the mutants showed negative effect on Y511 phosphorylation except for previously known mutant Y511F (9). Only one of the mutants (Btk-SH3) showed significant reduction in SLP-76 interaction, which might be caused by disruption of the SH3 domain protein interactions, and resulting impact on functionality.

All mutants showed significant impact on PLCγ phosphorylation, which hints at the importance of integrity different domains of Itk for Itk functionality, and involvement of different mechanisms in loss of function of Itk molecule by different mutations. We were the first to show this via quantitative method in a relevant $Itk^{-/-}$ system.

We were also the first to show that the same effect is observed as well on Th2 cytokine production in Th2 skewed $Itk^{-/-}$ thymocytes transfected with Itk mutants. This data directly links mutations in Itk domains with clinically relevant cytokines, and shows that they follow similar pattern to previously shown effects on IL2 (9). Nonskewed cells showed no difference in Th2 cytokine production neither by ELISA, nor by ICCS, confirming previously available research (87).

Our work involved systematic and comprehensive study of the effects of important mutations in SH3, SH1, and PH domain, and we were able to show their impact on different levels using complementary approaches, which will hopefully prove useful for characterization of other clinically relevant mutations in Itk or other kinases in order to gather extensive information on functionality of the kinases of interest. The information gathered about Itk could also prove useful for the further research and characterization of this important kinase, complete understanding of details of its regulation, and possible use of this knowledge in design of selective Itk activity modulators of therapeutic significance for common diseases such as asthma.

APPENDIX 1. EXPERIMENTAL PROTOCOLS

General reagents

10x PBS (1L)

- 80g NaCl
- 2g KCl
- 14.4g Na_2HPO_4
- 2.4g KH_2PO_4

Adjust pH to 7.4

Add DIUF H_2O to 1L

Autoclave

0.5M Tris, pH 7.5 (100 ml)

- 6.06g Tris
- Add DIUF H_2O to 100ml

Adjust with HCl to pH 7.5,

Filter

Keep at +4^{o}C

1M Tris, pH 7.5 (500 ml)

- 60.5g Tris
- Add DIUF H_2O to 500ml

Adjust with HCl to pH 7.5

Filter

Keep at +4^{o}C

0.5M EDTA, pH 8.0 (100 ml)

- 18.6g EDTA
- DIUF H_2O to 100ml

Adjust with HCl to pH 8.0

Filter

Keep at +4^{o}C

10N NaOH

- 20g NaOH
- Add DIUF H_2O to 50ml

Store in 50 ml Falcon tube at room temperature

Cell maintenance

Counting cells

Materials:

10% Erythrosin B in PBS

Protocol:

1. Resuspend cells by vigorously shaking the flask
2. Under the sterile flow hood transfer 0.1 ml of suspension into the Eppendorf tube using 1 ml disposable pipette
3. Add 0.1 ml 10% Erythrosin B
4. Mix
5. Inject under cover glass
6. Count under the microscope
    a. Count all cells in big square grid
        - Include borderline cells from down and right
        - Exclude borderline cells from up and left
    b. Number of cells counted will be equivalent to millions of cells in 50 ml of medium
    c. To get number of cells per ml, multiply by 20,000

Separation of live cells with Histopaque

Materials:

Histopaque (3 ml per sample)

15 ml Falcon tubes (2 per sample)

PBS

RPMI

Protocol:

1. Add 3 ml of histopaque on the bottom on 15 ml Falcon tube
2. Resuspend cells in 10 ml RPMI
3. Layer cell suspension on top of the histopaque
4. Pellet 30 min at 1,500 RPM
5. Transfer middle layer with 1 ml pipette into new 15 ml Falcon tube
6. Wash 2x
    a. Add 10 ml of PBS or RPMI
    b. Resuspend
    c. Pellet 5 min at 1,000-1,500 RPM in TC centrifuge
    d. Spill out supernatant
7. Now live cells are in the pellet

Growing cells

Preparation of RPMI or DMEM Medium (1L)

- Add 5 ml L-Glu
- Add 5 ml Pen/Strep (do not add for medium in Lipofectamine transfection)
- Add 5 ml HEPES

- Mix

Suspension cells (JTag, E6.1, Raji, DO11.10)

Materials:

FCS (5 ml per sample)

RPMI (45 ml per sample + resuspension volume)

Cells

75 cm^2 flasks

Protocol:

1. Count cells
2. Prepare a 75 cm^2 flask
    - Add 5 ml FCS (10% final concentration)
    - Add X ml RPMI where X = 45 - volume of cell suspension
3. Pellet cells at 1,000-1,500 RPM for 5 min in TC centrifuge
4. Resuspend pellet in RPMI
5. Add to a flask (amount of cells added should be ~0.2-0.5x10^6 per ml final concentration, 10-25x10^6 per 75 cm^2 flask)
    - Cells should be grown to reach 0.5-1.2x10^6 cells per ml at the day of the experiment
    - Change medium every 48 hours

Changing medium for suspension cells

1. Count cells
2. Pellet 5 min at 1,500 RPM in TC centrifuge
3. Resuspend pellet in RPMI
4. Transfer needed amount into new flask with prepared medium

Adherent cells (293T, HEK293)

1. Check confluency
2. Prepare a 75 cm^2 flask
    - Add 5 ml FCS (10% final concentration)
    - Add X ml DMEM where X = 45 - volume of cell suspension
3. Carefully spill away medium from old flask
4. Add 2 ml Trypsine
5. Rotate to cover bottom of the flask evenly
6. Wait 5 min
7. Rotate flask until all cells detach
8. Add 5 ml DMEM
9. Resuspend cells
10. Add to a flask (amount of cells added will depend on confluency)

Freezing cells

Materials:

At least $5x10^6$ cells per tube

Freezing medium (90% FCS, 10% DMSO)

- 9 ml FCS
- 1 ml DMSO

Cryovials

Cotton Box

Protocol:

1. Count cells
2. Resuspend at $5x10^6$ cells per ml in freezing medium
3. Transfer 1 ml per cryovial
4. Seal vials tightly
5. Put into a cotton box
6. Put into -80^oC freezer for 24 hours
7. Transfer into liquid nitrogen tank
8. Record in log

Thawing cells

Materials:

75 cm^2 flask

Full medium

- 5 ml FCS
- 45 ml RPMI (DMEM)

Protocol:

1. Take a vial out of the liquid nitrogen
2. Transfer into 37^{o}C water bath until it thaws
3. Bring under the sterile flow hood
4. Wash the surface of the vial with ethanol
5. Open the vial
6. Wash the rim of the vial with ethanol
7. Transfer content into 75 cm^2 flask with full medium and put into CO_2 incubator
8. Record container and shelf number into log journal

Cell transfections

Biorad

Materials:

20x10^6 cells needed per one sample

75 cm^2 flasks (one per sample)

FCS (5 ml per sample)

RPMI (45 ml per sample)

Protocol:

1. On ice (+4^{o}C)
    - Label cuvettes

- Add 20 μg DNA per cuvette

2. Pellet cells 5 min at 1,000-1,500 RPM in TC centrifuge in 50 ml Falcon tubes
3. Resuspend pellet in RPMI
4. Pellet cells 5 min at 1,000-1,500 RPM in TC centrifuge in same tubes
5. Dilute pellet with RPMI to concentration $40x10^6$ cells per ml ($20x10^6$ per 0.5 ml)
6. Transfer 0.5 ml of cell suspension into cuvette under the sterile flow hood
7. Put on ice (+4^{o}C) for 20 min
8. Electroporate at 0.25 V
9. Put back on ice for 5 min
10. Transfer content of the cuvette into prepared 75 cm^2 flasks with full medium (RPMI with L-Glu, pen/strep, and 10% serum) under the sterile flow hood
11. Put into CO_2 incubator (37^{o}C, 5% CO_2)
12. Expect maximum expression level 48 hours after transfection

Lonza JTag transfection

Materials:

Solution V

FCS

RPMI

5 cm^2 dishes or 6-well plates

15 ml Falcon tubes

Amaxa cuvettes

Protocol:

1. Pre-warm Solution V
2. In 5 cm^2 plastic cell culture dishes or 6-well cell culture plates
    - Add 0.2 ml FCS
    - Add 1.8 ml RPMI
3. Count cells
4. Pellet cells 5 min at 1,500 RPM in TC centrifuge
5. Resuspend pellet at $5x10^6$ cells per ml
6. Add 1 ml suspension into new 15 ml Falcon tube
7. Add 10 ml RPMI
8. Mix
9. Pellet 5 min at 1,500 RPM in TC centrifuge
10. Resuspend pellet in 100 µl Solution V
11. Add 5 µg DNA

12. Transfer to Amaxa cuvette
13. Insert into Amaxa apparatus
14. Select program S-18
15. Press X
16. Transfer into dishes or wells
17. Expect maximum expression level 24 hours after transfection

Lonza mouse thymocyte transfection

Materials:

Mouse

Isofluoreine

1,000 ml Beaker

Ethanol

Surgery set

Regular transfer pipettes

70 µl nylon filter

Syringe plunger

Erythrocyte Lysis Buffer

Full Lonza Medium (FCS, Component A, and Glu-supplemented)

Supplemented Nucleofector Solution

Component B

RPMI

12-well cell culture plates

15 ml Falcon tubes

50 ml Falcon tubes

Lonza cuvettes

Lonza transfer pipettes

Protocol:

Preparations:

1. Pre-warm
    - Nucleofector Solution
    - Lonza Medium
    - Component B
2. In 12-well cell culture plate (for each experimental well)
    - Add 1.5 ml Lonza Medium
    - Add 15 µl Component B
    - Mix
3. Transfer 12-well cell culture plate with medium into CO_2 incubator for 30 min
4. Prepare 10 ml RPMI medium in 15 ml Falcon tube on ice (+4^{o}C)
5. Prepare 1000ml beaker
    - Add 2 kimwipes on the bottom
    - Add 5 drops of Isofluoreine
    - Cover

Sacrifice:

1. Take out the mouse by the tail
2. Put into the beaker
3. Cover
4. Wait while mouse gets anesthetized (stops heavy breathing)
5. Take the mouse out
6. Perform cervical dislocation by holding a mouse at the base of the neck and pulling its tail until cranium is disconnected
7. Turn the mouse over
8. Sterilize the rib cage and belly area with ethanol

9. Take the skin near the middle of the area with index and thumb fingers
10. Lift the skin over rib cage
11. Make a small horizontal cut through the skin
12. Flay the rib cage by pulling the skin off with fingers in head direction until skin is removed from the rib cage

13. Locate the breast bone
14. Take a pelvic membrane under the breast bone with a forceps
15. Make a small horizontal cut through the membrane
16. Expand the cut horizontally to the right by cutting the membrane under the rib cage till ½ the distance from the breast bone

Isolating the Thymus:

1. Take the lower end of the breastbone with a forceps
2. Lift the breastbone slightly
3. While lifting the breastbone, cut the rib cage close to the breastbone on the right side in forward direction
    - Cut enough to make heart and thymus accessible
    - Do not proceed outside the rib cage, because it will immediately fill the rib cage with blood from nearby arteries
4. Operating with two forcepses open the rib cage
5. Grab the thymus gently with one forceps
6. Using small scissors, separate thymus from surrounding tissues
    - Do not puncture the heart!
7. Put thymus into the prepared medium on ice

Thymocyte isolation:

1. Transfer under the sterile flow hood
2. Put 70 μm nylon filter into the 50 ml Falcon tube
3. Using transfer pipette
4. Wet the nylon filter
5. Transfer the thymus onto the filter
6. Squish the thymus with syringe plunger using circular motions until thymus goes through the filter
7. Wash the filter with leftover medium
8. Pellet cells 5 min at 1,500 RPM in TC centrifuge

9. Lyse erythrocytes
    - Add 10ml Erythrocyte Lysis Buffer
    - Put on ice (+4^{o}C) for 5 min
    - Spin 5 min at 1,500 RPM in TC centrifuge
10. Resuspend the pellet in 10 ml RPMI

11. Count cells
12. Take out the needed amount (10x10^{6} cells per transfection)
13. Aliquot into Eppendorf tubes
14. Spin at 1,500 RPM in TC centrifuge

Nucleofection:

1. Prepare Eppendorf tubes with DNA (10 µl, 2 µg/µl, or 5 µl control GFP plasmid)
2. Take out the 12-well cell culture plate from CO_2 incubator and place under the sterile flow hood

3. Process each sample separately from here till transfer into 12 well plate

4. Aspirate supernatant above the pellet (aspirating it completely is critical!)
5. Resuspend the pellet in Nucleofector (100 µl per transfection, do not keep them in Nucleofector longer than 15 min!)
6. Transfer immediately to Eppendorf tubes with DNA (100 µl cell suspension per tube)
7. Mix using supplied transfer pipette

8. Transfer into Lonza cuvette
9. Electroporate with Amaxa machine
    - Select X-001 program
    - Press “X” button
10. Transfer immediately into a well of medium in 12-well cell culture plate
11. Mix

12. After all transfections are done move the plate into the CO_2 incubator for 24hr (37^oC, 5% CO_2)
13. Expect maximum expression level at 24-48 hours after transfection
14. The cells are capable of getting stimulated 3 hr after transfection

Lipofectamine

Materials:

10 cm cell culture dishes

- 24 µg DNA
- 60 µl Lipofectamine
- 2x750 µl medium

2 cm cell culture dishes

- 4 µg DNA
- 10 µl Lipofectamine
- 2x250 µl medium

Protocol:

1. Plate cells to be at 90-95% confluency at the day of the transfection

2. Dilute DNA in medium

3. Mix Lipofectamine
4. Dilute appropriate amount of Lipofectamine in 0.75 ml medium
    - Wait 5 min at room temperature
    - No more than 25 min
5. Mix DNA and Lipofectamine solutions in Eppendorf tube
    - Wait 20 min at room temperature
    - No more than 6 hrs

6. Transfer mixture to the cell culture dish
7. Distribute evenly

8. Incubate cells 24 hrs in CO_2 incubator (37^oC, 5% CO_2) for maximum expression

Reference

Lipofectamine 2000 Manual. Invitrogen, 2006

E.coli transfection

Materials:

Antibiotics

- Kanamycin 20 mg/ml H_2O
- Ampicillin 50 mg/ml H_2O

SOC medium

E.coli DH5α strain aliquots

Agar plates (10 cm with or without antibiotic)

- 15 g agar per 1L LB
- Autoclave for at least 30 min
- Cool down to 50^{o}C
- Add 5 ml Amp or Kan
- Spill into plates while still hot
    - Do it quickly
    - Fill plates about half way
    - Burn the bubbles with flame
- Let solidify overnight

Protocol:

1. Transfer aliquoted E.coli from -80^{o}C freezer into wet ice (+4^{o}C)
2. Thaw 30 min
3. Pre-warm agar plates in 37^{o}C warm room
4. Pre-warm SOC medium in 37^{o}C water bath
5. Add 1-5 µl DNA into DH5α tubes
6. Mix
7. 30 min on ice (+4^{o}C)
8. Prepare 42^{o}C water bath
9. Put tubes into the water bath for 45 sec
10. Immediately transfer to ice (+4^{o}C) and cool for 2 min
11. Take off the ice
12. Add 200 µl preheated SOC medium
13. Put into 37^{o}C shaker for 1 hr
14. Transfer 250 µl cell suspension onto agar surface and spread under flame
15. Put into 37^{o}C warm room
16. Plates should be placed upside down
17. Colonies will appear 24-36 hrs after transfection
    - Can be stored at +4^{o}C

DNA

Ethanol precipitation

Materials:

3.0 M Sodium Acetate, pH 5.2 (100 ml)

- 40.8 g per 100 ml H_2O

Protocol:

1. Add sodium acetate stock to the DNA solution to final concentration 0.3M
2. Mix
3. 1 hr on ice (+4^{o}C)
4. Centrifuge at 12,000 g for 15 min at +4^{o}C
5. Remove supernatant
6. Half-fill the tube with 70% ethanol
7. Centrifuge 12,000 RPM 10 min at +4^{o}C
8. Remove supernatant
9. Allow leftovers to evaporate in the sterile flow hood
10. Dissolve dry DNA pellet in needed volume of H_2O

Miniprep

Materials:

Day 1:

Colonies of E.coli on agar plate transfected with appropriate DNA

2xYT or LB

Glass culture tubes or 15ml Falcon tubes

Antibiotic (1000x Amp or 500x Kan)

Day 2:

15 ml Falcon tubes

Purification Resin

Minicolumns

Resuspension Solution, pH 7.5 (500 ml)

Add 3.94 g Tris

Add 1.86 g EDTA

Add 50 mg RNAse A

Add DIUF H_2O to 400 ml

Adjust pH to 7.5

Add DIUF H_2O to 500 ml

Keep at +4^oC

Lysis Solution (500 ml)

Add 25 g SDS

Add 4 g NaOH

Add DIUF H_2O to 500 ml

Keep at room temperature

Neutralization solution, pH 4.8 (500 ml)

Add 64.77 g potassium acetate

Add H_2O to 500 ml

Adjust pH

Keep at $+4^oC$

Column Wash, pH 7.5 (1L)

Add 7.85 g potassium acetate

Add 16.6 ml 0.5M Tris

Add 80 µl 0.5M EDTA

Add 579 ml 95% Ethanol

Add H_2O to 800 ml

Adjust pH

Add H_2O to 1L

Protocol:

Day 1:

1. Add 5 ml LB into glass culture tubes
2. Add 50 µl of resistance antibiotic (Kan or Amp)
3. Pick a colony from the agar plate using 200 µl pipette tip
4. Transfer into glass culture tube with medium
5. Shake in 37^{o}C bacterial shaker for 24 hours

Day 2:

1. Transfer cell suspension into 15 ml Falcon tubes
2. Pellet 5 min at 5,000 RPM (speed 6 at 10 min at larger centrifuge)
3. Spill out supernatant

Optional stopping point 1 (+4^{o}C, not more than 24 hrs)

4. Resuspend in 0.5 ml Resuspension Buffer
5. Transfer into Eppendorf tubes
6. Has to be finished in 5 min no matter what!!!
    - Add 0.5 ml Lysis Buffer
    - Mix by inverting tubes several times
7. Add 0.5 ml Neutralizing Buffer
8. Pellet 5 min at 13,400 or 15,000 RPM (the highest for the centrifuge)

Optional stopping point 2 (-20^{o}C)

9. Label minicolumns
10. Attach syringes
11. Attach minicolumns to the vacuum manifold
12. Add 0.5 ml purification resin
13. Add supernatant
14. Turn on the vacuum pump
15. After solution goes through completely, add 2 ml Wash Buffer
16. After buffer goes through column – unattach column from vacuum manifold and from syringe
17. Put minicolumn into clean Eppendorf tube
18. Cut the lid off
19. Pellet at 10,000 RPM for 5 min
20. Put minicolumn into new Eppendorf tube
21. Cut the lid off
22. Add 50 µl of slightly warm DIUF H_2O
23. Wait 5 min
24. Pellet at 15,000 RPM for 5 min
25. Transfer solution into new Eppendorf tubes
26. Store at -20^{o}C

Megaprep

Materials:

Day 1:

Colonies of E.coli on agar plate transfected with appropriate DNA

1L LB medium per sample

Antibiotic (1000x Amp or 500x Kan)

Day 2:

Large plastic Megaprep tubes (2 per sample)

Smaller plastic Megaprep tubes (at least 4 per sample, preferably 7 per sample)

Megaprep Columns (1 per sample)

50 ml Falcon tubes (2 per sample)

Purification Resin (5 ml per sample)

Resuspension Solution (30 ml per sample)

Lysis Solution (30 ml per sample)

Neutralization solution (30 ml per sample)

Column Wash (25 ml per sample)

70% ethanol (10 ml per sample)

Protocol:

Day 1:

1. Autoclave 1 L of LB in 2 L conical flask
2. Wait until cools down to 30^{o}C
3. Add 5 ml Amp or Kan

4. Pick a colony from the agar plate using 200 µl pipet tip
5. Put into prepared 1L medium
6. Shake in 37^{o}C bacterial shaker for 24-48 hours

Day 2:

1. Transfer cell suspension into two large Megaprep tubes per DNA construct
2. Pellet 20 min at 5,500 RPM (5,000 g)
3. Spill out supernatant

   Optional stopping point 1 (+4^{o}C, not more than 24 hrs)

4. Resuspend pellets from both tubes in 30 ml Resuspension Buffer
5. Transfer into 3 smaller Megaprep tubes 10 ml each
6. Has to be finished in 5 min no matter what!!!
   - Add 10 ml Lysis Buffer for each small Megaprep tube
   - Mix by inverting tubes several times
7. Add 10 ml Neutralizing Buffer
8. Mix thoroughly
9. Centrifuge 20 min at 10,000 RPM (14,000 g)

   Optional stopping point 2 (+4^{o}C)

10. Filter the supernatant through Watman paper filter into graduated cylinder
11. Add 0.7x volume of Isopropanol
12. Mix

13. Transfer into 4 small Megaprep tubes
14. Pellet 20 min at 10,000 RPM (14,000 g)

    Optional stopping point 3 (+4^{o}C)

15. Spill away supernatant
    - Pipette out all liquid (CRITICAL!)
    - Let dry open for ~30 min-1 hr
16. Add 4 ml H_2O to dissolve DNA in the first tube, then when pellet dissolves, transfer resulting solution to the next tube. Do for all 4 tubes.

17. Label Megaprep columns
18. Attach columns to the vacuum manifold

19. Add 5 ml Purification resin (shake well before use)
20. Add DNA Solution

21. Turn on the vacuum pump and apply vacuum
22. After solution goes through completely, add 25 ml Wash Buffer
23. After wash buffer goes through completely, add 5 ml 70% ethanol
24. After ethanol goes through column completely, unattach column from vacuum manifold and from syringe
25. Put column into 50 ml Falcon tube
26. Pellet at 1,500 RPM for 5 min
27. Put column into new 50 ml Falcon tube
28. Add 4 ml of warm (60-70^{o}C) PCR-grade DIUF H_2O into the column
29. Wait 5 min

30. Pellet at 1,500 RPM for 5 min

31. Transfer solution into new Eppendorf tubes

32. Store at -20^{o}C

DNA Quantification on the spectrophotometer

1. In Eppendorf tubes (1:200 dilution)
    - Add 5 µl DNA
    - Add 995 µl H_2O
2. Turn UV on spectrophotometer On
3. Select dsDNA, Short Oligo or Long Oligo
4. Blank with H_2O
5. Until run out of samples:
    a. Enter dilution and sample name
    b. Dry cuvette using kimwipes
    c. Transfer sample into cuvette
    d. Measure
    e. Wash cuvette with H_2O
6. Print out measurement results
7. Turn off UV

DNA gel electrophoresis

Materials:

General

50x TAE

- Add 242 g Tris
- Add 57.1 g glacial Acetic acid
- Add 100 ml 0.5M EDTA, pH 8.0
- Add DIUF H_2O to 1 L

6x Loading Dye

10% Ethidium Bromide in H_2O (toxic, wear gloves)

2 Log DNA Ladder

- Dilute 1:1:4 (2 Log DNA ladder stock : 6x Loading Dye : H_2O)

Small gel

50 ml 1x TAE for gel preparation

1x TAE for chamber (~200 ml)

0.4 g agarose

3 µl 10% Ethidium Bromide

Big gel

150 ml 1x TAE for gel preparation

1x TAE for chamber (~1 L)

1.2 g agarose

8 µl 10% Ethidium Bromide

Detection limit is ~20 ng DNA, maximum per lane ~20 µg.

Use small gel for analytical digests/PCR, big gel for preparative digests.

Protocol:

1. Prepare gel
    a. Weigh agarose in conical flask
    b. Add appropriate amount of 1x TAE
    c. Microwave ~5 min (until no grains of agarose are visible)
        - Take out and mix each 1 min
        - Do not let it boil!
    d. Take out
    e. Add appropriate amount of 10% Ethidium Bromide
    f. Mix
    g. Spill into form
    h. Add comb
    i. Wait ~1 hr until solidifies
2. Take out the comb
3. Transfer cast gel into chamber
4. Fill chamber with 1x TAE buffer so it covers the gel completely + ~1 mm over the gel

5. Add 6x Loading Dye to samples
    - 2 µl 6x Loading Dye for small gel
    - 20 µl 6x Loading Dye for Insert
    - 24 µl 6x Loading Dye for Backbone
6. Load wells
    a. Small gel
        - 7 µl sample per well
        - 5 µl ladder into marker wells
    b. Big gel
        - 60 µl sample per well
        - 5 µl ladder into marker wells
7. Connect apparatus
    - Red is "+", should be farther from wells than "-"
    - DNA goes to "+"
8. Turn it on
9. Adjust settings
    - 500 V : 250 mA : 100 W
    - Constant voltage 120 V
10. Hit Start
11. Turn off after the blue marker reaches the bottom of the gel
12. Image the gel on GelImager and save into a flash card
13. Proceed with extraction or throw away

DNA Extraction from TAE-buffered agarose gel

1. Cut the band from the gel under UV light
    - Make a cut far from the other bands to prevent contamination
2. Weigh agarose gel slice in an Eppendorf tube

3. Add 3 volumes of Ultra Salt (0.3 ml per 0.1 g of gel slice)
4. Incubate at 55^{o}C until gel slice melts completely (~5 min when the Ultra Salt is fresh)
    - Do not heat above 60^{o}C
    - Mix occasionally by inverting the tube

5. Resuspend Ultra Bind Beads until homogenous (break sediment with pipette tip if exists, otherwise vortex)
6. Add beads to the melted gel
    - 5 µl plus 1 µl per 1 µg of DNA expected
7. Resuspend gently several times with pipette tip
8. Wait 5 min at room temperature constantly mixing

9. Spin down beads for 15 sec using short spin button on the centrifuge (max speed set for 12,000 RPM)
10. Discard supernatant

11. Wash pellet with Ultra Wash (shake before use) using pipette tip to resuspend
12. Spin down beads for 15 sec using short spin button on the centrifuge (max speed set for 12,000 RPM)
13. Remove all traces of Ultra Wash
14. Resuspend in H_2O
    - Use volume of H_2O that is 2x volume of Ultra Bind used
15. Wait 5 min at room temperature
16. Pellet 5 min at maximum speed (14,000 RPM)
17. Transfer supernatant into a new Eppendorf tube
18. Measure DNA concentration

Cloning

Analytical restriction digest

1. Add in sequential order
    a. 6-7 µl DNA
    b. 2 µl BSA/NEB Mix
        - 1:1 BSA/NEB Buffer
    c. 1 µl RE1
    d. 1 µl RE2 (if applicable)

2. Mix
3. Put into 37^{o}C water bath overnight
4. Run on small DNA gel

Preparative restriction digest

Materials (per one digest):

DNA Source Vector (40 µg)

BSA (10 µl)

NEB Buffer (10 µl)

Restriction enzymes (5 µl each)

Antarctic Phosphatase (10 µl)

Antarctic Phosphatase Buffer (12 µl)

Protocol:

1. Mix in sequential order:
    a. 40 µg DNA
    b. X H_2O (X=70-DNA solution volume)
    c. 10 µl BSA
    d. 10 µl NEB Buffer
2. Perform restriction 1
    a. 5 µl RE1
    b. Transfer into 37^{o}C water bath for 2 hr (better overnight)
    c. Heat inactivate according to enzyme
    d. Pellet 5 min at 5,000 RPM
3. Perform restriction 2
    a. 5 µl RE2
    b. Transfer into 37^{o}C water bath for 2 hr (better overnight)
    c. Heat inactivate according to enzyme
    d. Pellet 5 min at 5,000 RPM
4. Dephosphorylate backbone on 5 min end (Backbone ONLY!!! With Insert proceed to next step)
    a. Add 12 µl AP (Antarctic Phosphatase) buffer
    b. Add 10 µl AP Enzyme
    c. 1 hr in 37^{o}C water bath
    d. 15 min at 65^{o}C

    e. Pellet 5 min at 10,000 RPM

5. Run on a big DNA gel
    a. Load the wells with spacing, so bands do not get contaminated while cutting
6. Extract bands
7. Store at -20^{o}C

Ligation

Materials:

10x T4 DNA Ligase Buffer

T4 DNA Ligase

Protocol:

1. Add to the Eppendorf tube
    a. DNA
    b. 2 µl 10x T4 DNA Ligase Buffer (shake well to dissolve precipitate after thawing)
    c. Add H_2O to 18 µl
2. Spin down
3. Add 2 µl T4 DNA Ligase
4. Mix with the pipette tip
5. Leave overnight at room temperature
6. Reaction can be scaled up or down as needed

Amount of DNA:

- 120 ng backbone or titrate for the best amount
- 2:1 insert:backbone ratio by molar amount or titrate for the best ratio

DNA Methylation

Materials:

NEB Buffer 2
200x SAM
SssI

Protocol:

1. Make 10x SAM solution
    - 10 µl SAM stock (200x) + 190 µl H_2O
2. In an Eppendorf tube (can be scaled up)
    - Add 1 µg DNA
    - Add 2 µl NEB Buffer 2
    - Add 2 µl 10x SAM
    - Add H_2O to 19 µl
    - Add 1 µl SssI (4U)
3. Transfer into 37^{o}C water bath overnight

    Store at -20^{o}C

PCR

<u>Platinum Blue Supermix Taq Polymerase</u>

Use for routine PCR of short fragments (~1 kb)

1. Add to PCR tube
    a. 45 µl Supermix
    b. 1 µl DNA template (~200 ng)
    c. 2 µl FWD primer (6.4 pM)
    d. 2 µl REV primer (6.4 pM)
    e. Mix by pipetting
        - Avoid bubbles

- Avoid getting content on the wall of the tube

2. Set the PCR cycler program

1.	T=94°C 02:00	{Initial denaturation, activation of polymerase}
2.	T=94°C 00:30	{Denaturation}
3.	T=55°C 00:30	{Primer Annealing}
4.	T=72°C 07:00	{Elongation. One minute per kb of the product, 7min for 7kb}
5.	GOTO 2 REP 35	{Cycle operator}
6.	T=72°C 10:00	{Final elongation to get rid of unfinished molecules}
7.	HOLD 4°C	

Platinum Taq Hi-FI Polymerase

Use for long fragments or for mutagenesis

1. Add to PCR tube
    a. 5 µl HiFi Buffer
    b. 1.5 µl 10 mM dNTP mix
    c. 1 µl 50 mM $MgSO_4$
    d. 2-5 µl DNA template (~200 ng for regular PCR, ~30 ng for site directed mutagenesis)
    e. 1 µl FWD primer (6.4 pM)
    f. 1 µl REV primer (6.4 pM)
    g. H_2O to 49 µl
    h. Mix by pipetting

i. 1 µl HiFi Polymerase

j. Mix by pipetting

- Avoid bubbles
- Avoid getting content on the wall of the tube

2. Set the PCR cycler program

1. T=94°C 02:00
2. T=94°C 00:30
3. T=55°C 00:30
4. T=68°C 01:00 {One minute per kb of the product, 1min for 1kb}

5. GOTO 2 REP [20-30]
6. T=68°C 10:00
7. HOLD 4°C

Site-directed mutagenesis

1. Design primers
2. Methylate template DNA
3. PCR
   a. Platinum Taq HiFi polymerase
   b. Methylated DNA as a template
4. Set the PCR cycler program

1. T=94°C 02:00
2. T=94°C 00:30
3. T=55°C {temperature in the middle row, usually start from 55°C}

   00:30 +0.0° +0:00 {temperature and time increments for each subsequent cycle}

   R=3.0°/s +0.0°S {speed of the cooling/heating and increment for subs. cycles}

   G=3.0 {usually 3.0°, use more or less when needed}

   {temperature increment between center and most outside wells, rises left to right, limit 10°C}

8. T=68°C 07:00 {One minute per kb of the product, 7 min for 7 kb}
4. GOTO 2 REP 20 {More cycles will not increase mutation yield}
5. T=68°C 10:00
6. HOLD 4°C

5. Transfect E.coli with PCR product
6. Plate on the agar plate
7. Prepare Minipreps of minimum 3 colonies from each plate
8. Check by restriction digest
9. Send samples approved by digests for sequencing

Subcloning routines

Direct Subcloning from PCR

1. Run PCR product on the gel
2. Extract DNA from the band
3. Digest PCR product with restriction enzymes
4. Cut target vector backbone with restriction enzymes and dephosphorylate with AP
5. Inactivate RE
6. Proceed with ligation

TOPO cloning

1. Mix in sequential order
    a. 2 µl PCR product
    b. 1 µl Salt Solution
    c. 2 µl H_2O
    d. 1 µl TOPO Vector
2. 30 min at room temperature
3. Transform E. coli with resulting mixture

Subcloning from another vector

1. Preparative digest of vectors containing backbone and insert
2. Extract DNA from the gel
3. Measure DNA concentration
4. Ligate Backbone and Insert

Sequencing

1. Mix
    a. 0.5-1 µg DNA
    b. 1 µl sequencing primer (6.4 pM final concentration in sequencing tube)
    c. Add H_2O to 12 µl
2. Label SS
3. Spin down drops
4. Take to Sequencing facility

General Western Protocol

Reagents

NP-40 Lysis Buffer (1 L)

- Add 10 ml NP-40
- Add 40 ml 0.5M Tris
- Add 8.8 g NaCl
- Add 0.8 ml 0.5M EDTA
- Add H_2O to 1 L
- Keep at +4^oC

2x Laemmli Buffer (100ml)

- 25 ml 500 mM Tris-HCl, pH 6.8
- 20 ml Glycerol
- Add

    - 3.1 g DTT
    - 4 g SDS
    - 0.2 g Bromphenol blue
- Add DIUF H_2O to 100ml
- Keep at +4^oC

Lysis Buffer preparation (0.5 ml per sample) HAS TO BE FRESH!

- 1 ml NP-40
- 1 µl Leupeptin
- 5 µl Apotonin
- 5 µl Pepstatin A
- 10 µl Na Orthovanadate (fresh!)
    - 18 mg per 1 ml H_2O
- 10 µl PMSF (toxic, wear gloves)
    - Have to add just before use because half-life in water solution is 30 min
- Put on ice (+4^oC)

IP

1. Lyse 5-20x10^6 cells in 0.5 ml NP-40 Lysis buffer
    - Same number of cells for each sample for equal loading
2. 1 hr on WOD
3. Pellet 20 min at 14,000 at +4^{o}C
4. Transfer supernatant into new tubes
    - 10 µl into Lysate tube (if applicable)
    - Rest into IP tube

    Lysate tube
    - Proceed to sample preparation

    IP tube
5. Add IP antibody
    - 5 µg for αGFP, αSLP-76 and αLAT
    - 4 µg for αItk
6. Leave overnight on WOD
7. Add 30 µl PGS (Protein G Sepharose)
8. WOD 1 hr
9. Wash 2x with 1 ml NP-40 Lysis Buffer
10. Remove supernatant with narrow pipette tip
11. Proceed to sample preparation

Sample preparation

1. Add 10 µl 2x Laemmli buffer to 10 µl sample

   Optional stopping point (+4^{o}C)

2. Boil 5 min
3. Pellet 1 min at 13,400 RPM
4. Proceed to loading the gel immediately!

Electrophoresis

Materials:

Hardware

Gel backing

Aluminum Plate

Spacers (2)

Glass plate

Large glass plate

Solutions

30% Acrylamide (100 ml, toxic, use gloves)

- Add 29 g Acrylamide
- Add 1g N,N'-methylenebisacrylamide
- Add DIUF H_2O to 100 ml
- Heat to 37^{o}C

- Store in dark bottle at room temperature or at +4^{o}C. Store no more than 2 months.
- Check pH before use (7.0 or less)

4x Lower Buffer, pH 8.8 (100 ml)

- Add 18.7 g Tris
- Add 0.4 g SDS
- Add H_2O to 80 ml
- Adjust pH
- Add H_2O to 100 ml
- Keep at +4^{o}C

4x Upper Buffer, pH 6.8 (100 ml)

- Add 6.05 g Tris
- Add 0.4 g SDS
- Add H_2O to 80 ml
- Adjust pH
- H_2O to 100 ml
- Keep at +4^{o}C

5x Running Buffer, pH 8.3 (1 L)

- Add 15.1 g Tris
- Add 94 g Glycine (less Glycine will result in lower resolution)
- Add 5 g SDS

- Add H_2O to 1 L
- Do not adjust pH
- Keep at +4^oC

1x WTB, pH 8.0 (1 L)

- Add 50 ml methanol
- Add 3.03 g Tris
- Add 14.41 g Glycine
- Add H_2O to 800 ml
- Adjust pH
- Add H_2O to 1 L
- Keep at +4^oC

10% Ammonium Persulfate in H_2O (prepare fresh!)

Protocol:

1. Gel Assembly
    a. Assemble in following order bottom to top:
        - Gel Backing
        - Aluminum plate
        - Spacers
        - Glass Plate
    b. Holding the assembly together put the part opposite to electrode connector on large glass plate
    c. Surfaces have to be leveled, so there are no leaks
    d. Put 4 clamps on sides, starting from lower right corner, and going diagonally

2. Prepare 10 ml of acrylamide gel in 15 ml falcon tube

Protein size	% gel	30% Acrylamide	4x Lower Buffer	H_2O
>100 kD	6	2	2.5	5.5
	7.5	2.5	2.5	5
<100 kD	9	3	2.5	4.5

3. Plug
    a. Transfer 1 ml of acrylamide gel from #2 into Eppendorf tube
        - Add 10 µl 10% APS
        - Add 5 µl TEMED

- Mix

b. Pipette at the bottom of the assembly between glass plate and aluminum plate

c. Wait for ~5 min to solidify

4. Lower Gel (Resolving)

a. 9 ml of acrylamide gel left from #2

- Add 45 µl APS
- Add 9 µl TEMED
- Mix

b. Pipet 7 ml in 1 ml increments against glass plate alternating left and right side

c. Add H_2O to top of aluminum plate to make a straight line gel and prevent the access of oxygen

d. Wait 30 min to solidify

e. Control for solidifying – leftover gel in Falcon tube

5. Dry Lower Gel with Whatman filter paper

6. Upper Gel (Stacking)

a. In 15 ml Falcon tube

- Add 670 µl 30% Acrylamide
- Add 1.25 ml 4x Upper Buffer
- Add 3 ml H_2O
- Add 25 µl APS

- Add 10 µl TEMED
- Mix

b. Pipette to the top of the aluminum plate

c. Get rid of the bubbles

d. Insert a comb

e. Wait 30 min to solidify

f. Control for solidifying – leftover gel in Falcon tube

g. Mark well location with a thin marker

7. Electrophoresis

a. Move lover clamps on gel assembly up

b. Transfer gel assembly from Large Glass Plate to Gel Chamber

c. Fill assembly and chamber with 1x Running Buffer

d. Carefully take out the comb

e. Load prepared samples

- 5 µl ladder
- Up to 30 µl sample

f. Set limits 500 V, 200 mA, 100 W. Constant Current 18 mA.

g. Run until blue line reaches the plug

8. Transfer

a. Wash PVDF membrane in Methanol

b. Wash 2x with H_2O

c. Soak in Western Transfer Buffer

- Blotting paper (2 sheets)
- PVDF membrane

d. Sandwich

- Put one piece of blotting paper on the bottom metal plate
- Remove the gel from the gel assembly using one of the spacers
    - Take one of the spacers off
    - Using a spacer, carefully take glass plate off
    - Cut upper gel off
    - Cut plug off
    - Pick the underside of the gel with spacer and carefully separate from aluminum plate
    - Put upside down on a wet blotting paper on metal plate
- Put membrane on top of the gel
- Put second sheet of blotting paper on top
- Roll out bubbles at each step
- Cover with the second metal plate
- Screw tight
- Spill away leftover WTB from apparatus

e. Transfer to the membrane

- Set limits 0.4 mA, 14 V
- Run 1.5 hr (can be left overnight)

9. Separate the membrane from the sandwich
10. Dry the membrane between two sheers of blotting paper
11. Proceed to Blotting

Blotting

Materials:

Solutions

Blocking Buffer (500 ml)

- Add 25 g BSA
- Add TBST to 500 ml
- Keep at -20^{o}C

1x TBST, pH 7.4 (2 L)

- Add 2.5 g Tris
- Add 17.5 g NaCl
- Add 2 ml Tween-20
- Add H_2O to 1.6 L
- Adjust pH
- Add H_2O to 2 L
- Keep at +4^{o}C

1x Stripping Buffer, pH 6.8

- Add 7.88 g Tris
- Add 20 g SDS
- Add 7 ml β-ME
- Add TBST to 100 ml
- Adjust pH
- Keep at room temperature

Protocol:

1. Prepare membrane
    a. Mark ladder
    b. Write membrane description
    c. Do everything with ballpoint pen
2. Activate PVDF membrane with Methanol in blotting tray
    a. Quickly move tray so ink does not smear
3. Wash 2x with H_2O

4. Add 15 ml Blocking Buffer (if first use or after stripping)
5. Block 1 hr on rocker

6. If membrane was used before, check for signal
    a. wash 3x 10 min with TBST
    b. expose to film (steps 14-16)

c. If there is a signal, strip in blotting tray:

- Add 50 ml 1x Stripping Buffer
- 30 min on rocker
- Go to step 6a
- Stripping buffer is reusable

d. After successful stripping, go to step 4

7. Prepare Antibody solutions in 15 ml Falcon tubes

a. Mix solvent

- 7.5 ml TBST
- 7.5 ml Blocking Buffer

b. Add antibody

MαpY (30µl) 1:500	MαH902 (30µl) 1:500	MαItk (15µl) 1:1,000	MαGFP (15µl) 1:1,000	MαLAT (15µl) 1:1,000	RαSLP (15µl) 1:1,000	GαM (3 µl) 1:5000	GαR (1.5µl) 1:10,000

c. Mix

- Add 15 µl 10% Thimerosal after use
- Can be stored at 4^{o}C

8. Remove Blocking buffer from the tray

9. Add 15 ml of 1^{o} Antibody into the blotting tray

10. 1 hr rocking
11. Wash 3x 5 min with 15 ml TBST

12. Add 15 ml of 2^{o} HRP-Conjugated Antibody into the blotting tray
13. 30 min rocking
14. Wash 3x 10 min with 15 ml TBST
15. Apply luminescent kit
    a. Transfer membrane to Serene Wrap, face side on the wrap
    b. Add 3 ml H_2O_2 (Peroxide) on top of the membrane
    c. Add 3 ml Luminol (Enhancer) on top of the membrane
    d. Seal Saran Wrap
    e. Check for leaks and reseal if needed
16. Expose film for 3 min in the darkroom
17. Develop film
18. Depending on the signal, decrease or increase exposure
19. Do at least 3 exposures

Specific Western Based Assays

<u>Protein expression</u>

1. Transfect constructs expressing protein of interest (start with $20x10^6$ cells per sample)
    - Need additional $20x10^6$ as nontransfected control
2. IP with anti-protein or anti-tag antibody

3. Run on Western Gel
4. Blot with anti-protein or anti-tag antibody

CoIP

1. Transfect both constructs expressing proteins of interest using Biorad (start with $20x10^6$ cells per sample)
    a. Need additional $20x10^6$ cells as nontransfected control
2. IP (make 2 series):
    a. With αProtein 1
    b. With αProtein 2
3. Run on Western Gel
4. Blot both series with αProtein 1
5. Blot both series with αProtein 2

In vitro kinase assay

Materials:

Stock solutions

1. 1 M HEPES (ready purchased)
2. 100 mM ATP (ready purchased)
3. 200 mM $MnCl_2$
    - 2.52 g in 100 ml H_2O
4. 100 mM $MgCl_2$
    - 0.952 g in 100 ml H_2O
5. 200 mM DTT
    - 31 mg in 1 ml H_2O

Kinase buffer (10 ml)

1. Add 500 µl 1 M HEPES
2. Add 100 µl 200 mM $MnCl_2$
3. Add 20 µl 100 mM ATP
4. Add 1 ml 100 mM $MgCl_2$
5. Add 500 µl 200 mM DTT
6. Add H_2O to 100 ml

Protocol:

1. Transfect 293T or HEK293 cells with Itk constructs using Lipofectamine (start with one 10 cm cell culture plate with 90% confluency per sample)
2. After 24 hrs IP αItk or αGFP

   Kinase reaction
3. Wash pellet with 1 ml kinase buffer
4. Pellet for 10 sec at maximum speed
5. Discard supernatant

6. Resuspend pellet in 100 µl kinase buffer
7. Incubate 10 min in 37^{o}C water bath
8. Put on ice (+4^{o}C)
9. Pellet for 10 sec at maximum speed
10. Discard supernatant

11. Proceed with Sample Preparation for General Western immediately

    Western
12. Proceed with Electrophoresis in General Western Protocol
    a. Run on 7.5-9% PAAG

13. Blot αpY
14. Blot αItk

Transphosphorylation

1. Transfect cells with Itk constructs using Biorad (start with $20x10^6$ cells per sample)
    a. Need additional $20x10^6$ cells as nontransfected control

TCR Stimulation

2. Count cells
    - Need ~ 20 $x10^6$ cells per sample
3. Spin down cells 5 min at 1000 RPM
4. Wash 2x with RPMI
5. Resuspend pellet in 1 ml RPMI

6. Label tubes (Stimulated and NonStimulated for each sample)
    - Cool on ice (+4^{o}C)

7. 500 µl into S and NS tubes

Primary

8. Add 2.5 µg primary antibody (5 µg/ml final concentration)
    - 1.8 µl OKT3 into S tubes
    - 2.1 µl OKT9 (or UPC10) into NS tubes
9. Mix by inverting tubes

- 1 hr on ice

Secondary

10. Spin down cells 5 min at 1,500 RPM
11. Remove supernatant
12. Resuspend in 500 µl RPMI
13. Add 2.5 µg secondary antibody (5 µg/ml final concentration)
    - RαM uc (2.1 µl)
14. Mix by inverting tubes
15. 30 min on ice (+4^{o}C)

Stimulation

16. Place tubes into 37^{o}C water bath for required amount of time
17. Transfer to ice (+4^{o}C) immediately
18. Spin down cells 5 min at 1,500 RPM
19. Remove supernatant

Western

20. Proceed with general western protocol
21. IP αItk
    - 4 µg R-poly-αItk per sample

- Run on 7.5-9% PAAG

22. IP αCD3ε

- 3 µg OKT3 per sample
- Run on 9% PAAG

23. Blot αpY

24. Blot αItk

Microscopy protocols

JTag-Raji conjugation

1. Count Cells

   Raji marker staining

2. Spin Raji at 1,500 RPM 5 min in 50 ml Falcon tube
3. Aliquote 10 x10^6 cells into fresh 50 ml Falcon tube
4. Wash 2x with PBS
5. Resuspend in 500 µl PBS
6. Add 10 µl Cy-5
7. Wait 10 min in the dark on ice (+4^{o}C)
8. Wash 2x with PBS
9. Resuspend in 2 ml of RPMI

Spin Jurkat

10. Spin Jurkat at 1,500 RPM 5 min in 50 ml Falcon tube
11. Resuspend in RPMI at $5x10^6$ cells/ml

Raji stimulation

12. Transfer Raji cells into Eppendorf tubes
    - $2 x10^6$ cells per tube (400 µl)
    - Stimulated + 2 µl SEE (5 µg/ml)
    - Nonstimulated
13. Leave for 1.5 hr in 37°C CO_2 incubator (37°C, 5% CO_2), open tube lids
14. Transfer to ice (+4°C)

Conjugation

15. Fresh Eppendorf tubes on ice (+4°C)
    - Add 100 µl Raji ($5x10^5$ cells)
    - Add 100 µl Jurkat ($5x10^5$ cells)
16. Mix gently by inverting tubes
17. Spin 1,500 RPM for 5 min in TC centrifuge
18. Resuspend

Conjugate activation and fixing

19. Put tubes for stimulation into 37°C water bath for needed period of time (3 min is optimal)
20. Move to ice (+4°C) immediately
    a. Add ice-cold 200 µl 4% PF

b. Mix

c. Wait 10 min

d. Add 1 ml of ice-cold PBS

e. Mix

21. Spin 5 min at1,500 RPM in TC centrifuge

22. Remove supernatant

23. Proceed to slide preparation or Antibody Staining

Slide preparation for microscopy

Cover slides

1. Cover slides with poly-L-Lysine 100 µl per slide
2. Wait 30 min
3. Wash with H_2O
4. Let dry

Final slide preparation

5. Resuspend fixed cell pellet (1-2 $x10^6$ cells) in 40 µl PBS
6. Spread 20 µl per slide
7. Wait until slightly dries up
8. Drop 15 µl mounting medium (AVOID BUBBLES!!!)
    a. Preheat mounting medium at 60^oC
9. Put coverslip over the cells
10. Put in $+4^oC$ until hardens (overnight)
11. Slides can be used up to ~36 hrs after preparation

Antibody staining in the tube for microscopy

Detergent

1. Resuspend cell pellet in 1 ml 0.2% Tween-20
2. Wait 5 min
3. Spin 5 min at 1,500 RPM
4. Remove supernatant

Block with FCS

5. Resuspend in 1 ml 10% FCS
6. Spin 5 min at1,500 RPM
7. Remove supernatant

Block with IgG

8. Resuspend in 0.5 ml Murine IgG (100 µg/ml)
9. Wait 30 min
10. Spin 5 min at1,500 RPM
11. Remove super

Primary

12. Resuspend in 500 µl Primary Ab solution (20 µl stock + 480 µl 10% FCS)
13. 1 hr
14. Spin 5 min at1,500 RPM
15. Remove supernatant

Wash

16. Resuspend in 1 ml 10% FCS

17. Spin 1000 RPM for 5 min
18. Remove supernatant
19. Proceed to slide preparation

Imaging slides for FRET

Setting up hardware

1. Turn on Fluorescent lamp power source
2. Turn on Microscope
3. Plug Camera
4. Turn on PC

Fluorescence settings

5. Put Neutral Density filter in
6. Adjust fluorescent lamp intensity to 100%
7. Adjust microscope lamp output to standard 3200K level

Microscope setup

8. Run AxioVision Software
9. Load CFP/YFP/FRET APO setting

Microscopy

10. Take reference image at 200 ms
11. Measure brightest spot intensity
12. Select timing in a way that brightest spot in FRET channel will be still lower than maximum (16,000)

13. Image CFP/YFP/FRET/Cy5/DIC channels in 2x/1x/2x/1000ms/Auto timing
14. Save as Tiff

Image processing for FRET calculation

1. Run FRET Prim plugin

2. Select Epifluorescence images directory
3. Select Apotome images directory

4. Move rectangle over the center of the cell
5. Press “Crop&Align”
6. Press “Accept Rotation”

7. Select Background area on the surface of APC
8. Press “Correct for background”

9. For analysis press
    a. “Generate Eapp Image”
    b. “Build Isolinear Maps”
    c. Select area and press “Calculate Mean Eapp” to calculate Eapp directly in the selection

Flow Cytometry

PhosphoFlow/Actin Polymerization in JTag/Mouse Cells

Materials:

Cells

~$5x10^6$ cells per condition

RPMI Medium

Antibodies for stimulation

- JTag
  - OKT3
  - RαM
- Mouse cells
  - AHαCD3ε
  - GαAH
  - GαH (S+A, Dy405 conjugated)

Blocking Antibody

- Mouse IgG (11 µg/µl)

PMA 200 ng/ml

Ionomycin

- 1 mg Ionomycin in 1.33 ml DMSO

4% Paraformaldehyde

FACS buffer (500 ml)

- 2.5 g BSA
- 0.1 g NaN3
- Dissolve in PBS
- Keep at +4oC

Staining agents (Alexa 647 conjugated)

- αpItk (Y511)
- αpERK1/2 (T202/Y204)
- αpPLCγ1 (Y783)
- αpZAP70 (Y319)

Phalloidin

Protocol:

Prepare cells

1. Resuspend pellet to $10x10^6$ cells in 1 ml RPMI
2. Aliquot 0.5 ml cells into Eppendorf tubes on ice (+4^{o}C)

Stimulate

3. Stimulate cells (on ice, +4^{o}C)
    a. S
        - Add OKT3 (5 μg/ml, 1.8 μl) or αCD3ε (5 μg/ml, 5 μl) for maximum stimulation

- 1 μg/ml, 1 μl – best window for differences between mutants
- Mix

- 1 hr on ice
- Pellet 5 min at 4°C at 1,500 RPM in TC centrifuge

- Aspirate supernatant with pipette tip
- Resuspend the pellet in 500 μl of ice cold RPMI
- Add GαM (5 μg/ml, 2.1 μl) or 4.5 μl premixed GαAH (5 μg/ml, 4.1 μl) + Dy405-GαH (0.5 μl)
- Mix
- 30 min on ice (+4°C)

- 37°C water bath (1 min standard, multiple points for kinetics)
- Transfer immediately to ice (+4°C)

b. PMA-IM (pERK1/2 positive control)
   i. Add 0.5 μl PMA (1:10 working solution, 20 ng/ml final concentration)
   ii. Add 0.5 μl Ionomycin (10 μM/ml final concentration)
   iii. Wait 15 min at 37°C

c. NS

i. Same procedure, just do not add anything, and keep on ice (+4^{o}C) all the time

Fix

4. Add 500µL of ice cold 4% paraformaldehyde
5. Mix by inverting the tube
6. Incubate (fix) samples on ice at 4^{o}C for 10 minutes.

Permeabilize

7. Transfer to FACS tubes on ice (+4^{o}C)
8. Pellet 5 min at 4^{o}C at 1,500 RPM in TC centrifuge
9. Spill away supernatant
10. Resuspend the pellet in leftover supernatant by vigorously vortexing
11. Add 1 ml ice cold 100% methanol
12. Vortex
13. Incubate 20 min on ice or leave at 4^{o}C overnight

Block

14. Add 3 ml FACS buffer
15. Vortex
16. Pellet cells 5 min at 1,500 RPM in TC centrifuge and spill away supernatant
17. Add 3 ml FACS buffer
18. Vortex

1. Pellet cells 5 min at 1,500 RPM in TC centrifuge and spill away supernatant

2. Add 100 µl FACS buffer
3. Add 11 µg Mouse IgG (1 µl)
4. Vortex
5. Incubate for 1 hr at room temperature in the dark

6. Add 3 ml FACS buffer
7. Vortex
8. Pellet cells 5 min at 1,500RPM in TC centrifuge and spill away supernatant
9. Add 3 ml FACS buffer
10. Vortex
11. Pellet cells 5 min at 1,500 RPM in TC centrifuge and spill away supernatant

    Stain
12. Resuspend cells in 120 µl FACS buffer
13. Transfer 60 µl of cell suspension into new tubes
14. Add 40 µl of staining antibody mixture and mix by vortexing
    a. Antibody mixture
        i. Add buffer (total volume minus combined volume of staining agents used)
        i. Add staining agents (combine volumes when needed):

αCD4 2µl	αPLCγ 15µl	αpY511 15µl	αpERK1/2 15µl	αpZAP70 15µl	Isotype 0.3µl	Phalloidin 5µl	αpY 15µl

15. Vortex

16. Incubate (stain) in the dark at room temperature for 1 hr

17. Add 3 ml FACS buffer

18. Vortex

19. Pellet cells 5 min at 1,500 RPM in TC centrifuge and spill away supernatant

20. Add 3 ml FACS buffer

21. Vortex

22. Pellet cells 5 min at 1,500 RPM in TC centrifuge and spill away supernatant

23. Resuspend in 100 µl of FACS buffer for analysis

24. Analyze samples in the same day

Intracellular Cytokine staining in Mouse Thymocytes

Materials:

- Cells
  - ~5x106 cells per condition
- RPMI Medium
- Antibodies for stimulation
  - Mouse cells
    - AHαCD3ε
    - AHαCD28
    - GαAH
    - GαH (S+A, Dy405 conjugated)
- PMA 200ng/ml
- Ionomycin
  - 1mg Ionomycin in 1.33 ml DMSO
- 4% Paraformaldehyde
- ICCS buffer (500 ml), up to 6 months at $4^{o}C$
  - 5g BSA
  - 2.5g Saponin
  - 0.25g NaN_3
  - Dissolve in PBS
- Staining agents
  - αIFNγ, αIL4, αIL13

Protocol:

Prepare cells

1. Resuspend pellet to 10x106 cells in 1ml medium
2. Aliquot 0.5ml cells into Eppendorf tubes on ice

Stimulation Round 1

3. Stimulate cells (on ice)
    a. S
        - Add αCD3+αCD28 (5µg/ml each, 5µl)
        - 1hr on ice
        - Pellet 5 min at 4^{o}C at 1,500 RPM in TC centrifuge
        - Aspirate supernatant with pipet tip
        - Resuspend the pellet in 500µl of ice cold medium
        - Add GαAH (1.8µg/ml, 4.1µl, 7.38 µg/ml final)
        - 30 min on ice
        - Resuspend
        - Transfer to 24 well plate (wells contain 500µl RPMI, 20% FCS)
        - 37^{o}C CO_2 incubator (24hr)
    b. NS
        - Same procedure, just do not add anything

Stimulation Round 2

4. Stimulate cells (on ice)

    a. S

        - Add αCD3+αCD28 (1µg/ml each, 1µl)

        - 1hr on ice
        - Pellet 5 min at 4^{o}C at 1,500 RPM in TC centrifuge

        - Aspirate supernatant with pipet tip
        - Resuspend the pellet in 500µl of ice cold **complete** medium
        - Add GαAH (5µg/ml, 4.1µl) + Dy405-GαH (0.5µl)
        - 30 min on ice
        - Resuspend
        - Transfer to 24 well plate
        - Add 500µl complete medium with Brefeldin A (2µl/ml)

        - 37^{o}C CO_2 incubator (6hr)

    b. NS

        - Same procedure, just do not add anything

Fix

5. Transfer to FACS tubes
6. Add 1 µL of ice cold 4% paraformaldehyde
7. Mix by inverting the tube
8. Incubate (fix) samples on ice at 4^{o}C for 10 minutes.
9. Pellet
10. Spill supernatant

Block

25. Add 3ml ICCS buffer
26. Vortex
27. Pellet cells 5 min at1,500RPM on TC centrifuge and spill away supernatant
28. Add 3ml ICCS buffer
29. Vortex
30. Pellet cells 5 min at1,500RPM on TC centrifuge and spill away supernatant

31. Add 100µl ICCS buffer
32. Add 10µg Rat IgG (1µl)
33. Vortex
34. Incubate for 1hr on ice

35. Add 3ml ICCS buffer
36. Vortex
37. Pellet cells 5 min at1,500RPM on TC centrifuge and spill away supernatant
38. Add 3ml ICCS buffer
39. Vortex
40. Pellet cells 5 min at1,500RPM on TC centrifuge and spill away supernatant

Permeabilize

11. Resuspend cells in 120µl ICCS buffer
12. Transfer 60µl of cell suspension into new tubes
13. Add 40µl of staining antibody mixture and mix by vortexing
    a. Antibody mixture
        - Add ICCS buffer (total volume minus combined volume of staining agents used)
        - Add staining agents (combine volumes when needed):

αCD4 2µl	αIFNγ 1µl	αIL4 1µl	αIL13 1µl

14. Incubate (stain) in the dark at room temperature for 1hr

15. Add 3ml ICCS buffer
16. Vortex
17. Pellet cells 5 min at1000 RPM in TC centrifuge and aspirate supernatant

18. Add 3ml ICCS buffer

19. Vortex

20. Pellet cells 5 min at1000 RPM in TC centrifuge and aspirate supernatant

21. Resuspend in 100µl of FACS buffer for analysis

22. Analyze samples in the same day

ELISA

Materials:

Coating buffer (500 ml) 0.1M Na_2CO_3, pH 9.3

1.8g $NaHCO_3$

398mg Na_2CO_3

200 ml H_2O

Adjust pH to 9.5

Add H2O

Filter

Keep at +4oC

Assay Diluent (200ml)

1% BSA in PBS, pH 7.4

1g BSA

20ml 10x PBS

150ml H2O

Dissolve

Add H2O

Filter

Keep at +4oC

Wash Buffer (2L)

200ml 10x PBS

1 ml Tween-20

Add H_2O to final volume

Filter

Store at +4^oC

Stop Solution (100 ml)

6.8ml 14.7M H3PO4

Add H2O to final volume

Keep at room temperature

96-well plates

Capture antibody

Biotynilated detection antibody

Streptavidin-peroxidase

TMB substrate

Recombinant cytokine standards

Multichannel pipette

Pipette tips

Multichannel pipette basins

15ml falcon tubes

Protocol:

Coating

Equilibrate coating buffer to room temperature

Prepare 1ml capture antibody solution in coating buffer per column of wells

- Dilute 1/250 (4µl per 1ml final solution)
- Transfer into pipet basin

Add 100µl per well

Cover plate

Overnight at +4oC

Blocking

Flick away contents of the wells

Wash 3x with 250µl Wash Buffer

Flick plate after each wash

Add 200 µl assay diluent per well

1hr at room temperature

Flick plate

Wash 3x with wash buffer

Flick after each wash

Adding standards

Dilute standards in assay diluent to 2ng/ml

- 19 µl IL4 (107ng/ml) per ml
- 2 µl IL13 (1,000ng/ml) per ml

- 2 µl IL5 (1,000ng/ml) per ml
- 6 µl IFNγ (33ng/ml) per ml

Use two well columns in duplicate as standard columns

Add 50 µl assay diluent into all standard column wells except row B

Add 100 µl standard solution into row B of standard columns

Transfer 50 µl from row B to row C

Mix

Change tips

Transfer 50 µl into next row

Mix

Repeat until reach row H

Discard 50 µl solution from row H

Adding samples

Add 50 µl samples into each sample well

Use duplicates if possible

1hr at room temperature

Adding detection antibody solution

Wash 5x with 250 µl wash buffer

Dilute detection antibody and streptavidin-HRP in assay diluent

IL4 (per ml assay diluent)

2 µl detector antibody per ml

4 µl streptavidin-HRP

IL13 (per ml assay diluent)

4 µl detector antibody per ml

4 µl streptavidin-HRP

IL5 (per ml assay diluent)

4 µl detector antibody per ml

4 µl streptavidin-HRP

IFNγ (per ml assay diluent)

4 µl detector antibody per ml

4 µl streptavidin-HRP

Add 100 µl per well

Adding substrate

Equilibrate TMB substrate to room temperature

Wash 7x with 250 µl wash buffer

Add 100 µl TMB to each well

Incubate 30 min at room temperature

Adding stop solution

Add 50 µl stop solution per well

Measure at 450nm (with 650nm background subtraction)

APPENDIX 2. LIST OF PRIMERS USED FOR SUBCLONINGS AND SITE-DIRECTED MUTAGENESIS

NCIns REV
'TTTTTCTCTAGAGGCTGGTCTGCAGATAAAGCCCAGCTTCTGCGATTT'

FP-CIns FWD
'GCTTATCTGCAGCTCCTAACCATGGTGAGC'

FP-CIns REV
'GTTTTTTCTCTAGAATCTGAGTCCGGACTTGTACAGCTCGTCC'

N-TERM FP FWD
'TGCGGAATTCTTCCTCGAGCGGCTCAATCGATGAACAACTTCATCCTCCT'

N-TERM FP REV
'GAGCTGTACAAGTCCGGACTCAGATCTCGAGCGGC'

C-TERM FP FWD
'ATCTCGAGCGGCTCAATCGA'

C-TERM FP REV
'GTGATCTAGAGTGATTAAAGCGCTTC'

ItkFWD Seq1
'ATGAACAACTTCATCCTCCTCCT'

ItkFWD Seq1
'CCATCCAAGAATGCTTCAAA'

ItkFWD Seq2
'CTACGTGGCTGAGAAGTATG'

ItkFWD Seq4
'TTGCTGCGGAGACCCTGCTG'

Btk-SH3 FWD
'CAGATCTCGAGCGGCTCAATCGATGAACAACTTCATCCTCC'

Btk-SH3 REV
‘ATCTGGTAGACATGACAG’

Itk-KLAPTA PPR FWD
‘TCAAAGAAGCCTCTTGCTCCTACTGCTGAAGACAAACA’

Itk-KLAPTA PPR REV
‘AAGAGGCTTCTTTGAAGCATTCTTG’

R265K REV
‘GACCATGAAAGCTCCTTCTTTACCTGTGTC’

R265K FWD
‘GGAGCTTTCATGGTCAAAGATTCCAGGACG’

K390R REV
‘GATGGCCACCTTGTCCTTGTTGAGCCAGTA’

K390R FWD
‘GGACAAGGTGGCCATCAGGACCATTCAGGAA’

Y511F FWD
‘ATTTGTCCTTGATGATCAATTTACCAGCTCCACGGGCA’

Y511F REV
‘ATTGATCAAGGACAAATCTTGTCATCC’

Y180 REV
‘CAAGGCAATGACCAGGGTTTCTTCAGG’

Y180E FWD
‘ACCCTGGTCATTGCCTTGGAGGACTACCAA’

Y180F FWD
‘ACCCTGGTCATTGCCTTGTTCGACTACCAA’

P287G REV
‘GTTCTCACTTATGATGGCCTTGGTGAA’

P287G FWD
‘GCCATCATAAGTGAGAACGGCTGTATAAAA’

APPENDIX 3. ITK CONSTRUCT MAPS

Designed by Ritz Zhang, San Diego State University, San Diego, CA)

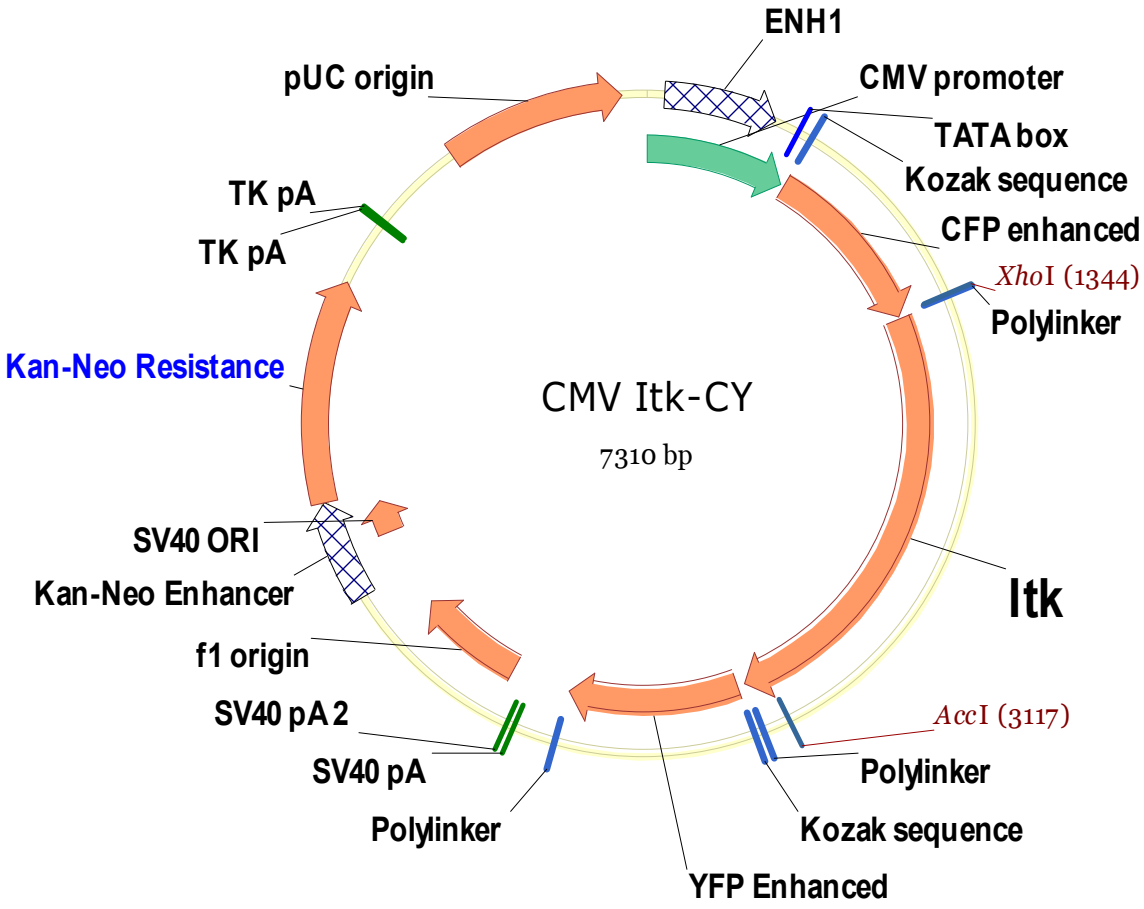

Figure 29. CMV Itk-CY construct

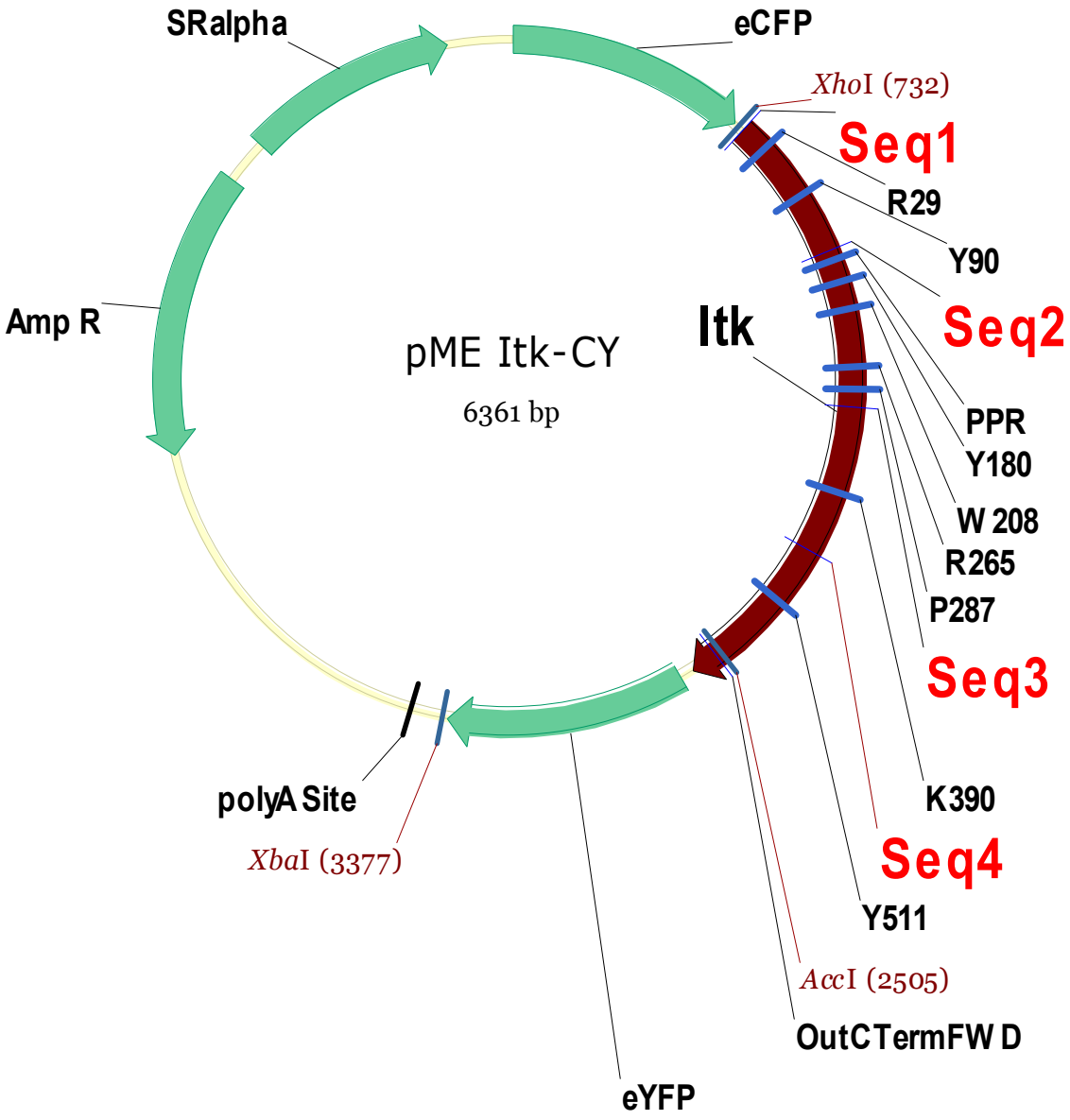

Figure 30. pME Itk-CY construct

Designed by Ritz Zhang, San Diego State University, San Diego, CA.

Sites for directed mutagenesis are marked, as well as sequencing primer binding sites.

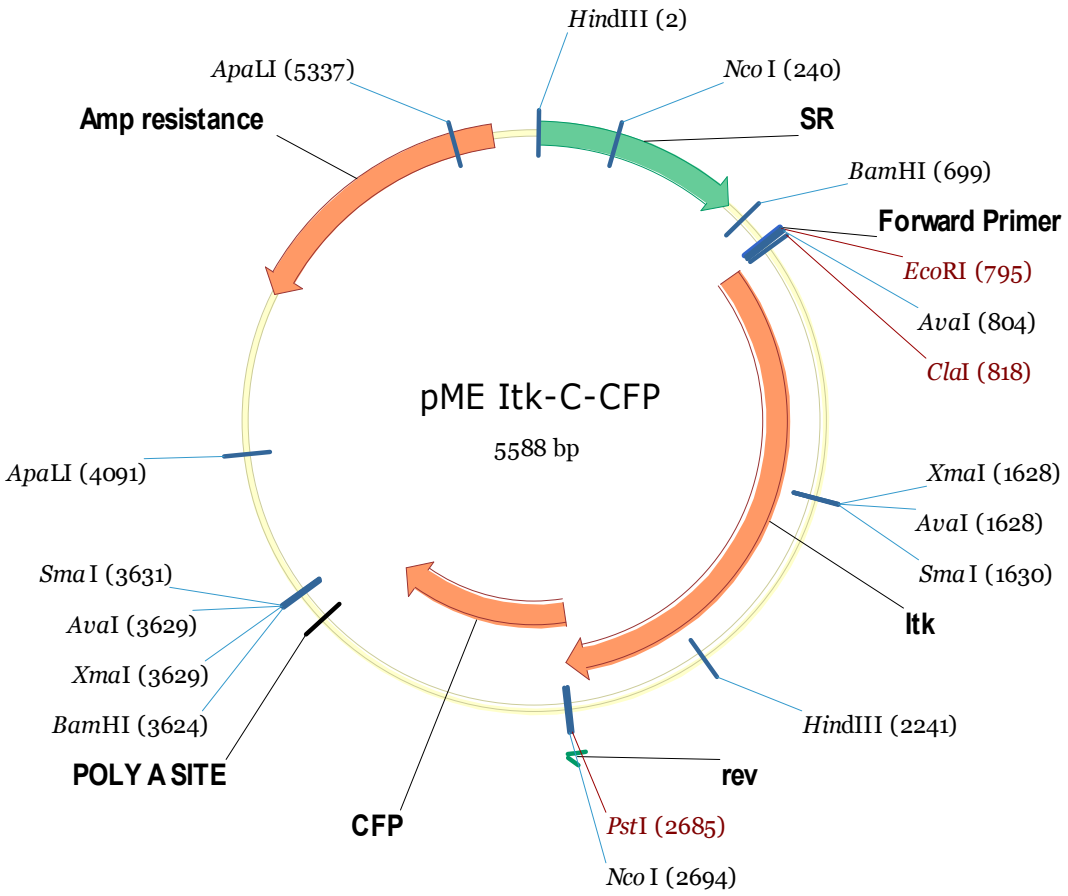

Figure 31. pME Itk-C-CFP construct

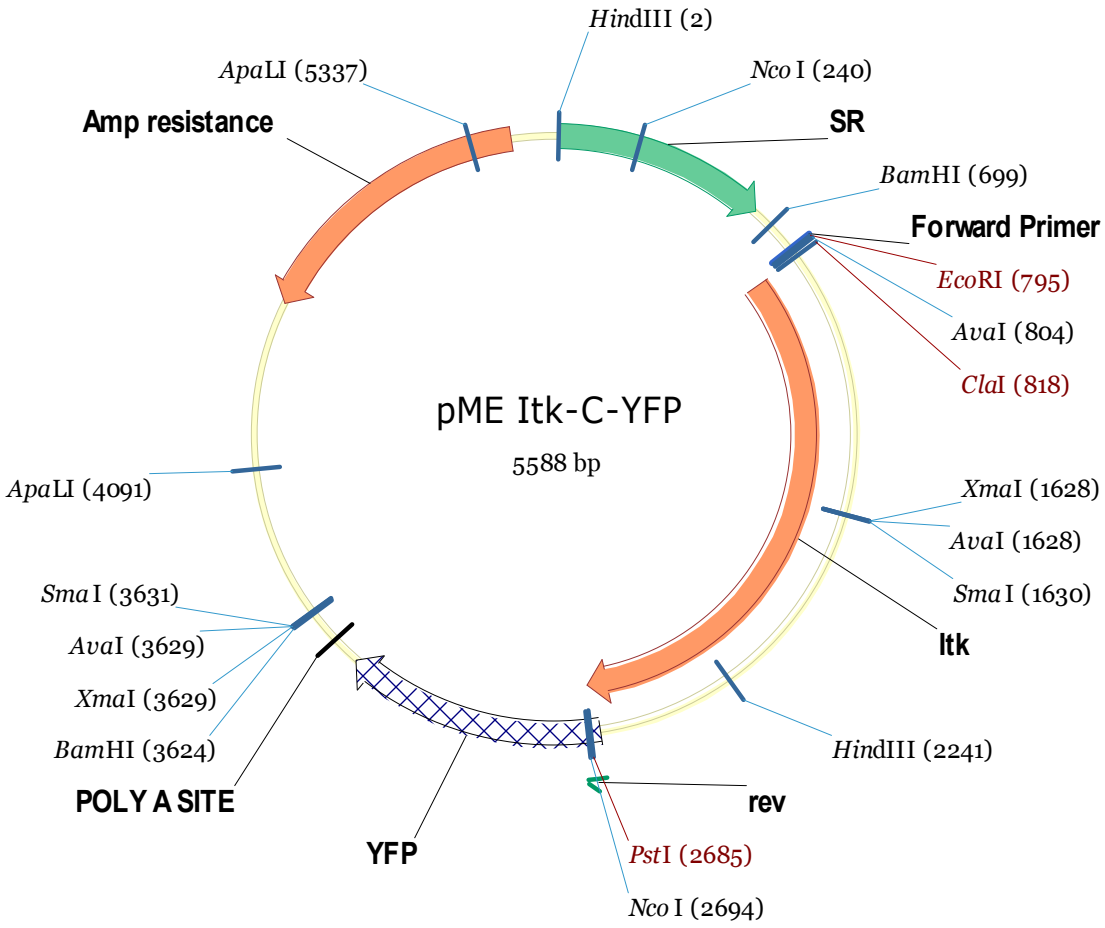

Figure 32. pME Itk-C-YFP construct

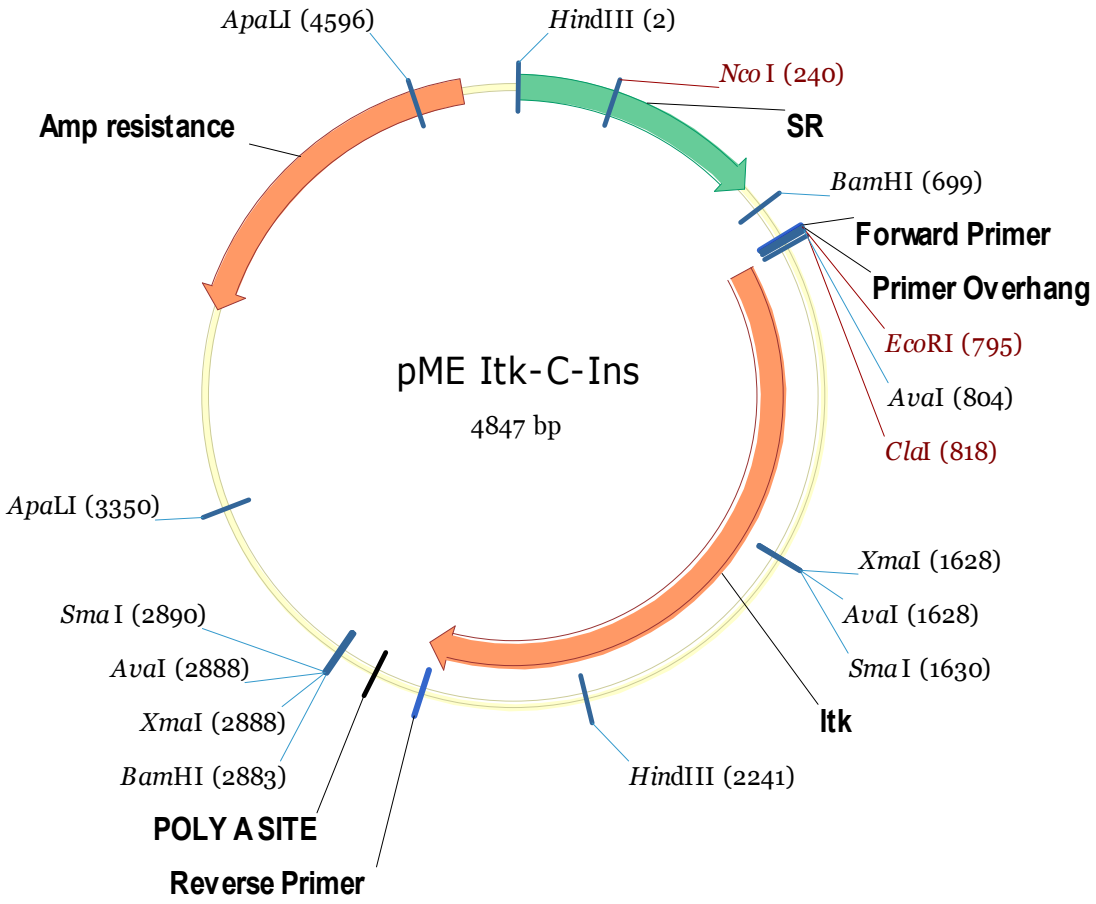

Figure 33. pME Itk-C-Ins construct

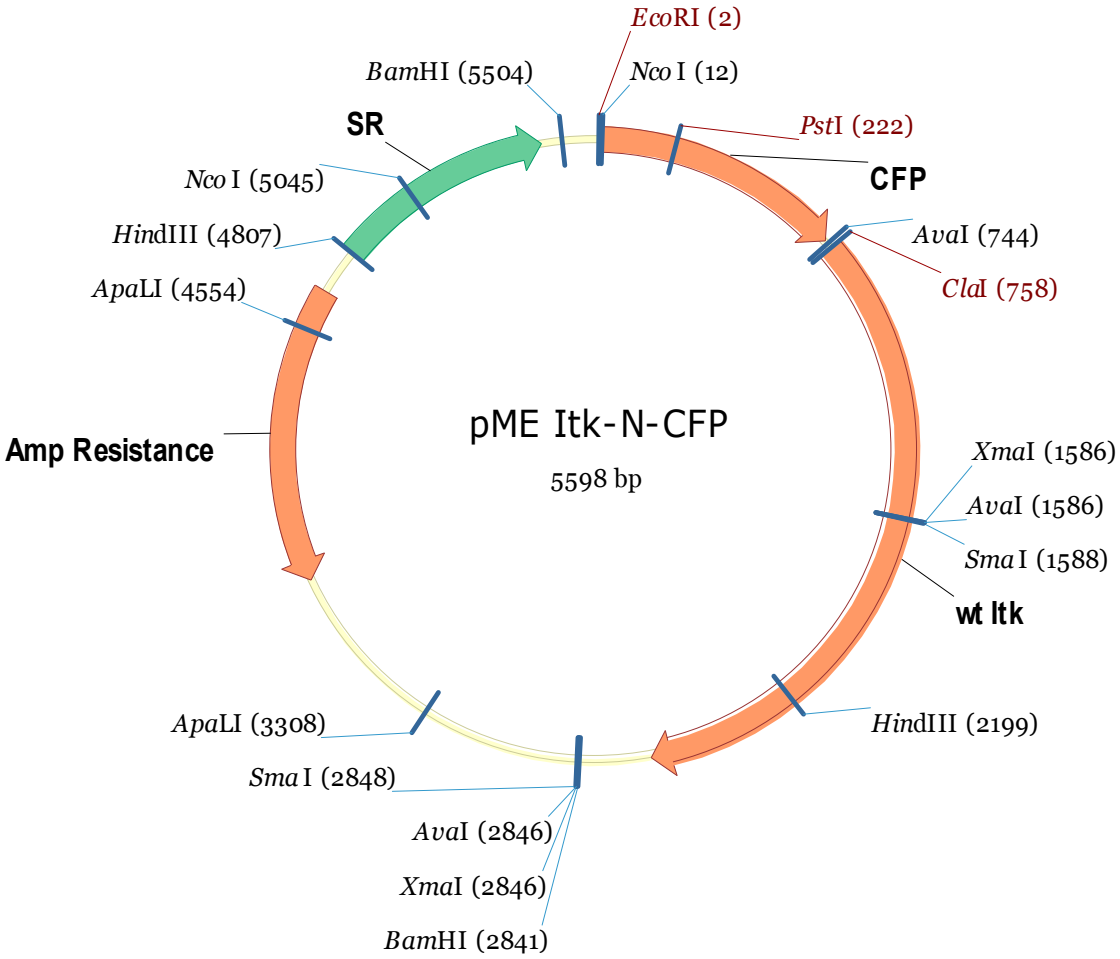

Figure 34. pME Itk-N-CFP construct

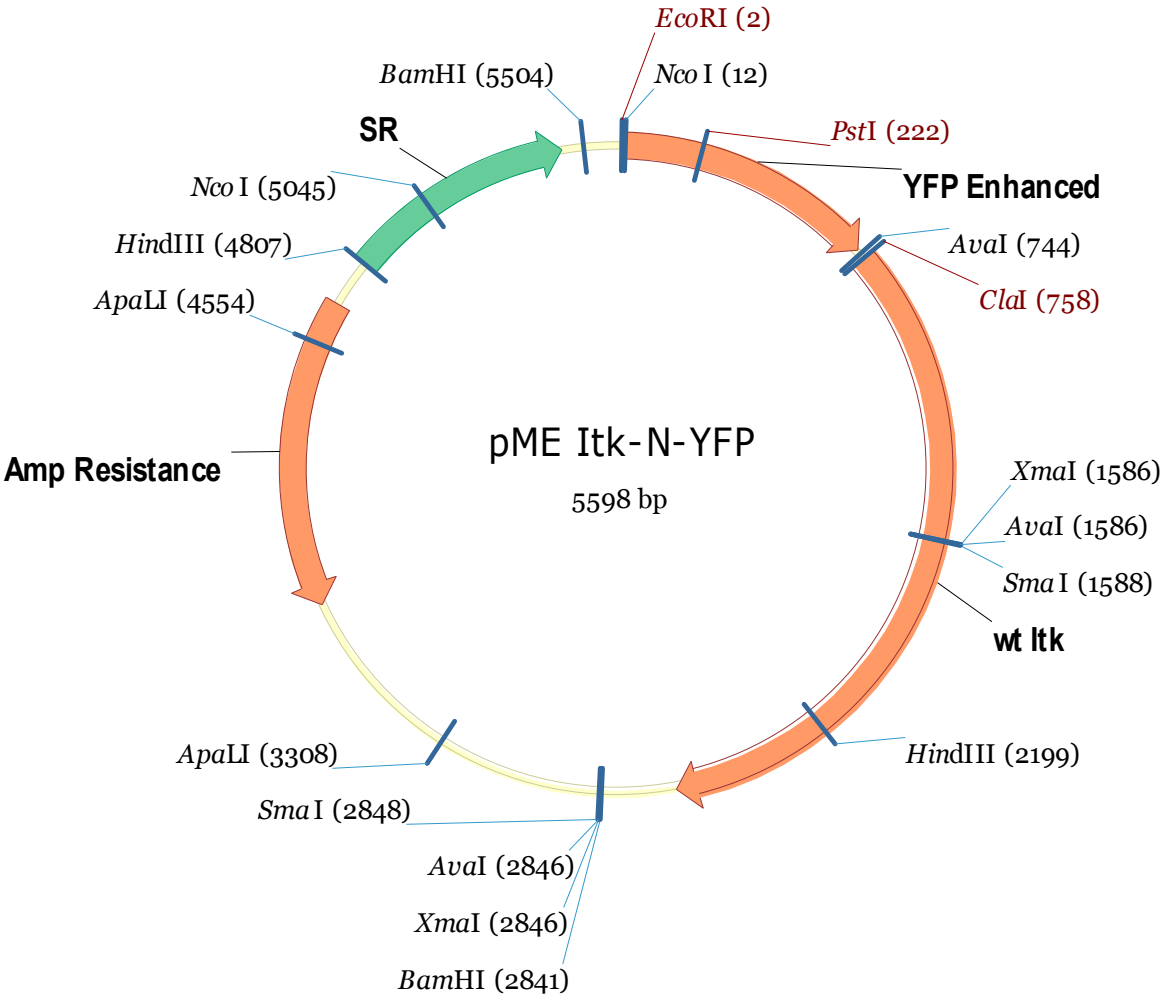

Figure 35. pME Itk-N-YFP construct

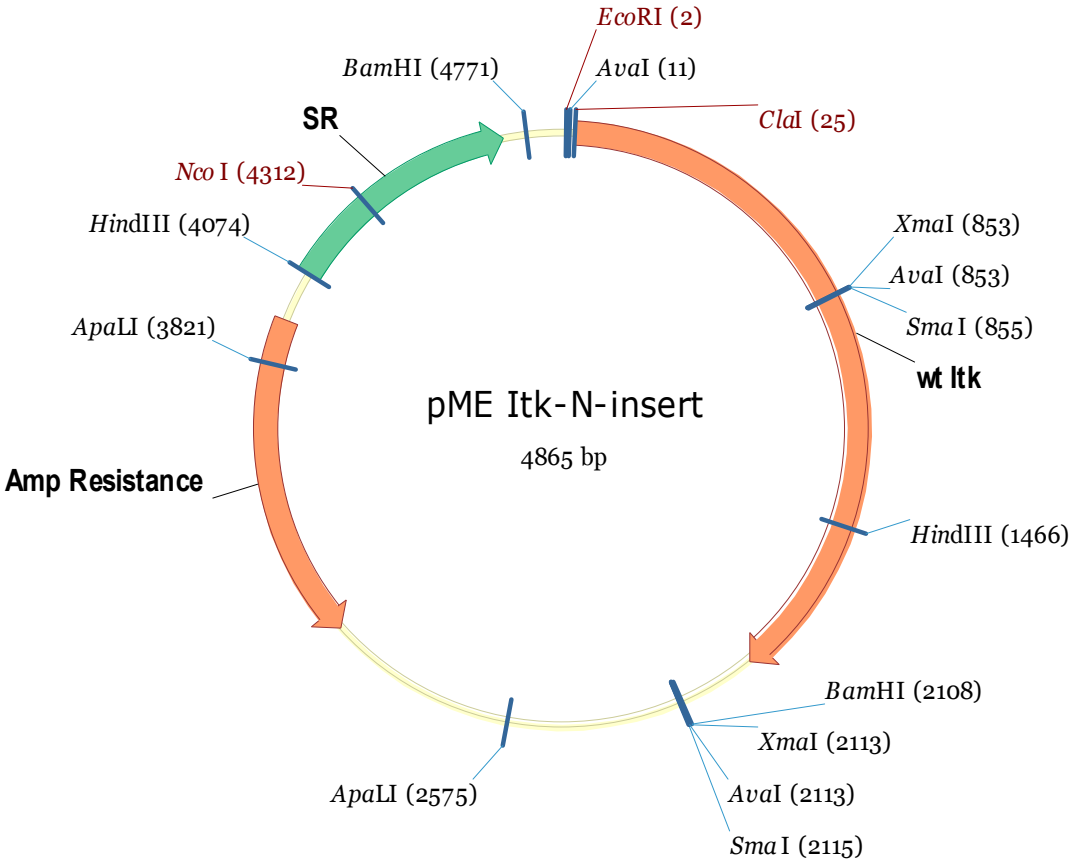

Figure 36. pME N-Insert construct

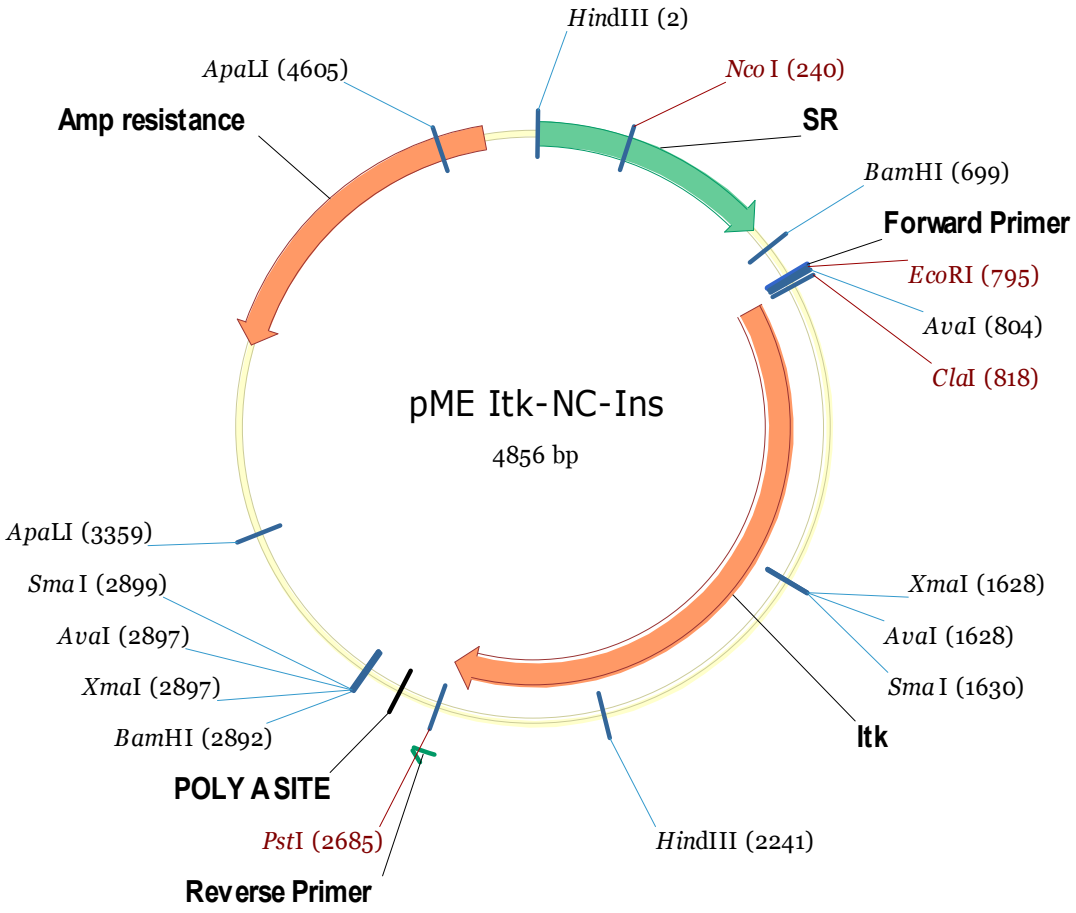

Figure 37. pME Itk-NC-Insert construct

APPENDIX 4. SOURCE CODE OF IMAGEJ PLUGIN

---------- Fret_Prim.java ----------

```
import java.io.*;
import ij.*;
import ij.io.*;
import ij.gui.*;
import ij.plugin.*;
import ij.plugin.frame.*;
import ij.plugin.filter.*;
import ij.process.*;
import java.awt.*;
import java.util.*;
import ij.measure.*;
import java.lang.Math.*;
import java.awt.image.*;
import java.awt.event.*;

public class FRET_Prim implements PlugIn {

  ImagePlus img;
  double[] cg = new double[3];
  double[] bg_dta = new double[10];
  double b_cutoff = 1;
  String dir;
  String nme;
  int crpd = 0;
  int iflag = 0;
  double apo_flag = 1;
  double mask_over_background = 10;
  int[] upper;
  ImageProcessor ch_p;
  ImagePlus bg_msrs;
  ImageStatistics bg_is;
  ImageProcessor[] vmaskk;
  double angle = 0;
  boolean cs_outline_flag = true;

  public FRET_Prim() {
    img  = null;
  }
```

```
  public void run(String arg) {
    cg[0] = 0.4279;
    cg[1] = 1.011;
    cg[2] = 5.151;

    DirectoryChooser dc = new DirectoryChooser("Open Epi Directory...");
      String dir = dc.getDirectory();
//    dc = new DirectoryChooser("Open Apo Directory...");
      String dir_apo = dir; // dc.getDirectory();

    File fle = new File(dir);
    FilenameFilter ss = new FilenameFilter(){
      public boolean accept(File dir, String name) {
        return name.endsWith(".tif") && name.indexOf("_c") !=-1;
      }
    };
    String[] children = fle.list(ss);

    File flee = new File(dir_apo);
    String[] children_apo = flee.list(ss);

    ImagePlus[] prm = new ImagePlus[children.length+2];
    Opener opnr = new Opener();
    int j = 0;
    for (int i=0; i<children.length; i++){
      prm[i+j] = opnr.openImage(dir+children[i]);
      if (i>1 && i<4){
        prm[i+j+1] = opnr.openImage(dir_apo+children_apo[j]);
        j++;
      }
    }

    ImageStack imss = new ImageStack(1382,1034);   //(1382,1034)/1388,1040;
     for (int k=0; k<children.length+2; k++){
       imss.addSlice("cc"+k, prm[k].getProcessor());
     }
    ImagePlus acb_imp = new ImagePlus("RAW", imss);
    CustomCanvas bc_cc = new CustomCanvas(acb_imp);
     new BackgroundCorrectorWindow(acb_imp, bc_cc);
  }

ImagePlus alt_getFRETImage (ImageStack imgs, ImageProcessor msk_imp){
```

```
    ImageProcessor[] iplus_all = new ImageProcessor[3];

    for (int i=0;i<3; i++){
      iplus_all[i] = imgs.getProcessor(i+1).duplicate().convertToFloat();
    }

    float cy_diff, numerator, divisor, eapp_val;
    ImageProcessor eapp_prcsr = iplus_all[0].duplicate();

//  Calculate Eapp using T.Zal formula
    for (int i=0; i<400; i++){
      for (int j=0; j<400; j++){
        cy_diff = iplus_all[2].getf(i,j) - iplus_all[1].getf(i,j)*(float)cg[1];
        numerator =  cy_diff - iplus_all[0].getf(i,j)*(float)cg[0];
        divisor   =  cy_diff + ((float)cg[2] - (float)cg[1])*iplus_all[0].getf(i,j);
        eapp_val  =  (numerator/divisor)*100;
        if (java.lang.Float.isNaN(eapp_val)) eapp_val = 0;
        eapp_prcsr.setf(i,j, eapp_val);
      }
    }

//  Convert Mask to Unitary
    ImageProcessor umask = msk_imp.duplicate();
    umask.add(-254);
    umask.min(0);

//  Apply Mask
    eapp_prcsr.copyBits(umask,0,0, Blitter.MULTIPLY);
    eapp_prcsr.filter(0);
    eapp_prcsr.min(0.0);
    eapp_prcsr.max(30);


//  Return Final Eapp Image
    ImagePlus eapp_img = new ImagePlus("Eapp", eapp_prcsr);

    return eapp_img;
  }

ImagePlus getFRETImage (ImageStack imgs, ImageProcessor msk_imp){
    double corr_guy;
    ImagePlus[] iplus_all = new ImagePlus[3];

//  get adjusted channel signals
```

```
    for (int i=0;i<3; i++){
     ImageProcessor ipx = imgs.getProcessor(i+1).duplicate().convertToFloat();
     switch(i) {
        case 0:
          corr_guy = cg[0];
        case 1:
          corr_guy = cg[1];
        case 2:
          corr_guy = 1;
        default:
          corr_guy = 1;
      }
     ipx.multiply(corr_guy);
     iplus_all[i] = new ImagePlus("s"+i, ipx);
    }
//  Calculate Eapp using T.Zal formula
    ImageProcessor ipPFN = iplus_all[2].getProcessor().duplicate();
    ipPFN.copyBits(iplus_all[1].getProcessor(), 0, 0, Blitter.SUBTRACT);
    ImageProcessor ipFNN = ipPFN.duplicate();

    ipPFN.copyBits(iplus_all[0].getProcessor(), 0, 0, Blitter.SUBTRACT);
    ImageProcessor tmp_prcs = iplus_all[0].getProcessor().duplicate();
    tmp_prcs.multiply(cg[2] - cg[1]);  //*1000
    ipFNN.copyBits(tmp_prcs, 0, 0, Blitter.ADD);
    ipPFN.multiply(1000);

    ImageProcessor eapp_prcsr = ipPFN.duplicate();
    eapp_prcsr.copyBits(ipFNN.duplicate(), 0, 0, Blitter.DIVIDE);

//  Convert Mask to Unitary
    ImageProcessor umask = msk_imp.duplicate();
    umask.add(-253);
    umask.min(0);

//  Apply Mask
    float a;
    eapp_prcsr.copyBits(umask,0,0, Blitter.MULTIPLY);
    for (int i=0; i<400; i++){
      for (int j=0; j<400; j++) {
        a = eapp_prcsr.getf(i,j);
        if (java.lang.Float.isNaN(a)) eapp_prcsr.setf(i,j,0);
      }
    }
//    eapp_prcsr.multiply(0.1);
```

```
   eapp_prcsr.filter(0);
//    eapp_prcsr.min(0.0);
//    eapp_prcsr.max(30);


//  Return Final Eapp Image
   ImagePlus eapp_img = new ImagePlus("Eapp", eapp_prcsr);

   return eapp_img;
  }

ImagePlus getFRETNImage (ImageStack imgs, ImageProcessor msk_imp){
   double corr_guy;
   ImagePlus[] iplus_all = new ImagePlus[3];
//  get adjusted channel signals
   for (int i=0;i<3; i++){
     ImageProcessor ipx = imgs.getProcessor(i+1).duplicate().convertToFloat();
     switch(i) {
        case 0:
          corr_guy = cg[0];
        case 1:
          corr_guy = cg[1];
        case 2:
          corr_guy = 1;
        default:
          corr_guy = 1;
      }
     ipx.multiply(corr_guy);
     iplus_all[i] = new ImagePlus("s"+i, ipx);
   }
//  Calculate Eapp using NFRET formula
   ImageProcessor ipPFN = iplus_all[2].getProcessor().duplicate();
   ipPFN.copyBits(iplus_all[1].getProcessor(), 0, 0, Blitter.SUBTRACT);
   ImageProcessor ipFNN = ipPFN.duplicate();

   ipPFN.copyBits(iplus_all[0].getProcessor(), 0, 0, Blitter.SUBTRACT);

   ImageProcessor nfret_prcs = iplus_all[0].getProcessor().duplicate();
   nfret_prcs.multiply(cg[2]);
   nfret_prcs.copyBits(iplus_all[1].getProcessor(), 0, 0, Blitter.MULTIPLY);

   ImageProcessor nfret_prcsr = ipPFN.duplicate();
   nfret_prcsr.copyBits(nfret_prcs.duplicate(), 0, 0, Blitter.DIVIDE);
```

```
//  Convert Mask to Unitary
    ImageProcessor umask = msk_imp.duplicate();
    umask.add(-253);
    umask.min(0);

//  Apply Mask
    nfret_prcsr.copyBits(umask,0,0, Blitter.MULTIPLY);
    nfret_prcsr.multiply(100000);
    nfret_prcsr.min(0.0);

//  Return Final Eapp Image
    ImagePlus fretn_img = new ImagePlus("FRETN", nfret_prcsr);

    return fretn_img;
  }

ImagePlus getNFRETImage (ImageStack imgs, ImageProcessor msk_imp){
    double corr_guy;
    ImagePlus[] iplus_all = new ImagePlus[3];
//  get adjusted channel signals
    for (int i=0;i<3; i++){
      ImageProcessor ipx = imgs.getProcessor(i+1).duplicate().convertToFloat();
      switch(i) {
          case 0:
            corr_guy = cg[0];
          case 1:
            corr_guy = cg[1];
          case 2:
            corr_guy = 1;
          default:
            corr_guy = 1;
       }
      ipx.multiply(corr_guy);
      iplus_all[i] = new ImagePlus("s"+i, ipx);
    }
//  Calculate Eapp using NFRET formula
    ImageProcessor ipPFN = iplus_all[2].getProcessor().duplicate();
    ipPFN.copyBits(iplus_all[1].getProcessor(), 0, 0, Blitter.SUBTRACT);
    ImageProcessor ipFNN = ipPFN.duplicate();

    ipPFN.copyBits(iplus_all[0].getProcessor(), 0, 0, Blitter.SUBTRACT);

    ImageProcessor nfret_prcs = iplus_all[0].getProcessor().duplicate();
    nfret_prcs.copyBits(iplus_all[1].getProcessor(), 0, 0, Blitter.MULTIPLY);
```

```
    nfret_prcs.sqrt();

    ImageProcessor nfret_prcsr = ipPFN.duplicate();
    nfret_prcsr.copyBits(nfret_prcs.duplicate(), 0, 0, Blitter.DIVIDE);

//  Convert Mask to Unitary
    ImageProcessor umask = msk_imp.duplicate();
    umask.add(-253);
    umask.min(0);

//  Apply Mask
    nfret_prcsr.copyBits(umask,0,0, Blitter.MULTIPLY);
    nfret_prcsr.multiply(10);
    nfret_prcsr.min(0.0);
//    nfret_prcsr.max(30);

//  Return Final Eapp Image
    ImagePlus fretn_img = new ImagePlus("NFRET", nfret_prcsr);

    return fretn_img;
  }

double eapp_mean_calc(ImagePlus raw_stack, Roi rroi){
    double[] dta = new double[10];
    double value_a = cg[0];
    double value_d = cg[1];
    double value_g = cg[2];
    ImageStack ims = raw_stack.getStack();
    if (iflag==0 && (rroi==null || !rroi.isArea())) {
          IJ.error("No selection: Whole Image data will be calculated");
    }
    ImagePlus tmm;
    ImageProcessor channel_processor;
    ImageStatistics acb_is;
    for (int i=1; i<4;i++){
      channel_processor = ims.getProcessor(i).duplicate();
      tmm = new ImagePlus("ChP", channel_processor);
      tmm.setRoi(rroi);
      acb_is = tmm.getStatistics();
      tmm.trimProcessor();
      dta[i-1] = acb_is.mean;
    }

    double temp_nominator   = dta[2] - (value_a*dta[1]) - (value_d*dta[0]);
```

```
    double temp_denominator = dta[2] - (value_a*dta[1]) + (value_g - value_d)*dta[0];
    double eapp_wh = temp_nominator/temp_denominator*100;
    if (temp_nominator<0 || temp_denominator<0)   { eapp_wh = 0;}
    eapp_wh = ((double)Math.round(eapp_wh*100))/100;

    return eapp_wh;
  }

ImageProcessor mask_creator(ImageProcessor src, double lower, double upper){
    ImageProcessor target = src.duplicate().convertToByte(2<1);
    for (int j=0; j<src.getHeight(); j++) {
      for (int k=0; k<src.getWidth(); k++){
        float value = src.getf(j,k);
        if (value>=lower && value<=upper)
           target.set(j,k,255);
        else
           target.set(j,k, 0);
      }
    }
    return target;
}

public ImagePlus get_isolinear(ImageProcessor ip, double lower, int
decimal_point_flag){
    ImagePlus msrmts = new ImagePlus("Measurement", ip);
    msrmts.killRoi();
    ImageStatistics acb_is = msrmts.getStatistics();

    double upr = acb_is.max;
    double diff = (upr - lower)/10;

    ImageProcessor isolinear_proc = ip.duplicate();
    isolinear_proc = isolinear_proc.convertToRGB();
    Color filler = new Color(0,0,0);
    isolinear_proc.fill();
    ImagePlus isolinear = new ImagePlus("Isolinear Map", isolinear_proc);

    // Surface No.          0   1   2   3   4   5   6   7   8   9  10  11
          int[] r_level = {0,  23,   0,   0,   0, 255, 255, 255, 255, 255,   0,  0};
          int[] g_level = {0,   0,   0,  93, 255, 255, 201,   0,   0, 255,   0,  0};
          int[] b_level = {0, 139, 255,   9,  19,   0,   0,   0, 134, 255,   0,  0};

    int cntr = 0;
    int locator;
```

```
    ImageProcessor iso_mask  = ip.duplicate();
    Font font = new Font("SansSerif", Font.PLAIN, 9);
    isolinear_proc.setFont(font);
    isolinear_proc.setAntialiasedText(true);
    ImageProcessor fla, vmask, vmask_p;
    ImageProcessor[] mask_arr = new ImageProcessor[10];

    for (int i = 9; i>0; i--){
       isolinear_proc.resetRoi();
       mask_arr[i] = mask_creator(iso_mask, lower+diff*i, upr);
    }
    int from, to;
    double from_d, to_d;

    for (int i = 0; i<10; i++){
       locator = 350-i*35;
       fla = mask_arr[i];
       filler = new Color(r_level[i],g_level[i],b_level[i]);
       isolinear.setColor(filler);
       isolinear_proc.fill(fla);
       isolinear_proc.setRoi(335, locator, 60, 30);
       isolinear_proc.fill();
       filler = new Color(0,0,0);
       isolinear.setColor(filler);
       if (cntr<9){
         if (decimal_point_flag == 1){
           from = (int)lower+(int)diff*(i-1);
           to = (int)lower+(int)diff*(i);
           isolinear_proc.drawString(" "+from+" to "+to, 335, locator+30);
         } else {
           from_d = (double)Math.round((lower+diff*(i-1))*100)/100;
           to_d = (double)Math.round((lower+diff*(i))*100)/100;
           isolinear_proc.drawString(" "+from_d+" to "+to_d, 335, locator+30);
         }
       }
       else {
           isolinear_proc.drawString(" "+(lower+diff*(i-1))+" to "+upr, 335,
locator+30);
       }
    }

    return isolinear;
}
```

```
public void makebutton(String name, Button btn, Panel panel, ActionListener e) {
        btn = new Button(name);
        btn.addActionListener(e);
        panel.add(btn);
       }

public void drawBar(ImagePlus iplus) {
       int width = 20;
       int height = 368;
       int x = 360;
       int y = 20;
       byte[] rLUT,gLUT,bLUT;
       int mapSize = 0;
       ImageProcessor ip = iplus.getProcessor();

       java.awt.image.ColorModel cm = ip.getColorModel();
       IndexColorModel m = (IndexColorModel)cm;
       mapSize = m.getMapSize();
       rLUT = new byte[mapSize];
       gLUT = new byte[mapSize];
       bLUT = new byte[mapSize];
       m.getReds(rLUT);
       m.getGreens(gLUT);
       m.getBlues(bLUT);

       double colors = mapSize;
       int start = 0;
       int ctrr = 22;
       Font font = new Font("SansSerif", Font.PLAIN, 9);
       ip.setFont(font);
       ip.setAntialiasedText(true);

       float flt;
       for (int i = 0; i<height; i++) {
          ctrr++;
          int iMap = start + (int)Math.round((i*colors)/height);
          if (iMap>= mapSize)
             iMap = mapSize - 1;

          ip.setColor(new Color(rLUT[iMap]&0xff, gLUT[iMap]&0xff,
bLUT[iMap]&0xff));
          int j = height - i - 1;
          ip.drawLine(x, j+y, width+x, j+y);
          if (ctrr>22) {
```

```
            ctrr = 0;
            ip.setColor(new Color(255&0xff, 255&0xff, 255&0xff));
            ip.drawLine(x-20,j+y-8,x,j+y-8);
            flt =(float)Math.round(ip.getf(x+5, j+y)*100)/100;
            ip.drawString(" "+flt, x-25, j+y-6);
          }
        }

        ip.setColor(new Color(255&0xff, 255&0xff, 255&0xff));
        ip.moveTo(x,y);
        ip.lineTo(x+width,y);
        ip.lineTo(x+width,y+height);
        ip.lineTo(x,y+height);
        ip.lineTo(x,y);

}

ImageProcessor[] getChannelMasks(ImageStack imstk){
        ImagePlus tmpp;
        ImageProcessor acb_ip, mskk, sdsd, raji_mskk, raji_sdsd;
        ImageProcessor[] channel_mask_array = new ImageProcessor[3];

        double[] up = new double[10];
        for (int i=1; i<imstk.getSize(); i++){
           acb_ip = imstk.getProcessor(i);
           tmpp = new ImagePlus("TMPP", acb_ip);
           acb_ip.resetRoi();
           bg_is = tmpp.getStatistics();
           up[i] = (double)bg_is.max;
         }
         if (apo_flag == 1) {
           mskk = imstk.getProcessor(4).duplicate();
           channel_mask_array[0] =  mask_creator(mskk, up[4]/5, up[4]); //YFP Apo
Mask
           raji_mskk = imstk.getProcessor(6).duplicate();
           channel_mask_array[1] =  mask_creator(raji_mskk, up[6]/7, up[6]); //Cy5 Apo
Mask
        } else {
           mskk = imstk.getProcessor(2).duplicate();
           sdsd =  mask_creator(mskk,
(double)bg_dta[2]*(double)mask_over_background, up[2]);
           raji_mskk = imstk.getProcessor(5).duplicate();
           raji_sdsd =  mask_creator(raji_mskk,
(double)bg_dta[5]*(double)mask_over_background, up[5]);
```

```
        }

        channel_mask_array[2] =
channel_mask_array[0].duplicate().convertToByte(2<1); //contact site
        channel_mask_array[2].copyBits(channel_mask_array[1].convertToByte(2<1),
0, 0, Blitter.AND);
        return channel_mask_array;
}


 class CustomCanvas extends ImageCanvas {
       CustomCanvas(ImagePlus imp) {
          super(imp);
       }
 }

 class BackgroundCorrectorWindow extends StackWindow implements
ActionListener {
       Button button1, button2, button3, button4, button5;

       BackgroundCorrectorWindow(ImagePlus imp, ImageCanvas ic) {
          super(imp, ic);
          setLayout(new FlowLayout());
          remove(sliceSelector);
          addPanel();
          imp.setRoi(0,0,400,400);
       }

       void addPanel() {
          setFont(new Font("Helvetica", Font.PLAIN, 14));

          Panel panel = new Panel();
          panel.setLayout(new GridLayout(11, 1));
            makebutton("Crop & Align", button1, panel, this);
            panel.add(new Label(""));
            makebutton("Rotate", button2, panel, this);
            makebutton("Accept Rotation", button3, panel, this);
            panel.add(new Label(""));
            makebutton("Correct for Background", button4, panel, this);
            panel.add(new Label(""));
            makebutton("Parameters", button5, panel, this);
            panel.add(new Label(""));
            panel.add(new Label("Select channel"));
            panel.add(sliceSelector);
```

```
    add(panel);
    pack();
}

public void actionPerformed(ActionEvent e) {
    String b = e.getActionCommand();
    if (b=="Crop & Align") {
      if (crpd == 1){
       IJ.error("Already cropped");
       return;
      }
      Rectangle selector = imp.getRoi().getBounds();
      imp.killRoi();
      int x_bnd = (int)selector.getX();
      int y_bnd = (int)selector.getY();

      Roi lrg_selector = new Roi (x_bnd-100, y_bnd-100, 600, 600);
      imp.setRoi(lrg_selector);
      IJ.run("Crop");
      imp.killRoi();
      IJ.runPlugIn("StackRegAlt ", imp.getTitle());
      imp.killRoi();

      ImageStack imstk = imp.getStack();
      ImageProcessor[] channel_mask_array = getChannelMasks(imstk);

      ColorProcessor cp = new ColorProcessor(600, 600);
      byte[] red, green, blue;
      red = (byte[])channel_mask_array[1].getPixels();
      green = (byte[])channel_mask_array[0].getPixels();
      blue = (byte[])channel_mask_array[2].getPixels();
      cp.setRGB(red, green, blue);

      ic = new CustomCanvas(imp);
      new BackgroundCorrectorWindow(imp, ic);
      imp.killRoi();
      crpd = 1;

      ImagePlus rotator_merge = new ImagePlus("Rotator Merge", cp);
      rotator_merge.show();
    }
    if (b=="Rotate") {
      double merge_angle=0;
      ImagePlus cp = WindowManager.getImage("Rotator Merge");
```

```
            Roi rotr = cp.getRoi();
            if (rotr.isLine()){
              Rectangle rct = rotr.getBounds();
              merge_angle = rotr.getAngle(rct.x, rct.y, rct.x + rct.width, rct.y +
rct.height);
            } else {
              IJ.log("This macro requires a straight line selection");
            }
            angle = angle + merge_angle;

            cp.getProcessor().rotate(merge_angle);
            cp.updateAndDraw();
            WindowManager.putBehind();
          }
          if (b=="Accept Rotation") {
            ImagePlus cp = WindowManager.getImage("Rotator Merge");
            cp.hide();

            for (int i=0; i<imp.getStackSize(); i++){
              imp.setSlice(i+1);
              imp.getProcessor().rotate(angle);
            }

            imp.killRoi();
            Roi crpp_roi = new Roi (100, 100, 400, 400);
            imp.setRoi(crpp_roi);
            IJ.run("Crop");

            imp.setSlice(1);
            imp.updateAndDraw();

            ic = new CustomCanvas(imp);
            new BackgroundCorrectorWindow(imp, ic);
            imp.killRoi();
          }
          if (b=="Correct for Background"){
            ImageStack bgs = imp.getStack();
            Roi bg_roi = imp.getRoi();
            if (bg_roi==null || !bg_roi.isArea()) {
                IJ.error("No selection: Select background area");
                return;
            }
            imp.setRoi(bg_roi);
```

```
            ImageStack bgss = new ImageStack(400, 400);
            for (int i=1; i<bgs.getSize()+1;i++){
              ch_p = bgs.getProcessor(i);
              bg_msrs = new ImagePlus("ChP"+i, ch_p);
              bg_msrs.setRoi(bg_roi);
              bg_is = bg_msrs.getStatistics();
              bg_dta[i] = bg_is.mean;
              bg_msrs.killRoi();
              if (i<4) ch_p.add(bg_dta[i]*(-1)*b_cutoff);
              bgss.addSlice("Background Subtracted "+i, ch_p);
            }
            WindowManager.closeAllWindows();
            imp = new ImagePlus("Background Corrected", bgss);
            ic = new CustomCanvas(imp);
            imp.setTitle("Eapp Calculator");
            new EappWindow(imp, ic);

          }
          if (b=="Parameters"){
            GenericDialog gd = new GenericDialog("Parameters");
                  gd.addNumericField("Background Cutoff:", b_cutoff, 1);
            gd.showDialog();
            if (gd.wasCanceled()) return;

            b_cutoff = gd.getNextNumber();
           }
      }
}

class EappWindow extends StackWindow implements ActionListener {

      Button button1, button2, button3, button4, button5, button6, button7;

      EappWindow(ImagePlus imp, ImageCanvas ic) {
         super(imp, ic);
         setLayout(new FlowLayout());
         remove(sliceSelector);
         addPanel();
      }

      void addPanel() {
         setFont(new Font("Helvetica", Font.PLAIN, 14));

         Panel panel = new Panel();
```

```
        panel.setLayout(new GridLayout(13, 1));
          makebutton("Generate Eapp Image", button1, panel, this);
          makebutton("Build isolinear maps", button2, panel, this);
          panel.add(new Label(""));
          makebutton("Calculate mean Eapp", button3, panel, this);
          makebutton("Calculate Eapp Grid", button4, panel, this);
          panel.add(new Label(""));
          makebutton("Localization Index", button5, panel, this);
          panel.add(new Label(""));
          makebutton("Parameters", button6, panel, this);
          makebutton("Save Results...", button7, panel, this);
          panel.add(new Label(""));
          panel.add(new Label("Select channel"));
          panel.add(sliceSelector);
        add(panel);
        pack();
      }

      public void actionPerformed(ActionEvent e) {
        String b = e.getActionCommand();

        if (b=="Generate Eapp Image") {
          ImageStack imstk = imp.getStack();

          ImageProcessor[] channel_mask_array = getChannelMasks(imstk);
          ImagePlus eapp_show_alt_img = alt_getFRETImage (imstk,
channel_mask_array[0]);

          ContrastEnhancer ce = new ContrastEnhancer();
          ce.stretchHistogram(eapp_show_alt_img, 0.5);
          eapp_show_alt_img.show();

          LutLoader fh = new LutLoader();
          fh.run("C:/Sci/ImageJ/luts/16_colors.lut");
          drawBar(eapp_show_alt_img);

          iflag = 1;
          Roi yy = imp.getRoi();
          double eapp_drw = eapp_mean_calc(imp, yy);
          iflag = 0;
          eapp_show_alt_img.setColor(Color.YELLOW);
          eapp_show_alt_img.getProcessor().drawString("Mean Eapp:"+eapp_drw, 20,
20);
          eapp_show_alt_img.updateAndDraw();
```

```
            if (cs_outline_flag){
               ImagePlus cs_img = new ImagePlus ("Contact Site",
channel_mask_array[2]);
               cs_img.show();
               channel_mask_array[2].setThreshold(255, 255,
ImageProcessor.NO_LUT_UPDATE);
               IJ.runPlugIn("ij.plugin.filter.ThresholdToSelection", "");
               Roi xx = cs_img.getRoi();
               cs_img.hide();

               double eapp_cs_drw = eapp_mean_calc(imp, xx);
               eapp_show_alt_img.getProcessor().drawString("Mean Eapp CS:
"+eapp_cs_drw, 20, 40);
               eapp_show_alt_img.setColor(Color.BLACK);
               xx.drawPixels(eapp_show_alt_img.getProcessor());
               eapp_show_alt_img.updateAndDraw();
            }

         }
         if (b=="Calculate mean Eapp"){
            Roi zz = imp.getRoi();
            double ee = eapp_mean_calc(imp, zz);
            IJ.log(Double.toString(ee));
         }
         if (b=="Calculate Eapp Grid"){
            Roi zz = imp.getRoi();
            double ee = eapp_mean_calc(imp, zz);
            IJ.log(Double.toString(ee));
         }
         if (b=="Localization Index"){
            Roi zz = imp.getRoi();
            imp.setSlice(2);
            IJ.run("Plot Profile");
         }

         if (b=="Build isolinear maps") {
            ImageStack imstk = imp.getStack();
            ImageProcessor acb_ip, tst;
            ImageProcessor[] channel_mask_array = getChannelMasks(imstk);
            ImagePlus eapp_show_img, cs_img;
            ImageProcessor [] isomaps = new ImageProcessor[3];

            eapp_show_img = alt_getFRETImage (imstk, channel_mask_array[0]);
```

```
            tst = eapp_show_img.getProcessor();
            channel_mask_array[0].add(-253);

//              cs_img = new ImagePlus ("Contact Site", channel_mask_array[2]);
//              cs_img.show();
            channel_mask_array[2].setThreshold(255, 255,
ImageProcessor.NO_LUT_UPDATE);
            IJ.runPlugIn("ij.plugin.filter.ThresholdToSelection", "");
//              Roi xx = cs_img.getRoi();
//              cs_img.hide();

            for (int i=1; i<3; i++){
               acb_ip  = imstk.getProcessor(i).duplicate();
               acb_ip.copyBits(channel_mask_array[0].convertToShort(2<1), 0, 0,
Blitter.MULTIPLY);
               acb_ip.filter(0);
               isomaps[i-1] =
get_isolinear(acb_ip,(int)bg_dta[i]*(int)mask_over_background, 1).getProcessor();
            }
            isomaps[2] = get_isolinear(tst, 1, 0).getProcessor();

            Font font = new Font("SansSerif", Font.BOLD, 12);
            String label = " ";
            for (int i=0; i<3; i++){
                isomaps[i].setFont(font);
                isomaps[i].setAntialiasedText(true);
                isomaps[i].setColor(Color.YELLOW);
                switch (i){
                  case 0: label ="CFP";break;
                  case 1: label ="YFP";break;
                  case 2: label ="Eapp";break;
                }
//                if (cs_outline_flag){
//                  isomaps[i].setColor(Color.BLACK);
//                  xx.drawPixels(isomaps[i]);
//                  isomaps[i].drawString("Isolinear map of "+label+" distribution.
Contact site outlined in black.", 20, 20);
//                } else {
                  isomaps[i].drawString("Isolinear map of "+label+" distribution.", 20,
20);
//                }
            }
```

```
            ImagePlus presenter = new ImagePlus("Isolinear Maps",
channel_mask_array[0]);
            ImageProcessor presenter_ip = presenter.getProcessor().convertToRGB();
            presenter_ip = presenter_ip.resize(1220, 410);
            presenter = new ImagePlus("Isolinear Maps", presenter_ip);
            presenter_ip = presenter.getProcessor();
            presenter_ip.setColor(Color.WHITE);
            presenter_ip.fill();
            int spacer=0;
            for (int i=0; i<3;i++){
               presenter_ip.copyBits(isomaps[i], spacer+5, 5, Blitter.COPY);
               spacer+=405;
            }
            presenter.show();
          }

          if (b=="Parameters"){
            GenericDialog gd = new GenericDialog("Parameters");
                  gd.addNumericField("Value a (YFP Bleedthrough):", cg[0], 4);
                  gd.addNumericField("Value d (CFP Bleedthrough):", cg[1], 4);
                  gd.addNumericField("Value G:", cg[2], 4);
                  gd.addNumericField("Mask Over Background:",
mask_over_background, 2);
                  gd.addNumericField("Apotome Mask:", apo_flag, 0);
                  gd.addCheckbox("Outline  contact site", false);
            gd.showDialog();
            if (gd.wasCanceled()) return;

            cg[0] = gd.getNextNumber();
            cg[1] = gd.getNextNumber();
            cg[2] = gd.getNextNumber();
            mask_over_background = gd.getNextNumber();
            apo_flag = gd.getNextNumber();
            cs_outline_flag = gd.getNextBoolean();
          }
          if (b=="Save Results..."){
            WindowManager.putBehind();
            FileSaver fs = new FileSaver(WindowManager.getCurrentImage());
            IJ.log(dir);
                fs.saveAsTiff(dir);
          }
      }
 }
```

WORKS CITED

1. Smith C.I., Islam T.C., Mattsson P.T., Mohamed A.J., Nore B.F., Vihinen M. The Tec family of cytoplasmic tyrosine kinases: mammalian Btk, Bmx, Itk, Tec, Txk and homologs in other species. *Bioessays* **2001,** *23* (5), pp. 436-446

2. Czar M.J., Debnath J., Schaeffer E.M., Lewis C.M., Schwartzberg P.L. Biochemical and genetic analyses of the Tec kinases Itk and Rlk/Txk. *Biochemical Society Transcripts* **2001,** *29* (6), pp. 863-867

3. Joseph R.E., Min L., Andreotti A.H. The linker between SH2 and kinase domains positively regulates catalysis of the Tec family kinases. *Biochemistry* **2007,** Vol. *46,* pp. 5455-5462

4. Joseph R. E., Fulton B.D., Andreotti A.H. Mechanism and functional significance of Itk phosphorylation. *Journal of Molecular Biology* **2007,** Vol. *373,* pp. 1281-1292

5. Colgan J., Asmal M., Neagu M., Yu B., Schneidkraut J., Lee Y., Sokolskaja E., Andreotti A.H., Luban J. Cyclophilin A regulates TCR signal strength in CD4+ T cells via a proline-directed conformational switch in Itk. *Immunity* **2004,** Vol. *21,* pp. 189-201

6. Min L., Fulton B.D., Andreotti A.H. A case study of proline isomerization in cell signaling. *Frontiers in Bioscience* **2005,** Vol. *10,* pp. 385-397

7. Gibson S., Leung B., Squire J.A., Hill M., Arima N., Goss P., Hogg D., Mills G.B. Identification, cloning, and characterization of a novel human T-cell-specific tyrosine kinase located at the hematopoietin complex on chromosome 5q. *Blood* **1993,** *82* (5), pp. 1561-1572

8. Brown K., Long J.M., Vial S.C.M., Dedi N., Dunster N.J., Renwick S.B., Tanner A.J., Frantz J.D., Fleming M.A., Cheetham G.M.T. Crystal structures of interleukin-2 tyrosine kinase and their implications for the design of selective

inhibitor. *The Journal of Biological Chemistry* **2004,** *279* (18), pp. 18727-18732

9. Wilcox H.M. and Berg L.J. Itk phosphorylation sites are required for functional activity in primary T cells. *The Journal of Biological Chemistry* **2003,** *278* (39), pp. 37112-37121

10. Cheetham G.M. Novel protein kinase inhibitors and molecular mechanisms of autoinhibition. *Current opinion in Structural Biology* **2004,** Vol. *24,* pp. 700-705

11. Lin T.-A., McIntyre K.W., Das J., Liu C., O'Day K.D., Penhallow B., Hung C.-Y., Whitney G.S., Shuster D.J., Yang X.X., Townsend R., Postelnek J., Spergel S.H., Lin J., Moquin R.V., Furch J.A., Kamath A.V., Zhang H., Wityak J., Kanner S.B. Selective Itk inhibitors block T-cell activation and murine lung inflammation. *Biochemistry* **2004,** Vol. *43,* pp. 11056-11062

12. Kashem M.A., Nelson R.M., Yingling J.D., Pullen S.S., Prokopowicz A.S., Jones J.W., Wolak J.P., Rogers G.R., Morelock M.M., Snow R.J., Homon C.A., Jakes S. Three mechanistically distinct kinase assays compared: measurement of intrinsic ATPase activity identified the most comprehensive set of Itk inhibitors. *Journal of Biomolecular Screening* **2007,** *12* (X), pp. 1-14

13. Snow R.J., Abeywardane A., Campbell S., Lord J., Kashem M.A., Khine H.H., King J., Kowalski J.A., Pullen S.S., Roma T., Roth G., Sarko C.R., Wilson N.S., Winters M.P., Wolak J.P., Cywin C.L. Hit-to-lead studies on benzimidazole inhibitors of Itk: Discoveryof a novel class of kinase inhibitors. *Bioorganic & Medicinal Chemistry Letters* **2007,** Vol. *17,* pp. 3660-3665

14. Charrier J.-D., Miller A., Kay D.P., Brenchley G., Twin H.C., Collier P.N., Ramaya S., Keily S.B., Durrant S.J., Knegtel R.M.A., Tanner A.J., Brown K., Curnock A.P., Jimenez J.-M. Discovery and structure - activity relationship of 3-aminopyrid-2-ones as potent and selective interleukin-2 inducible T-cell kinase (Itk) inhibitors. *The Journal of Medicinal Chemistry* **2011,** Vol. *54,* pp. 2341-2350

15. Bunnell S.C., Diehn M., Yaffe M.B., Findell P.R., Cantley L.C., Berg L.J. Biochemical interactions integrating Itk with the T cell receptor-initiated signaling cascade. *The Journal of Biological Chemistry* **2000,** *275* (3), pp. 2219-

2230

16. Joseph R.E., Min L., Xu R., Musselman E.D., Andreotti A.H. A remote substrate docking mechanism for the Tec family tyrosine kinases. *Biochemistry* **2007,** Vol. *46,* pp. 5595-5603

17. Joseph R.E. and Andreotti A.H. Controlling the activity of the Tec kinase Itk by mutation of the phenylalanine gatekeeper residue. *Biochemistry* **2010,**

18. Brazin K.N., Mallis R.J., Fulton D.B., Andreotti A.H. Regulation of the tyrosine kinase Itk by the peptidyl-prolyl isomerase cyclophilin A. *Proceedings of National Academy of Sciences* **2002,** *99* (4), pp. 1899-1904

19. Schwartzberg P.L. The many faces of Src: multiple functions of a prototypical tyrosine kinase. *Oncogene* **1998,** Vol. *17,* pp. 1463-1468

20. Andreotti A.H. Native state proline isomerization: an intrinsic molecular switch. *Biochemistry* **2003,** *42* (32), pp. 9515-9524

21. Pletneva E.V., Sundd M., Fulton D.B., Andreotti A.H. Molecular details of Itk activation by prolyl isomerization and phospholigand binding: the NMR structure of the Itk SH2 domain bound to a phosphopeptide. *Journal of Molecular Biology* **2006,** Vol. *357,* pp. 550-561

22. Gothel S.F. and Marahiel M.A. Peptidyl-prolyl cis-trans isomerases, a superfamily of ubiquitous folding catalysts. *Cellular and Molecular Life Science* **1999,** Vol. *55,* pp. 423-436

23. Mallis R.J., Brazin K.N., Fulton B.D., Andreotti A.H. structural characterization of a proline-driven conformational switch within the Itk SH2 domain. *Nature Structural Biology* **2002,** *9* (12), pp. 900-905

24. Brazin K.N., Fulton B.D., Andreotti A.H. A specific intermolecular association between the regulatory domains of a Tec family kinase. *The Journal of Molecular*

Biology **2000,** Vol. *302,* pp. 603-623

25. Breheny P.J., Laederach A., Fulton B.D., Andreotti A.H. Ligand specificity modulated by prolyl imide bond cis/trans isomerization in the Itk SH2 domain: a quantitative NMR study. *Journal of American Chemical Society* **2003,** *125* (51), pp. 15706-15707

26. Su Y.-W., Zhang Y., Schweikert J., Koretzky G.A., Reth M., Wienands J. Interaction of SLP adaptors with the SH2 domain of Tec family kinases. *European Journal of Immunology* **1999,** Vol. *29,* pp. 3702-3711

27. Ching K.A., Grasis J.A., Tailor P., Kawakami Y., Kawakami T., Tsoukas C.D. TCR/CD3-induced activation and binding of Emt/Itk to Linker of Activated T Cell Complexes: requirement for the Src homology 2 Domain. *The Journal of Immunology* **2000,** pp. 256-262

28. Severin A., Joseph R.E., Boyken S., Fulton B., Andreotti A.H. Proline isomerization preorganizes the Itk SH2 domain for binding to the Itk SH3 domain. *Journal of Molecular Biology* **2009,** Vol. *387,* pp. 726-743

29. Qi Q., Sahu N., August A. Tec kinase Itk forms membrane clusters specifically in the vicinity of recruiting receptors. *The Journal of Biological Chemistry* **2006,** *281* (50), pp. 38529-38534

30. Severin A., Fulton B.D., Anrdeotti A.H. Murine Itk SH3 domain. *Journal of Biomolecular NMR* **2008,** Vol. *40,* pp. 285-290

31. Hansson H., Okon M.P., Smith E.C.I., Vihinen M., Hard T. Intermolecular interactions between the SH3 domain and the proline-rich TH region of Bruton tyrosine kinase. *FEBS Letters* **2001,** Vol. *489,* pp. 67-70

32. Andreotti A.H., Bunnell S.C., Feng S., Berg L.J., Schreiber S.L. Regulatory intramolecular association in a tyrosine kinase of the Tec family. *Nature* **1997,** Vol. *385,* pp. 93-97

33. Qi Q. and August A. The Tec family kinase Itk exists as a folded monomer in vivo. *The Journal of Biological Chemistry* **2009,** *284* (43), pp. 29882-29892

34. Min L., Wu W., Joseph R.E., Fulton B.D., Berg L., Andreotti A.H. Disrupting the intermolecular self-association if Itk enhances T cell signaling. *The Journal of Immunology* **2009,** Vol. *184,* pp. 1-8

35. Grasis J.A., Guimond D.M., Cam N.R., Herman K., Magotti P., Lambris J.D., Tsoukas C.D. In vivo significance of ITK-SLP-76 interaction in cytokine production. *Molecular Cell Biology* **2010,** *30* (14), pp. 3596-3609

36. Hao S. and August A. The proline rich region of the Tec homology domain of Itk regulates its activity. *FEBS Letters* **2002,** Vol. *525,* pp. 53-58

37. Hansson H., Mattsson P.T., Allard P., Haapaniemi P., Vihinen M., Smith E.C.I., Hard T. Solution structure of the SH3 domain from Bruton Tyrosine Kinase. *Biochemistry* **1998,** Vol. *37,* pp. 2912-2924

38. Laederach A., Cradic K.W., Brazin K.N., Zamoon J., Fulton B.D., Huang X.-Y., Andreotti A.H. Competing modes of self-association in the regulatory domains of Bruton's tyrosine kinase: intramolecular contact versus asymmetric homodimerization. *Protein Science* **2002,** Vol. *11,* pp. 36-45

39. Nisitani S., Kato R.M., Rawlings D.J., Witte O.N., Wahl M.I. In situdetection of activated Bruton's tyrosine kinase in the Ig signaling complex by phosphopeptide-specific monoclonal antibodies. *Proceedings of National Academy of Sciences* **1999,** Vol. *96,* pp. 2221-2226

40. Pursglove S.E., Mulhern T.D., Mackay J.P., Hinds M.G., Booker G.W. The solution structure and intramolecular associations of the Tec kinase Src Homology 3 domain. *The Journal of Biological Chemistry* **2002,** *277* (1), pp. 755-762

41. McCarthy Morrough L., Hinshelwood S., Costello P., Cory G.O.C., Kinnon C. The SH3 domain of Bruton's tyrosine kinase displays altered ligand binding

properties when auto-phosphorylated in vitro. *European Journal of Immunology* **1999,** Vol. *29,* pp. 2269-2279

42. Laederach A., Cradic K.W., Fulton B.D., Andreotti A.H. Determinants if intra versus intermolecular self-association within the regulatory domains of Itk. *The Journal of Molecuar Biology* **2003,** Vol. *329,* pp. 1011-1020

43. Laederach A., Cradic K.W., Fulton B.D., Andreotti A.H. Determinants of intra versus intermolecular association within the regulatory domains of Rlk and Itk. *The Journal of Molecular Biology* **2003,** Vol. *329,* pp. 1011-1020

44. Marengere L.E.M., Okkenhaug K., Clavreul A., Couez D., Gibson S., Mills G.B., Mak T.W., Rottapel R. The SH3 domain of Itk/Emt binds to proline-rich sequences in the cytoplasmic domain of the T cell costimulatory receptor CD28. *The Journal of Immunology* **1997,** Vol. *159,* pp. 3220-3229

45. Hansson H., Smith E.C.I., Hard T. Both proline-rich sequences in the TH region of Bruton's tyrosine kinase stabilize intermolecular interactions with the SH3 domain. *FEBS Letters* **2001,** Vol. *508,* pp. 11-15

46. Zhou H.-X. Quantitative relation between intermolecular and intramolecular binding of Pro-rich peptides to SH3 domains. *Biophysical Journal* **2006,** Vol. *91,* pp. 3170-3181

47. Hyvonen M. and Saraste M. Structure of the PH domain and Btk motif from Bruton's tyrosine kinase: molecular explanations for X-linked agammaglobulinaemia. *The EMBO Journal* **1997,** *16* (12), pp. 3396-3404

48. Kurosaki T. and Kurosaki M. Transphosphorylation of Bruton's tyrosine kinase on tyrosine 551 is critical for B cell antigen receptor function. *The Journal of Biological Chemistry* **1997,** *272* (25), pp. 15595-15598

49. Huang Y.H., Grasis J.A., Miller A.T., Xu R., Soonthorvacharin S., Andreotti A.H., Tsoukas C.D., Cooke M.P., Sauer K. Positive regulation of Itk PH domain function by soluble IP4. *Science* **2007,** Vol. *316,* pp. 886-889

50. Woods M.L., Kivens W.J., Adelsman M.A., Qiu Y., August A., Shimizu Y. A novel function for the Tec family tyrosine kinase Itk in activation of [beta]1 integrins by the T-cell receptor. *The EMBO Journal* **2001,** *20* (6), pp. 1232-1244

51. Ching K.A., Kawakami Y., Kawakami T., Tsoukas C.D. Emt/Itk associates with activated TCR complexes: role of the pleckstrin homology domain. *The Journal of Immunology* **1999,** pp. 6006-6013

52. Yang W.-C., Ching K.A., Tsoukas C.D., Berg L.J. Tec kinase signaling in T cells is regulated by phosphatidylinositol 3-kinase and the Tec pleckstrin homology domain. *The Journal of Immunology* **2001,** pp. 387-395

53. Li Z., Wahl M.I., Eguinoa A., Stephens L.R., Hawkins P.T., Witte O.N. Phosphatidylinositol 3-kinase-[gamma] activates Bruton's tyrosine kinase in concert with Src family kinases. *Proceedings of National Academy of Sciences* **1997,** Vol. *94,* pp. 13820-13825

54. Kojima T., Fukuda M., Watanabe Y., Hamazato F., Mikoshiba K. Characterization of the pleckstrin homology domain of Btk as an inositol polyphosphate and phosphoinositide binding domain. *Biochemical and Biophysical Research and Communication* **1997,** Vol. *236,* pp. 333-339

55. Vihinen M., Zvelebil M.J.J., Zhu Q., Broomans R.A., Ochs H.D., Zegers B.J.M, Nilsson L. Waterfield M.D., Smith E. Structural basis for pleckstrin homology domain mutations in X-linked agammaglobulinemia. *Biochemistry* **1995,** Vol. *34,* pp. 1475-1481

56. Law C.-L., Chandran K.A., Sidorenko S.P., Clark E.A. Phospholipase C[gamma]1 interacts with conserved phosphotyrosyl residues in the linker region of Syk and is a substrate for Syk. *Molecular and Cellular Biology* **1996,** *16* (4), pp. 1305-1315

57. Braiman A., Barda-Saad M., Samelson L.E. Recruitment and activation of PLC[gamma]1 in T cells: a new insight into old domains. *The EMBO Journal* **2006,** Vol. *25,* pp. 774-784

58. Everett KL BunneyTD, Yoon Y, Rodrigues-Lima F, Harris R, Driscoll, P.C., Abe K., Fuchs H., de Angelis M.H., Yu P., Cho W., Katan M. Characterization of phospholipase C gamma enzymes with gain-of-function mutations. *The Journal of Biological Chemistry* **2009,** *284* (34), pp. 23083-23093

59. Nurieva R.I., Chuvpilo S., Wieder E.D., Elkon K.B., Locksley R., Serfling E., Dong C. A costimulation-initiated signaling pathway regulates NFATc transcription in T lymphocytes. *The Journal of Immunology* **2007,** Vol. *179,* pp. 1096-1103

60. Rao A., Luo C., Hogan P.G. Transcription factors of the NFAT family: regulation and function. *Annual Review of Immunology* **1997,** Vol. *15,* pp. 707-747

61. Kane L.P., Lin J., Weiss A. Signal transduction by the TCR for antigen. *Current Opinion in Immunology* **2000,** *12* (3), pp. 242-249

62. Heyeck S.D., Wilcox H.M., Bunnell S.C., Berg L.J. Lck phosphorylates the activation loop tyrosine of the Itk kinase domain and activates Itk kinase activity. *The Journal of Biological Chemistry* **1997,** *272* (40), pp. 25401-25408

63. Chan A.C., Dalton M., Johnson R., Kong G., Wang T., Thoma R., Kurosaki T. Activation of ZAP-70 kinase activity by phosphorylation of tyrosine 493 is required for lymphocyte antigen receptor function. *The EMBO Journal* **1995,** *14* (11), pp. 2499-2508

64. Shim E.Y., Jung S.H., Lee J.R. Role of two adaptor molecules SLP-76 and LAT in the PI3K signaling pathway in activated T-cells. *The Journal of Immunology* **2011,** pp. 2926-2935

65. Bogin Y., Ainey C., Beach D., Yablonski D. SLP-76 mediates and maintains activation of the Tec family kinase Itk via the T cell antigen receptor-induced association between SLP-76 and Itk. *Proceedings of National Academy of Sciences* **2007,** *104* (16), pp. 6638-6643

66. Beach D., Gonen R., Bogin Y., Reischl I.G., Yablonski D. Dual role of SLP-76 in

mediating TCR-induced activation of PLC[gamma]1. *The Journal of Biological Chemistry* **2007,** *282* (5), pp. 2937-2946

67. Yablonski D., Kuhne M.R., Kadlecek T., Weiss A. uncoupling of nonreceptor tyrosine kinases from PLC-[gamma]1 in an SLP-76-deficient T cell. *Science* **1998,** Vol. *281,* pp. 413-416

68. Jordan M.S., Sadler J., Austin J.E., Finkelstein L.D., Singer A.L., Schwartzberg P.L., Koretzky G.A. Functional hierarchy of the N-terminal tyrosines of SLP-76. *The Journal of Immunology* **2006,** Vol. *176,* pp. 2430-2438

69. Zhang W., Trible R.P., Samelson L.E. LAT palmitoylation: its essential role in membrane microdomain targeting and tyrosine phosphorylation during T cell activation. *Immunity* **1998,** Vol. *9,* pp. 239-246

70. Perrez-Villar J.J., Whitney G.S., Sitnick M.T., Dunn R.J., Venkatesan S., O'Day K., Schieven G.L., Lin T.-A., Kanner S.B. Phosphorylation pf the linker for activation of T-cells by Itk promotes recruitment of Vav. *Biochemistry* **2002,** Vol. *41,* pp. 10732-10740

71. Hundt M., Harada Y., De Giorgio L., Tanimura N., Zhang W., Altman A. Palmitoylation-dependent plasma membrane transport but lipid raft-independent signaling by linker for activation of T cells. *The Journal of Immunology* **2009,** *183* (3), pp. 1685-1694

72. Hundt M., Tabata H., Jeon M.S., Hayashi K., Tanaka Y., Krishna R., De Giorgio L., Liu Y.C., Fukata M., Altman A. Impaired activation and localization of LAT in anergic T cells as a consequence of a selective palmitoylation defect. *Immunity* **2006,** *24* (5), pp. 513-522

73. Dong S., Corre B., Nika K., Pellegrini S., Michel F. T cell receptor signal initiation induced by low-grade stimulation requires the cooperation of LAT in human T cells. *Plos One* **2010,** *5* (11),

74. Zhang W., Trible R.P., Zhu M., Liu S.K., McGlade J., Samelson L.E. Association od Grb2, Gads and phospholipase C-[gamma]1 with phosphorylated LAT

tyrosine residues. *The Journal of Biological Chemistry* **2000,** *275* (30), pp. 23355-23361

75. Andres P.G., Howland K.C., Dresnek D., Edmondson S., Abbas A.K., Krummel M.F. CD28 signals in the immature immunological synapse. *The Journal of Immunology* **2004,** Vol. *172,* pp. 5880-5886

76. Dennehy K.M., Elias F., Na S.-Y., Fischer K.-D., Hunig T., Luhder F. Mitogenic CD28 signals require the exchange factor Vav1 to enhance TCR signaling at the SLP-76-Vav-Itk signalosome. *The Journal of Immunology* **2007,** Vol. *178,* pp. 1363-1371

77. Liu K.Q., Bunnell S.C., Gurniak C.B., Berg L.J. T cell receptor-initiated calcium release is uncoupled from capacitative calcium entry in Itk-deficient T cells. *The Journal of Experimental Medicine* **1998,** *187* (10), pp. 1721-1727

78. Schaeffer E.M., Debnath J., Yap G., McVicar D., Liao X.C., Littman D.R., Sher A., Varmus H.E., Lenardo M.J., Schwartzberg P.L. Requirement for Tec kinases Rlk and Itk in T cell receptor signaling and immunity. *Science* **1999,** *284* (5414), pp. 638-641

79. Blomberg K.E., Boucheron N., Lindvall J.M., Yu L., Raberger J., Berglöf A., Ellmeier W., Smith C.E. Transcriptional signatures of Itk-deficient CD3+, CD4+ and CD8+ T-cells. *BMC Genomics* **2009,** *10* (233),

80. Yang W.C., Ghiotto M., Barbarat B., Olive D. The role of Tec protein-tyrosine kinase in T cell signaling. *The Journal of Biological Chemistry* **1999,** *274* (2), pp. 607-617

81. Schaeffer E.M., Yap G.S., Lewis C.M., Czar M.J., McVicar D.W., Cheever A.W., Sher A., Schwartzberg P.L. Mutation of Tec family kinases alters T helper cell differentiation. *Nature Immunology* **2001,** *2* (12), pp. 1183-1188

82. Quintana A., Griesemer D., Schwarz E.C., Hoth M. Calcium-dependent activation of T-lymphocytes. *Pflugers Archive* **2005,** *450* (1), pp. 1-12

83. Teixeira C., Stang S.L., Zheng Y., Beswick N.S., Stone J.C. Integration of DAG signaling systems mediated by PKC-dependent phosphorylation of RasGRP3. *Blood* **2003,** *102* (4), pp. 1414-1420

84. Lucas J.A., Atherly L.O., Berg L.J. The absence of Itk inhibits positive selection without changing lineage commitment. *The Journal of Immunology* **2002,** *168* (12), pp. 6142-6151

85. Schaeffer E.M., Broussard C., Debnath J., Anderson S., McVicar D.W., Schwartzberg P.L. Tec family kinases modulate thresholds for thymocyte development and selection. *The Journal of Experimental Medicine* **2000,** *192* (7), pp. 987-1000

86. Au-Yeong B.B., Katzman S.D., Fowell D.J. Itk-dependent signals required for CD4+ T cells to exert, but not gain, Th2 effector function. *The Journal of Immunology* **2006,** *176* (7), pp. 3895-3899

87. Miller A.T., Wilcox H.M., Lai Z., Berg L.J. Signaling through Itk promotes T helper 2 differentiation via negative regulation of T-bet. *Immunity* **2004,** *21* (1), pp. 67-80

88. Fowell D.J., Shinkai K., Liao X.C., Beebe A.M., Coffman R.L., Littman D.R., Locksley R.M. Impaired NFATc translocation and failure of Th2 development in Itk-deficient CD4+ T cells. *Immunity* **1999,** *11* (4), pp. 399-409

89. Mueller C. and August A. Attenuation of immunological symptoms of allergic asthma in mice lacking the tyrosine kinase ITK. *The Journal of Immunology* **2003,** *170* (10), pp. 5056-5063

90. Atherly L.O., Lucas J.A., Felices M., Yin C.C., Reiner S.L., Berg L.J. The Tec family tyrosine kinases Itk and Rlk regulate the development of conventional CD8+ T cells. *Immunity* **2006,** *25* (1), pp. 79-91

91. Readinger J.A., Mueller K.L., Venegas A.M., Horai R., Schwartzberg P.L Tec kinases regulate T-lymphocyte development and function: new insights into the

roles of Itk and Rlk/Txk. *Immonological Reviews* **2009,** *228* (1), pp. 93-114

92. Qi Q., Xia M., Hu J., Hicks E., Iyer A., Xiong N., August A. Enhanced development of CD4+ gammadelta T cells in the absence of Itk results in elevated IgE production. *Blood* **2009,** *114* (3), pp. 564-571

93. Broussard C., Fleischacker C., Horai R., Chetana M., Venegas A.M., Sharp L.L., Hedrick S.M., Fowlkes B.J., Schwartzberg P.L. Altered development of CD8+ T cell lineages in mice deficient for the Tec kinases Itk and Rlk. *Immunity* **2006,** *25* (1), pp. 93-104

94. Hu J., Sahu N., Walsh E., August A. Memory phenotype CD8+ T cells with innate function selectively develop in the absence of active Itk. *European Journal of Immunology* **2007,** *37* (10), pp. 2892-2899

95. Felices M., Yin C.C., Kosaka Y., Kang J., Berg L.J. Tec kinase Itk in gammadeltaT cells is pivotal for controlling IgE production in vivo. *Proceedings of the National Academy of Sciences* **2009,** *106* (20), pp. 8308-8313

96. Fischer A.M., Mercer J.C., Iyer A., Ragin M.J., August A. Regulation of CXC chemokine receptor 4-mediated migration by the Tec family tyrosine kinase ITK. *Journal of Biological Chemistry* **2004,** *279* (28), pp. 29816-29820

97. Takesono A., Horai R., Mandai M., Dombroski D., Schwartzberg P.L. Requirement for Tec kinases in chemokine-induced migration and activation of Cdc42 and Rac. *Current Biology* **2004,** *14* (10), pp. 917-922

98. Grünig G., Warnock M., Wakil A.E., Venkayya R., Brombacher F., Rennick D.M., Sheppard D., Mohrs M., Donaldson D.D., Locksley R.M., Corry D.B. Requirement for IL-13 independently of IL-4 in experimental asthma. *Science* **1998,** *282* (5397), pp. 2261-2263

99. Kim Y.K., Oh S.Y., Jeon S.G., Park H.W., Lee S.Y., Chun E.Y., Bang B., Lee H.S., Oh M.H., Kim Y.S., Kim J.H., Gho Y.S., Cho S.H., Min K.U., Kim Y.Y., Zhu Z. Airway exposure levels of lipopolysaccharide determine type 1 versus type 2 experimental asthma. *The Journal of Immunology* **2007,** *178* (8), pp. 5375-

5382

100. Ferrara T.J., Mueller C., Sahu N., Ben-Jebria A., August A. Reduced airway hyperresponsiveness and tracheal responses during allergic asthma in mice lacking tyrosine kinase inducible T-cell kinase. *Journal of Allergy and Clinical Immunology* **2006,** *117* (4), pp. 780-786

101. Sahu N., Mueller C., Fischer A., August A. Differential sensitivity to Itk kinase signals for T helper 2 cytokine production and chemokine-mediated migration. *The Journal of Immunology* **2008,** *180* (6), pp. 3833-3838

102. Sahu N., Morales J.L., Fowell D., August A. Modeling susceptibility versus resistance in allergic airway disease reveals regulation by Tec kinase Itk. *PLoS* **2010,** *5* (6),

103. Sahu N. and August A. Itk inhibitors in inflammation and immune-mediated disorders. *Current Topics in Medicinal Chemistry* **2009,** *9* (8), pp. 690-703

104. Lee S.-H., Chang A.-S., Park S.-W., Park J.S., Uh S.-T., Kim Y.H., Oh B., Lee J.-K., Park B.-L., Shin H.D., Park C.-S., Kimm K. the association of a single-nucleotide polymorphism of the IL-2 inducible T-cell kinase gene with asthma. *Annals of Human Genetics* **2011,** Vol. *75,* pp. 359-369

105. Wong F.W.S. Inhibitors of the tyrosine kinase signaling cascade for asthma. *Current Opinion in Pharmacology* **2005,** Vol. *5,* pp. 264-271

106. Wong F.W.S. and Leong K.P. Tyrosine kinase inhibitors: a new approach to asthma. *Biochimica et Biophysica Acta* **2004,** Vol. *1697,* pp. 53-69

107. Bonin A., Rausch A., Mengel A., Hitchcock M., Kruger M., Ahsen O., Merz c., Rose L., Stock C., Martin S.F., Leder G., Docke W.-D., Asadullah K., Zugel U. Inhibition of the IL-2-inducible tyrosine kinase (Itk) activity: a new concept for the therapy of inflammatory skin disease. *Experimental Dermatology* **2010,** Vol. *20,* pp. 41-47

108. Takata M. and Kurosaki T. A role of Bruton's tyrosine kinase in B cell antigen receptor-mediated activation of phospholipase C-[gamma]2. *The Journal of Experimatnat Medicine* **1996,** Vol. *184,* pp. 31-40

109. Huck K., Feyen O., Niehues T., Ruschendorf F., Hubner N., Laws H.-J., Telieps T., Knapp S., Wacker H.-H., Meindl A., Jumaa H., Borkhardt H. Girl homozygous for an IL-2-inducible T cell kinase mutation that leads to protein deficiency develop fatal EBV-associated lymphoproliferation. *The Journal of Clinical Investigation* **2009,** *119* (5), pp. 1350-1358

110. Streubel B., Vinatzer U., Wilheim M., Raderer M., Chott A. Novel t(5;9)(q33;q22) fuses Itk to Syk in unspecified peripheral T-cell lymphoma. *Leukemia* **2006,** Vol. *20,* pp. 313-318

111. Hussain A., Yu L., Faryal R., Mohammad D.K., Mohamed A.J., Smith E.C.I. TEC family kinases in health and disease - loss-of-function of Btk and Itk and the gain-of-function fusions Itk-Syk and Btk-Syk. *FEBS Journal* **2011,** pp. 1-10

112. Readinger J.A., Schiralli G.M., Jiang J.K., Thomas C.J., August A., Henderson A.J., Schwartzberg P.L. Selective targeting of ITK blocks multiple steps of HIV replication. *Proceedings of National Academy of Sciences* **2008,** *105* (18), pp. 6684-6689

113. Bachmann M.F., Littman D.R., Liao X.C. Antiviral immune responses in Itk-deficient mice. *The Journal of Virology* **1997,** *71* (10), pp. 7253-7257

114. Kim J.I., I.C. Ho., Grusby M.J., Glimcher L.H. The transcription factor c-Maf controls the production of interleukin-4 but not other Th2 cytokines. *Immunity* **1999,** *10* (6), pp. 745-751

115. Montoya M.C., Sancho D., Bonello G., Collette Y., Langlet C., He H.T., Aparicio P., Alcover A., Olive D., Sanchez-Madrid F. Role of ICAM-3 in the initial interaction of T lymphocytes and APCs. *Nature Immunology* **2002,** *3* (2), pp. 159-168

116. Zal T. and Gascoigne R.J. Photobleaching-corrected FRET efficiency imaging of live cells. *Biophysical Journal* **2004,** Vol. *86,* pp. 3923-3939

117. Zal T. and Gascoigne N.R.J. Using Live FRET imaging to reveal early protein-protein interactions during T cell activation. *Current Opinion in Immunology* **2004,** *16* (418), pp. 674-683

118. Krouwels F.H., Nocker R.E., Snoek M., Lutter R., van der Zee J.S., Weller F.R., Jansen H.M., Out T.A. Immunocytochemical and flow cytofluorimetric detection of intracellular IL-4, IL-5 and IFN-gamma: applications using blood- and airway-derived cells. *Journal of Immunological Methods* **1997,** *203* (1), pp. 89-101

119. Schulz K.R., Danna E.A., Krutzik P.O., Nolan G.P. Single-cell phospho-protein analysis by flow cytometry. *Current Protocols in Immunology* **2007,** *8* (8.17),

120. Krutzik P.O. and Nolan G.P. Intracellular phospho-protein staining techniques for flow cytometry: monitoring single cell signaling events. *Cytometry* **2003,** *55* (2), p. 61070

121. Takebe Y., Seiki M., Fujisawa J.-I., Hoy P., Yokota K., Arai K.-I., Yoshida M., Arai N. SR[alpha] promoter: an efficient and versatile mammalian cDNA expression system composed of the Simian Virus 40 early promoter and the R-U5 segment of human T-cell leukemia virus type 1 long terminal repeat. *Molecular and Cellular Biology* **1988,** *8* (1), pp. 466-472

122. Buschle M., Brenner M.K., Chen I.S.Y., Drexler H.G., Gognac S.M., Rooney C.M. Transfection and gene expression in normal and malignant primary B lymphocytes. *Journal of Immunological Methods* **1990,** Vol. *133,* pp. 77-85

123. Lorenz M., Yamaguchi H., Wang Y., Singer R., Condeelis J. Imaging sites of N-WASP activity in lamellipodia and invadopodia of carcinoma cells. *Current Biology* **2004,** Vol. *14,* pp. 697-703

124. Carreno L.J., Gonzales P.A., Kalergis A.M. Modulation of T cell function by TCR/pMHC binding kinetics. *Immunobiology* **2006,** *211* (1-2), pp. 47-64

125. Johnson H.M., Russell J.K., Pontzer C.H. Staphylococcal enterotoxin microbial superantigens. *FASEB* **1991,** Vol. *5,* pp. 2706-2712

126. Sahu N., Mueller C., Fischer A., August A. Differential sensitivity to Itk kinase signals for T helper 2 cytokine production and chemokine-mediated migration. *The Journal of Immunology* **2008,** *180* (6), pp. 3833-3838

127. Hayakawa K., Lin B.T., Hardy R.R. Murine thymic CD4+ T cell subsets: a subset (Thy0) that secretes diverse cytokines and overexpresses the V beta 8 T cell receptor gene family. *The Journal of Experimental Medicine* **1992,** *176* (1), pp. 269-274

128. Watanabe H., Numata K., Ito T., Takaqi K., Matsukawa A. Innate immune response in Th1- and Th2-dominant mouse strains. *Shock* **2004,** *22* (5), pp. 460-466

129. Berg L.J., Finkelstein L.D., Lucas J.A., Schwartzberg P.L. Tec family kinases in T lymphocyte development and function. *Annual Review in Immunology* **2005,** Vol. *23,* pp. 549-600

130. Mohamed A.J., Yu L., Bäckesjö C.M., Vargas L., Faryal R., Aints A., Christensson B., Berglöf A., Vihinen M., Nore B.F., Smith C.I. Bruton's tyrosine kinase (Btk): function, regulation, and transformation with special emphasis on the PH domain. *Immunological Reviews* **2009,** *228* (1), pp. 58-73

131. Monks C.R., Freiberg B.A., Kupfer H., Sciaky N., Kupfer A. Three-dimensional segregation of supramolecular activation clusters in T cells. *Nature* **1998,** *395* (6697), pp. 82-86

132. Hu Q., Davidson D., Schwartzberg P.L., Macchiarini F., Lenardo M.J., Bluestone J.A., Matis L.A. Identification of Rlk, a novel protein tyrosine kinase with predominant expression in the T cell lineage. *Journal of Biological Chemistry* **1995,** *270* (4), pp. 1928-1934

133. Shan X., Czar M.J., Bunnell S.C., Liu P., Liu Y., Schwartzberg P.L., Wange R.L.

Deficiency of PTEN in Jurkat T cells causes constitutive localization of Itk to the plasma membrane and hyperresponsiveness to CD3 stimulation. *Molecular Cell Biology* **2000,** *20* (18), pp. 6945-6957

134. Sommers C.L., Rabin R.L., Grinberg A., Tsay H.C., Farber J., Love P.E. A role for the Tec family tyrosine kinase Txk in T cell activation and thymocyte selection. *The Journal of Experimental Medicine* **1999,** *190* (10), pp. 1427-1438

135. Sommers C.L.,Huang, K., Shores E.W., Grinberg A., Charlick D.A., Kozak C.A., Love P.E. Murine txk: a protein tyrosine kinase gene regulated by T cell activation. *Oncogene* **1995,** *11* (2), pp. 245-251

136. Tomlinson M.G., Kane L.P., Su J., Kadlecek T.A., Mollenauer M.N., Weiss A. Expression and function of Tec, Itk, and Btk in lymphocytes: evidence for a unique role for Tec. *Molecular Cell Biology* **2004,** *24* (6), pp. 2455-2466

137. Yang W.C. and Olive D. Tec kinase is involved in transcriptional regulation of IL-2 and IL-4 in the CD28 pathway. *European Journal of Immunology* **1999,** *29* (6), pp. 1842-1849

138. Brandt E.B. and Sivaprasad U. Th2 Cytokines and Atopic Dermatitis. *Journal of Clinical Cellular Immunology* **2011,** *2* (3),

139. Oh C.K., Geba G.P., Molfino N. Investigational therapeutics targeting the IL-4/IL-13/STAT-6 pathway for the treatment of asthma. *European Respiratory Reviews* **2010,** *19* (115), pp. 46-54

140. Au-Yeung B.B. and Fowell D.J. A key role for Itk in both IFN gamma and IL-4 production by NKT cells. *The Journal of Immunology* **2007,** *179* (1), pp. 111-119